

The Sediment and Particulate Organic Carbon Cycle of Lake Melville,
Labrador: a Fjord Estuary undergoing Hydrologic and Climatic Change

by

Christina Michelle Kamula

A Thesis submitted to the Faculty of Graduate Studies of

The University of Manitoba

in partial fulfilment of the requirements of the degree of

MASTER OF SCIENCE

Department of Environment and Geography

University of Manitoba

Winnipeg

Copyright © 2015 by C. Michelle Kamula

ABSTRACT

To evaluate potential impacts of anthropogenic and climatic changes on Lake Melville, a fjard estuary that receives runoff from the Churchill River in Labrador, modern sedimentological processes, sources, and distribution of sediment and particulate organic carbon (POC) were investigated in recently deposited sediment (i.e., last 100-150 yrs.). This investigation showed that the Churchill River is the dominate source of sediment and terrestrial POC to the Lake Melville system, which could double following the proposed hydroelectric development on the Lower Churchill River. An examination of the sedimentary record revealed an increase in terrestrial POC deposited in recent years, implying increased delivery of terrestrial POC to the system since 1970. Box-model budgets quantified sources, sinks, and losses of sediment and terrestrial and marine POC to Lake Melville that can be used to assess changes to the system in the future from hydroelectric development and ongoing climatic change.

ACKNOWLEDGEMENTS

First, I would like to thank my supervisor, Dr. Zou Zou Kuzyk for her continuous support, guidance, encouragement, and positivity, and for providing me with the amazing opportunity to work in Labrador. The mentorship I received from Dr. Kuzyk motivate me to do better science but also helped me gain more confidence to continue pursuing a career in Arctic science. I would also like to thank Dr. Kuzyk and Dr. Gary Stern for supporting me as I pursued opportunities beyond my thesis work that allowed me to connect with Northerners and some of the finest scientists in Arctic research.

I am extremely grateful for the expertise and support I received from Dr. Robie Macdonald throughout the entire project but especially during the writing process. Thank you to Dr. David Lobb for assistance with data analysis and for his enthusiasm and guidance. I thank R. Laing, Captain C. Bannister and crew of R/V Nuliajuk, Captain J. Angnakok and crew of M/V What's Happening, A. Eastwood, Dr. Kuzyk, C. Webb, and A. Schartup for assistance in the field. Thank you to E. Slavicek, M. Yun, and M. Soon for their assistance with lab work. Special thanks to E. Wiley for logistical support and to Dr. McCullough for helping answering many science questions.

I thankfully acknowledge Tom Sheldon (Nunatsiavut) and Trevor Bell (MUN) for their commitment to Inuit health and well-being which led them to develop the project *Lake Melville: Avativut, Kanuittailinnivut (Our Environment, Our Health)* for which this research contributes to. Financial support from ArcticNet, NSTP, UMGF, and financial support from Dr. Kuzyk is gratefully acknowledged. I sincerely thank my family, especially my father Don Kamula, and friends at U of M and elsewhere for their support and encouragement. Finally, I thank Tom Guenther for his unceasing support and patience!

TABLE OF CONTENTS

ACKNOWLEDGEMENTS	iii
LIST OF FIGURES	vi
LIST OF TABLES	viii
Chapter 1 : General Introduction	1-1
1.1 Overview.....	1-1
1.2 Sediment and organic carbon cycling in coastal environments	1-1
1.3 Radionuclide Approach	1-5
1.4 Study area and incentive for research	1-9
1.5 Project overview and funding	1-13
1.6 Thesis objectives	1-14
1.7 Thesis overview	1-15
1.8 References.....	1-15
Chapter 2 : Patterns and Sources of Sediment and Particulate Organic Carbon in Lake Melville, Labrador, Canada: Inferences from ²¹⁰Pb, ¹³⁷Cs, and δ¹³C	2-1
2.1 Abstract	2-1
2.2 Introduction.....	2-2
2.3 Study area.....	2-4
2.3.1 <i>Overview</i>	2-4
2.3.2 <i>Geological Setting</i>	2-6
2.3.3 <i>Hydrology and oceanography</i>	2-7
2.4 Methods.....	2-8
2.4.1 <i>Sample collection</i>	2-8
2.4.2 <i>Radiochemical analysis</i>	2-10
2.4.3 <i>Calculation of sedimentation and mass accumulation rates</i>	2-12
2.4.4 <i>²¹⁰Pb_{ex} and ¹³⁷Cs inventories</i>	2-14
2.4.5 <i>Organic carbon and δ¹³C_{org} measurements</i>	2-16
2.4.6 <i>Calculation of the percentage of terrestrial and marine organic carbon</i>	2-16
2.4.7 <i>Modelling of organic carbon</i>	2-17
2.5 Results.....	2-18
2.5.1 <i>Porosity profiles</i>	2-18
2.5.2 <i>²¹⁰Pb, ²²⁶Ra, and ¹³⁷Cs radiochemistry</i>	2-20

2.5.3 Sedimentation and Mass Accumulation Rates	2-26
2.5.4 Inventories of $^{210}\text{Pb}_{\text{ex}}$ and ^{137}Cs	2-29
2.5.5 Distribution and profiles of organic carbon and $\delta^{13}\text{C}$	2-31
2.6 Discussion	2-34
2.6.1 Overview	2-34
2.6.2 Inputs of riverine sediment inferred from mass accumulation rates	2-34
2.6.3 Indications of riverine inputs, focusing, and boundary scavenging from ^{137}Cs and $^{210}\text{Pb}_{\text{ex}}$ inventories	2-38
2.6.4 Terrestrial and marine influence on sediment composition inferred from $\delta^{13}\text{C}_{\text{org}}$...	2-42
2.6.5 Inferences of Change from Profiles of $\delta^{13}\text{C}_{\text{org}}$ and OC.....	2-44
2.7 Conclusion	2-46
2.8 References.....	2-48
Chapter 3 : Sediment and particulate organic carbon budgets of Lake Melville, Labrador	3-1
3.1 Abstract.....	3-1
3.2 Introduction.....	3-2
3.3 Study Area	3-5
3.4 Methods.....	3-9
3.4.1 General approach	3-9
3.4.2 Sample collection	3-10
3.4.3 Radioisotope analysis and calculation of sedimentation rates.....	3-12
3.4.4 Stable Isotope and bulk organic carbon analysis	3-13
3.4.5 Calculations for organic carbon surface flux, burial and oxidation rates	3-13
3.5 Results and Discussion	3-15
3.5.1 Sediment sinks	3-15
3.5.2 Surface flux and rates of burial and oxidation of particulate organic carbon	3-18
3.5.3 Sediment input from rivers.....	3-24
3.5.4 Estimated inputs of terrestrial organic carbon from rivers.....	3-27
3.5.5 Estimated inputs from autochthonous primary production	3-29
3.5.6 Inputs from coastal erosion and resuspension.....	3-32
3.4.7 Exchange with Groswater Bay.....	3-33
3.6 Mass-balance and summary of budgets	3-34
3.6.1 Sediment budget	3-34

3.6.2 Particulate organic carbon budgets	3-37
3.7 Potential impacts of the Lower Churchill development on the sediment and particulate organic carbon budgets	3-39
3.8 References.....	3-41
Chapter 4 : Conclusion and suggestions for future work.....	4-1
4.1 Conclusions.....	4-1
4.2 Suggestions for future work.....	4-6
4.3 References.....	4-7
APPENDICES	
Appendix A: Description of core locations used in this study.....	A-1
Appendix B: Down-core data of radiochemistry, stable isotope, and organic carbon.....	B-1
Appendix C: Summary of autochthonous production.....	C-1

LIST OF FIGURES

Figure 1-1: An illustration of the cycling of ^{210}Pb in the environment (Kuzyk, 2015) (Used under permission obtained on November 27, 2015 from Dr. Zou Zou Kuzyk)	1-5
Figure 1-2. Map of Hamilton Inlet including Inuit Lands Region, Labrador Inuit Settlement Area, and communities of Rigolet, Happy-Valley Goose Bay (HVGB), and Northwest River (A). Map displaying the location of Lake Melville (B).....	1-11
Figure 2-1. Map of Hamilton Inlet including Groswater Bay, Lake Melville and Goose Bay, as well as major inflowing rivers (Churchill, Goose, Northwest, and Kenamu).	2-5
Figure 2-2. Locations where sediment cores and water samples were collected in 2013 and 2014.	2-9
Figure 2-3. Porosity profiles of sediment cores. Observed coarse particles in slice 20 and 21 cm of core 35 are shown as open dots. These sections had unusually low ^{210}Pb activities and were omitted from modelling.....	2-19
Figure 2-4. Profiles of total ^{210}Pb (black dot) and ^{226}Ra (open dot) activities for cores collected in 2013 and 2014. Total ^{210}Pb activities in cores 26, I13, and MT1 were counted indirectly by alpha.....	2-21

Figure 2-5. Profiles of measured (black point) and modelled (line) natural log $^{210}\text{Pb}_{\text{ex}}$ activity. Sedimentation rates beginning with “~” could not be validated using ^{137}Cs profiles and should be interpreted cautiously. Coarse grained material observed at depths of 20 and 21 cm in core 35 resulted in abnormally low activities, thus these sections were excluded from the modelling. Irregularly low $^{210}\text{Pb}_{\text{ex}}$ activities at depths 16 and 17 cm in core I12 were also excluded from the modelling. ^{210}Pb activities in core 26 were measured by alpha method.2-23

Figure 2-6. Down-core profiles of ^{137}Cs 2-25

Figure 2-7. ^{210}Pb -derived sedimentation (cm y^{-1}) and mass accumulation rates ($\text{g cm}^{-2} \text{y}^{-1}$) across Lake Melville. 2-27

Figure 2-8. $^{210}\text{Pb}_{\text{ex}}$ (A) and ^{137}Cs (B) inventories are compared to the expected inventory from direct atmospheric fallout (1.5 and 23.6 dpm cm^{-2} , respectively) (dashed horizontal line). Inventories are arranged along a west (Goose Bay) to east (Lake Melville) axis. The inventory of ^{137}Cs in core 26 was not available because background levels were not reached within the length of the core. $^{210}\text{Pb}_{\text{ex}}$ inventory in core 26 was estimated by extrapolating the $^{210}\text{Pb}_{\text{ex}}$ activity downwards to background levels. 2-30

Figure 2-9. A thematic map showing organic carbon content in surface sediment (0-1 cm) across Lake Melville. 2-31

Figure 2-10. Surface sedimentary $\delta^{13}\text{C}_{\text{org}}$ values (‰ relative to VPDB) across Lake Melville. 2-32

Figure 2-11. Profiles $\delta^{13}\text{C}_{\text{org}}$ (A) and percent contribution of terrestrial- and marine-type OC (B). Shading represents sediment containing 90% pre-1970 (surface) and post-1970 (bottom) while non-shaded areas are a mixture of both. 2-33

Figure 2-12. Mass accumulation rates (MAR, $\text{g cm}^{-2} \text{y}^{-1}$) (A), average porosity below the surface mixed layer (SML) (B), ^{137}Cs inventories (dpm cm^{-2}) (C), and ratio of ^{137}Cs to $^{210}\text{Pb}_{\text{ex}}$ inventories (D) plotted as a function of distance to the Churchill River. In C, the dashed line represents the expected ^{137}Cs inventory from direct atmospheric fallout. In D, the filled triangle represents the expected $^{137}\text{Cs}/^{210}\text{Pb}_{\text{ex}}$ inventory from direct atmospheric fallout. 2-35

Figure 2-13. Inventories of $^{210}\text{Pb}_{\text{ex}}$ and ^{137}Cs , and their ratios are compared across Lake Melville, and to the expected ratio in local soil from direct atmospheric fallout (shaded area). Cores with $^{210}\text{Pb}/^{137}\text{Cs}$ ratios that fall within the shaded area (i.e. high ^{137}Cs inventories), suggest additional terrigenous particles. Cores with $^{210}\text{Pb}/^{137}\text{Cs}$ ratios similar to soil (15.9), implies sediment focusing (black arrow), cores above the black arrow indicate an additional source of $^{210}\text{Pb}_{\text{ex}}$ 2-40

Figure 2-14. Relationships between ^{137}Cs inventories (dpm cm^{-2}) and mass accumulation rates (MAR, $\text{g cm}^{-2} \text{y}^{-1}$) (A) and $^{210}\text{Pb}_{\text{ex}}$ inventories (dpm cm^{-2}) and the percentage of marine OC within cores (B)..... 2-41

Figure 2-15. $\delta^{13}\text{C}$ (open dot) and OC content (black dot) plotted as a function of distance from the Churchill River. Site 29 (black triangle) was excluded from the OC regression analysis because this site is not considered a depositional area. 2-43

Figure 3-1. Map of Hamilton Inlet, major inflowing rivers (Churchill, Goose, Northwest, and Kenamu), smaller rivers (Sebaskachu, Mulligan and English) and Inuit lands, settlement, and community (Rigolet). 3-6

Figure 3-2. June 2013 salinity (A) and temperature (B) distribution of the water column of Goose Bay and Lake Melville. 3-8

Figure 3-3. Map of sample locations. All sediment cores were used to establish mass accumulation rates and the size of the sediment sink except core I11, which was mixed throughout. 3-11

Figure 3-4. Bathymetric map showing the division between Goose Bay and Lake Melville and between the western and eastern sections of Lake Melville (---). The inserted bar graph shows the seafloor area (km^2) to water depths (m). 3-17

Figure 3-5. First-order decay model (black line) fitted to profiles of total and marine organic carbon (black dots) shown as $\ln \text{g OC g sediment}^{-1}$ versus cumulative mass-depth (g cm^{-2}). 3-19

Figure 3-6. Calculated new primary production ($\text{g m}^{-2} \text{yr}^{-1}$) in Goose Bay and Lake Melville as estimated from a general empirical model and the surface fluxes of OC_{mar} in the sediment cores. 3-31

Figure 3-7. Mass balance budgets of sediment ($\times 10^8 \text{ kg yr}^{-1}$) (a), POC_{terr} ($\times 10^6 \text{ kg yr}^{-1}$) (b), and POC_{mar} ($\times 10^6 \text{ kg yr}^{-1}$) (c). Arrows pointing towards a box represent inputs, arrows pointing downwards represent sinks and curved arrows represent net oxidation. 3-36

LIST OF TABLES

Table 2-1. Sediment core properties and sedimentation rates and parameters. 2-28

Table 3-1. Properties of rivers draining into Lake Melville. 3-9

Table 3-2. Summary of mass accumulation rates and area of sea floor used to calculated sediment sink. 3-16

Table 3-3. Organic carbon surface fluxes and rates of burial and oxidation. 3-21

Table 3-4. Churchill River monthly TSS and discharge data used to estimate the suspended sediment input into the Lake Melville system. 3-25

Table 3-5. River TSS measurements.	3-26
Table 3-6. Concentrations of particulate organic carbon in river water.	3-27
Table 3-7. Monthly rates of POC_{terr} averaged to estimate the yearly inputs of POC_{terr} from the Churchill, Goose, and Northwest River.	3-28
Table 3-8. Measure $\delta^{13}\text{C}_{\text{org}}$ of riverine particulate organic matter.	3-29

Chapter 1 : General Introduction

1.1 Overview

This Master's thesis investigated sedimentary processes and the quantity, composition and fate of particulate organic carbon through Lake Melville, a fjard estuary in Labrador, Canada. This investigation used radioisotope (^{210}Pb and ^{137}Cs) and organic geochemical (organic carbon, $\delta^{13}\text{C}$) techniques to examine the sedimentary record and establish the fundamental sedimentary processes such as, sedimentation rates, within Lake Melville. As well, through this investigation into the sedimentary record identification and quantification of the major sources (i.e., terrestrial or marine), processes (i.e., deposition, lateral transport), and fate (i.e., oxidation, burial, export) of particulate organic carbon (POC) and sediment were established for Lake Melville.

1.2 Sediment and organic carbon cycling in coastal environments

Coastal environments and, in particular, estuaries are important regions for the transfer of sediment and organic carbon (OC) between land and the open ocean and thus are important in the overall global sediment and organic carbon cycles (Gattuso et al., 1998; Muller-Karger et al., 2005). In recent years, the fate of particulate organic carbon (POC) in coastal environments has received greater attention because the delivery, accumulation, and burial efficiency of sediment and POC in these environments is enhanced compared to open ocean regions, causing them to behave as 'filters' for materials undergoing transfer from land to the open ocean (Blair and Aller, 2012; Burdige, 2005, 2007). In addition to terrestrial inputs, estuaries also typically have high in situ biological carbon production (primary production). Thus, despite having been frequently

overlooked in global carbon budgets in the past, coastal environments are now recognized as a major OC sink, having the potential to regulate atmospheric CO₂ levels over glacial-interglacial time scales (Burdige, 2005; Smith et al., 2015). Moreover, an understanding of the source and fate of sediment and POC in coastal environments also provides a base from which to constrain local biogeochemical cycles (e.g., Dittmar and Kattner, 2003) and the fate of contaminants (e.g., Hare et al., 2010; Macdonald et al., 1991)

The terrestrial and marine type POC are each sourced, cycled, and degraded at different rates by varying mechanisms (Macdonald et al., 1998). Marine organic matter (OM) produced in the water column or sea ice includes photosynthesizing plankton, fecal pellets, and dead tissues, which are often easily degradable and referred to as labile (reactive) (Libes, 2011; Stein, 1991). As marine OM sinks from the euphotic zone through the water column, it undergoes remineralization, transforming to soluble forms (DOC, CO₂, NO₃⁴⁻). The vertical flux of OM from the euphotic zone to the seafloor thus depends on production, suspended biomass, season, grazing pressure, and depth of the water column (Klages et al., 2004; Suess, 1980; Wassmann, 1997; Wassmann et al., 2004). In deep (>1000 m) open ocean water where the period of settling of detritus through the water column is long, 99% of sinking detritus is remineralized before reaching the seafloor (Libes, 2011). In shallower (< 1000 m) shelves, 1-3% of primary production can reach the seafloor (Wassmann et al., 2004) while up to 6% of primary production has been reported for coastal environments such as Hudson Bay (depth ≤ 300 m) (Kuzyk et al., 2009).

Upon deposition on the seafloor, OM undergoes further degradation through the respiratory activities of benthic organisms. OM oxidation is generally most intense in the surface oxic zone of the sediments, and the fraction of the OM that gets buried or mixed deeper than this

zone may be preserved and buried for the long term in the sediment. The burial of OM and sequestration of OC in marine sediments depends on sedimentation rate and benthos activity/productivity (Stein et al., 2004). The stirring of sediment by benthic organisms (bioturbation) can support continued degradation of detritus below the sediment surface by delivering O₂ into subsurface sediment (10 cm to 1 m deep) (Libes, 2011).

In contrast to marine OM, terrigenous OM is often classified as refractory (unreactive) because it consists of intrinsically recalcitrant biomolecules such as the vascular plant material lignin and/or because of ‘protection’ from degradation by association with mineral surface area (Libes, 2011). Recent work suggests terrestrial OM may not be quite as resistant to degradation as previously thought (cf., Vonk et al., 2012). Nevertheless, marine POC tends to be preferentially consumed before terrigenous POC (POC_{terr}) resulting in a greater sink of terrestrial OM in coastal environments. Indeed, Burdige (2005) estimated that about one third of OM buried in marine sediments globally is terrigenous OM, with the majority efficiently buried in river dominated coastal regions.

Sediment and terrigenous POC_{terr} is sourced primarily by physical weathering of bedrock (Schlünz and Schneider, 2000) and erosion of surface soils and river banks. The materials are introduced into coastal environments by river runoff, coastal erosion, and aeolian transport. In some regions (e.g., Canadian Beaufort Sea near the Mackenzie River), the supply of sediment and POC_{terr} is dominated by river runoff, while in others (e.g., Siberian coastline), inputs from coastal erosion are the main sources of sediment and POC_{terr} (Rachold et al., 2000). Coastal erosion in Arctic and subarctic areas differs from that in temperate regions due to the short open-water season and the presence of ice in the marine and terrestrial environments (Lantuit et al.,

2012). Coastal geomorphology, presence of permafrost, storminess, and sea-ice conditions all influence the rate of sub-aerial erosion.

The development of hydroelectric dams and reservoirs (Déry et al., 2011) has major implications on the transfer of sediment (Gupta et al., 2012), POC_{terr} (Schäfer et al., 2002), and nutrients (Gong et al., 2006; Humborg et al., 2000) from land to coastal environments, with largely unknown impacts on the burial and sequestration of OC in marine sediment. Global estimates by Syvitski et al. (2005) and Vörösmarty et al. (2003) revealed that the retention of sediment and carbon within reservoirs has decreased the global sediment flux to coastal environments by approximately $1.4 \pm 0.3 \text{ Gt yr}^{-1}$ to $4\text{-}5 \text{ Gt yr}^{-1}$ and 1 to $3 \text{ Gt carbon yr}^{-1}$. In addition to the quantity of OC, the impoundment of rivers has been associated with changes in the composition of sediment (i.e., grain size) (Bogen and Bønsnes, 2001; Boyer-Villemaire et al., 2013) and POC (autotrophic to heterotrophic) (Friedl and Wüest, 2002) delivered downstream. Geomorphic changes (Power et al., 1996) in addition to altered nutrient fluxes can impact the downstream ecosystem.

Recent studies have also linked warming climate to increased freshwater discharge and seasonal variability to the Arctic Ocean (McClelland et al., 2006; Peterson et al., 2002) and other northern areas (Déry et al., 2005) which probably is associated with increased loads of sediment and POC_{terr} (ancient and fresh). Additionally, a warming climate resulting in rising sea levels (Alley et al., 2005), loss of sea ice (Jones et al., 2009), and thawing permafrost (Lantuit and Pollard, 2008; Payette et al., 2004) in the sub-arctic and arctic regions, has increased rates of coastal erosion, amplifying the delivery of sediment and POC_{terr} to coastal and marine environments (Rachold et al., 2000).

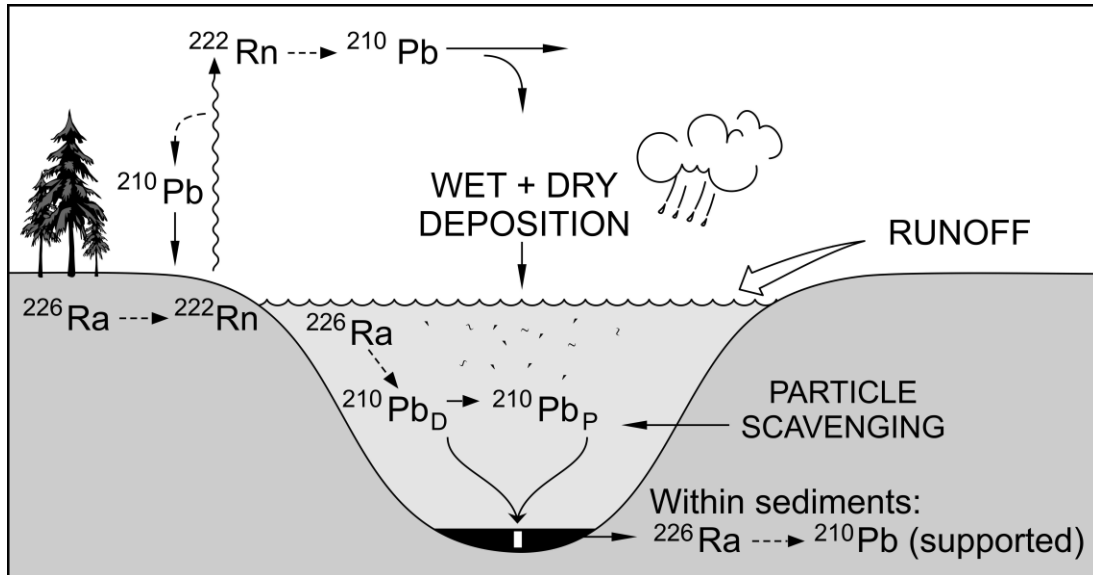
For a sub-basin of the Churchill River in central Labrador, Canada, Roberts et al. (2012) predicted that ongoing regional warming could increase annual stream flow by 9% over the 2041-2070 time period, with the greatest increase occurring in December. Since the 1990's, Labrador has experienced several warm winter anomalies (Finnis and Bell, 2015). Examination of air temperature records suggested these warm anomalies were associated with a positive atmospheric warming trend, which can be masked by high natural variability (Finnis and Bell, 2015). In addition to natural variability, Way and Viau (2014) argued that warming since 1998 in the Labrador region is also associated with anthropogenic forcing.

1.3 Radionuclide Approach

Radionuclides such as ^{210}Pb and ^{137}Cs bind to fine particles and accumulate in lacustrine, marine and estuarine basins (e.g., Figure 1-1), thus providing a means for interpreting the environment from which the particles were sourced and the mechanisms involved in their distribution and deposition. The naturally-occurring ^{210}Pb and fallout ^{137}Cs (a product of nuclear fission) are two of the most commonly used radionuclide tracers for studying deposition, erosion, and delivery of sediment.

First described by Goldberg (1963), the ^{210}Pb method has been used extensively for dating sediment since the 1970's (Appleby and Oldfield, 1978; Bruland et al., 1974; Carpenter et al., 1981; Koide et al., 1973; Koide et al., 1972; Krishnaswamy et al., 1971; Lavelle, 1985; Oguri et al., 2012; Smith et al., 2002; Sugai, 1990a; and many more) and is often the primary radionuclide tracer for assessing the modern sedimentary record (Kuzyk et al., 2015). As part of the decay series for ^{238}U , which is a ubiquitous radionuclide in soil and rock, ^{210}Pb (half-life 22.3 yrs.) in marine and estuarine sediment is derived from three sources (Figure 1-1).

Figure 1-1: An illustration of the cycling of ^{210}Pb in the environment (Kuzyk et al., 2015) (Used under permission obtained on December 4, 2015 from Springer publisher).



Firstly, ^{210}Pb is produced by *in situ* decay of ^{226}Ra (half-life 1620 yrs.) directly from the inorganic sediment. This type of ^{210}Pb is termed supported or background ^{210}Pb and is considered to be in radioactive equilibrium (production rate = decay rate) with ^{226}Ra , allowing for the indirect measurement of supported ^{210}Pb (Appleby, 2001).

Secondly, ^{210}Pb is produced in the atmosphere from the decay of ^{222}Ra (half-life 2.8 days), an inert gas that is produced by the decay of ^{226}Ra in soil. When produced near the soil surface, ^{222}Ra escapes to atmosphere and through a short (3-4 days) decay series, decays into ^{210}Pb (Turekian et al., 1977). Atmospheric ^{210}Pb is termed unsupported or excess ^{210}Pb ($^{210}\text{Pb}_{\text{ex}}$). Through dry or wet fallout, atmospheric $^{210}\text{Pb}_{\text{ex}}$ returns to the earth's surface and attached readily through ionic binding to sediment particles (Appleby, 2001; Appleby and Oldfield, 1992).

Thirdly, ^{210}Pb (also considered unsupported or excess ^{210}Pb) is produced from the direct decay of dissolved ^{226}Ra in surface water of the world's oceans (Krishnaswami and Cochran, 2011). When in contact with particulate matter, $^{210}\text{Pb}_{\text{ex}}$ produced in surface seawater binds almost irreversibly and is subsequently deposited to the seafloor (i.e., particle scavenged). A number of studies have associated particle scavenging of $^{210}\text{Pb}_{\text{ex}}$ with fluxes of organic matter (e.g., Cochran et al., 1990; Kuzyk et al., 2013; Moore and Dymondt, 1988; Oguri et al., 2012). This correlation allows for inventories of $^{210}\text{Pb}_{\text{ex}}$ to be used as a proxy for the productivity of the overlying water column (e.g., Fang et al., 2013; Shimmield et al., 1995; Wei et al., 2011).

Easily misinterpreted, geological processes such as sedimentation rate that are established from ^{210}Pb must be validated (Smith, 2001). This validation is commonly achieved using the transient tracer ^{137}Cs . First introduced into the atmosphere in 1945, ^{137}Cs (half-life 30.2 yrs.), a by-product of nuclear fission, was produced primarily between 1952 and 1962 from atmospheric nuclear weapons testing (Wright et al., 1999). The majority (57%) of its production took place between 1961 and 1962 (Wright et al., 1999). ^{137}Cs fallout peaked in 1963, mostly in the northern hemisphere where nuclear weapons testing primarily took place (Walling and He, 2000). As such, a 1963 fallout peak provides a good geochemical marker in unmixed sediment in the northern hemisphere. Previous studies have assessed the fallout distribution of ^{137}Cs from nuclear weapons testing (Hutchison-Benson et al., 1985; Monetti, 1996; Wright et al., 1999), with consensus that latitude, longitude, and precipitation are major controls on fallout. In some northern European regions, a second, more recent peak of ^{137}Cs can be seen in soil and sediment reflecting the Chernobyl accident of 1986 (Appleby, 2008).

The sorption of ^{137}Cs to particles and subsequent burial in the sediment record is associated with particle size (i.e., clay) (Staunton and Roubaud, 1997), mineralogical

composition (He and Walling, 1996), and concentration of cations (e.g., Na^+ , K^+ , Mg^{2+}) within the water column, which compete with ^{137}Cs for sorption sites (Lujanienė et al., 2010). The latter factor means that ^{137}Cs exhibits weaker particle reactivity in seawater compared to freshwater, which has lower concentration of cations. Thus, ^{137}Cs binds strongly to clays in the terrestrial environment and is delivered to coastal areas with erosion and fluvial transport of these clays; however, ^{137}Cs can be mobilized from the clays in certain sedimentary regimes (i.e., coupling of fresh and marine water as occurs in estuaries) (cf., Kuzyk et al., 2013; Kuzyk et al., 2009; Oughton et al., 1997; Sholkovitz et al., 1983). The differences in supply (steady-state vs. transient) and behaviour (i.e., degree of particle reactivity) of ^{210}Pb and ^{137}Cs in marine system provides a means for assessing sediment sources (i.e., terrestrial vs. marine) (e.g., Kuzyk et al., 2013; Smith et al., 2002).

In marine and estuarine sediment, the use of ^{210}Pb and ^{137}Cs is complicated by the vertical mixing of sediment by burrowing benthic organisms (bioturbation) and physical mixing by waves and tides. Bioturbation is by far the more dominant process in marine and estuarine sediment and can result in mixing as deep as 40 cm (Lavelle, 1985; Middelburg et al., 1997). This mixing significantly alters the lithostratigraphy of deposited sediment and the distribution of tracers, making it impossible to definitively assign dates to sediment layers (cf., Johannessen and Macdonald, 2012). Nevertheless, by including mixing (and compaction with depth) in the interpretation of sediment cores and validating with an independent tracer (i.e., ^{137}Cs), rates of accumulation and burial can be calculated from marine sediment (Lavelle, 1985; Robbins and Edgington, 1975; Smith, 2001). Kuzyk (2015) provides a thorough outline of the critical steps needed to overcome the problem of mixing and reliably interpret estuarine and marine sediment cores. Estimating these rates is a necessary first step for reconstructing the history of

contaminants (Macdonald et al., 1991) or constructing sediment and OC budgets (Johannessen et al., 2003; Kuzyk et al., 2009).

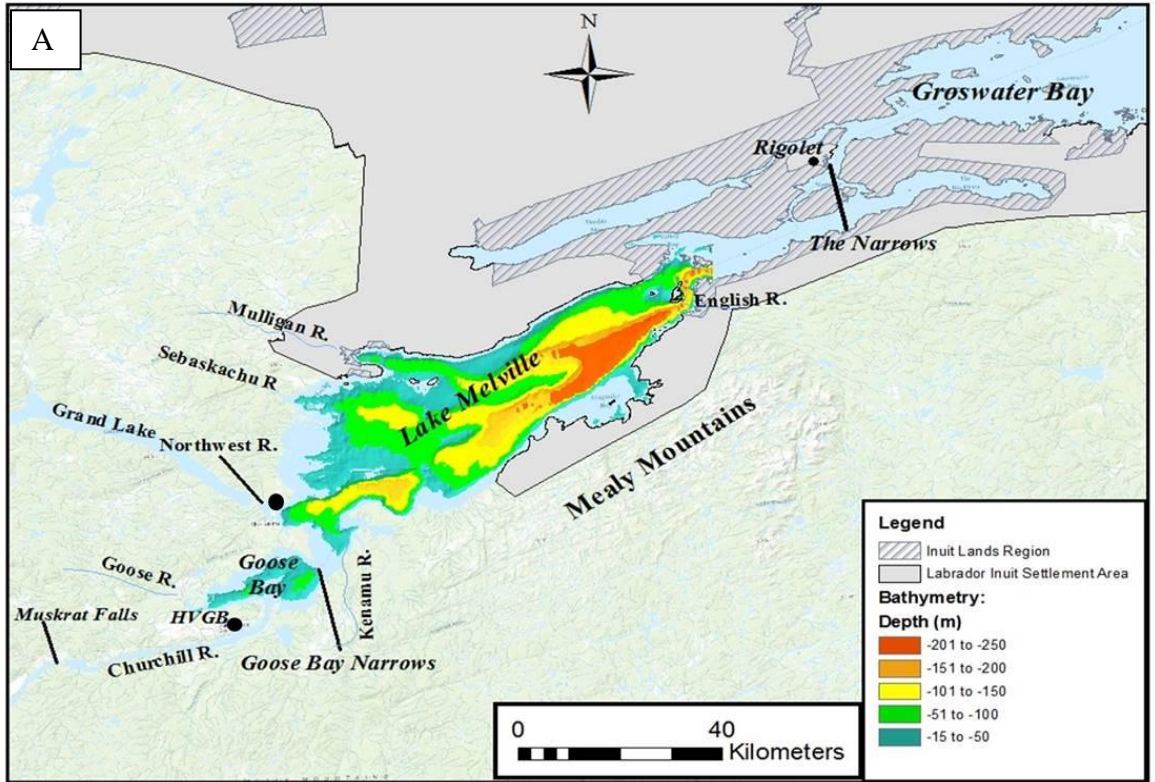
1.4 Study area and incentive for research

Lake Melville is a subarctic, ‘fjord’ estuary located in central Labrador, Canada (53.55°N and 59.58°W) (see Figure 1-2). Fjords are similar to the more commonly researched fjords in many respects, both having been carved by Pleistocene and Holocene glaciation and thus being characterized as drowned glacial valleys where fresh water from land runoff and saline ocean water mix, creating an estuarine circulation (Brown et al., 2012; Syvitski, 1987). Often (but not always) a shallow sill is located at the mouth of both fjords and fjards, which can restrict the exchange of water, sediment, and nutrients with the open ocean (Brown et al., 2012). However, common differentiating factors between fjords and fjards are topography, basin relief, depth, and bathymetry (Finkl, 2004; Perillo, 1995). In a fjord, the sill closes a long, narrow, very deep, uniform U-shaped basin with steep sidewalls and high relief topography (Perillo, 1995). In contrast, the shores of fjards are low-layering, often rocky, with basins of irregular shape and depth that frequently contain lateral terraces, shoals, rocky reefs (skerries), and islands (Carpenter, 2012; Fairbridge, 1968; Perillo, 1995)(Carpenter, 2012; Fairbridge, 1968; Perillo, 1995). Because of their low laying shoreline, Finkl (2004) proposed that fjards are formed by unconfined glacial erosion, while fjords are considered to be carved by linear glacial erosion. Another important difference is that fjards are generally located in temperate ecoregions and their tributaries flow through forested watersheds with deeper surficial deposits relative to fjords, which are commonly located at high latitudes where erosion resisted rock and thin surficial deposits, contain sparse vegetation (Carpenter, 2012; and references within). These differences

suggest dissimilarity in the type and quantity of sediment and OM deposited in the two environments.

Lake Melville is part of the Nunatsiavut Inuit Settlement Area. The community of Rigolet is located at the mouth of the fjard, while a number of beneficiaries reside in the communities of Happy Valley-Goose Bay (HVGB) and Northwest River at the fjard head. As part of Hamilton Inlet, the largest inlet on the Labrador coast, Lake Melville is connected to Groswater Bay and the Labrador Sea through a long narrow passageway known as the Narrows. Here, a shallow sill (30 m) restricts the landward flow of seawater, causing turbulent mixing between seawater and the export of surface freshwater (Bobbitt and Akenhead, 1982b). The mixing and cooling of marine and fresh water at the sill results in a bottom water salinity of about 28 in Lake Melville (Bobbitt and Akenhead, 1982b). The combination of upwelling at the Narrows (Lu et al., 2013) and inflowing freshwater runoff are thought to increase nutrients and productivity in this area, explaining an observed aggregation of feeding Common Minke Whales (*Balaenoptera acutorostrata*) from June to November (Chaulk et al., 2013).

Figure 1-2. Map of Hamilton Inlet including Inuit Lands Region, Labrador Inuit Settlement Area, and communities of Rigolet, Happy-Valley Goose Bay (HVGB), and Northwest River (A). Map displaying the location of Lake Melville (B).



From the Narrows, Lake Melville extends landward 130 km with a maximum depth of about 250 m. The basin features two large troughs, Grand and Mulligan that contain thick (> 400 m) deposits of unconsolidated marine sediment (Syvitski and Lee, 1997). A shallow (< 8 m), narrow passage known as Goose Bay Narrows, connects Lake Melville to Goose Bay, a western extension of the Lake. Collectively, Lake Melville and Goose Bay are referred to as the Lake Melville system (LMS).

The LMS captures ca. 45% of the total surface water runoff from the Labrador land mass (ca. $95 \text{ km}^3 \text{ yr}^{-1}$), which maintains a relatively fresh surface layer (10-20 m deep) across the LMS (Bobbitt and Akenhead, 1982b). The Churchill River, the largest river in Labrador with a mean discharge of ca. $1,700 \text{ m}^3 \text{ sec}^{-1}$ and drainage area of $92,500 \text{ km}^2$, is the dominant supply of freshwater. Since the early 1970s, the headwaters of the Churchill River have been regulated by the Churchill Falls hydroelectric generating station and Smallwood Reservoir. The flooding of the Smallwood Reservoir re-routed two rivers and flooded hundreds of kilometers of bog and muskeg, tripling the Churchill River's base flow in winter and decreasing flow by about 30% in summer (Bobbitt and Akenhead, 1982b). At the same time, the regulated flow has dampened short-term hydrological variation (Syvitski, 1987). Impacts from this hydroelectric development on the delivery of freshwater, sediment, terrestrial OM and other nutrients to the LMS have never been fully investigated.

At the time of this study, construction was just beginning on the Lower Churchill River hydroelectric project (LCRHP) at Muskrat Falls. Impoundment at Muskrat Falls and subsequent modification to the Churchill River's hydrology is expected to begin in 2016, when water will be held back to flood 41 km^2 of land and develop a reservoir behind Muskrat Falls. Although the Churchill River supplies ca. 60% of the total freshwater input to Lake Melville, the LCRHP's

downstream impact studies did not extend east of Goose Bay Narrows, making the implicit assumption that Lake Melville proper would not be impacted by the LCRHP (with the exception of mercury following flooding (Madden et al. 2014)). The development of the LCRHP and lack of environmental assessment of the downstream fjard has created concern around the future integrity of the ecosystem and Inuit ability to continue to use the fjard for harvesting country food, a central component of traditional Inuit culture and a necessity in the north where grocery costs are high.

1.5 Project overview and funding

This Master's Thesis was conducted as part of "Lake Melville: Avativut, Kanuittailinnivut (Our Environment, Our Health)" developed by the Nunatsiavut Government of Labrador and Memorial University of Newfoundland in collaboration with the University of Manitoba and funding from ArcticNet, a Network of Centres of Excellence in Canada. Lake Melville: Avativut, Kanuittailinnivut is the third phase of ArcticNet Nunatsiavut Nuluak, a project that works together with Inuit, centering on Inuit knowledge, to identify impacts of climate change and modernization on coastal ecosystems and Inuit communities of northern Labrador. The overall project objectives of Lake Melville: Avativut, Kanuittailinnivut are to:

- 1) establish baseline conditions of Inuit health and well-being and ecosystem integrity in Lake. Melville prior to hydroelectric development on the Lower Churchill River;
- 2) develop the science for monitoring any downstream effects of hydroelectric development in the context of ongoing climate change.

The research conducted for this Master's thesis contributes to the larger project by providing a high resolution examination of the modern sedimentary record and the cycling of particulates (sediment and carbon) in the LMS in the context of past and ongoing hydrologic and climate changes. The research presented here also provides a baseline from which changes to the system in the future can be assessed. Furthermore, this research provides support for other research by contributing to our understanding of various biogeochemical cycles (e.g., nutrients) and the cycling of contaminants such as total and methylmercury in the LMS. This research was funded by the Northern Scientific Training Program (NSTP) (to C.M. Kamula), and ArcticNet, the University of Manitoba, and the NSERC CERC program (Dr. Zou Zou Kuzyk).

1.6 Thesis objectives

In the context of hydrologic and climate changes, the objective for this Master's project was to use marine sediment together with other physical and chemical parameters and previously published data to investigate the rates of sedimentation and the quantity and composition of organic matter sourced, buried, and exported out of the LMS. This objective was accomplished by first using radionuclide and stable isotope methods to establish the fundamental processes taking place in the LMS and to document any changes recorded in the sediments (Chapter 2). Using this new understanding of the sediment and OC cycles in Goose Bay and Lake Melville, together with previously published data, budgets were developed to quantify the sources, sinks, and losses (Chapter 3). In quantifying these processes and fluxes, any changes to the delivery of sediment and OC to the LMS in the future can be measured. With the hydroelectric development of the Lower Churchill River expected to begin altering river runoff in 2016, the data presented in this

thesis is timely and will serve as an important baseline for the system while also providing predictions of changes to the system following impoundment at Muskrat Falls.

1.7 Thesis overview

This Master's thesis is organized into manuscript format and subdivided into four chapters. Chapter 1 provided the context for the following chapters by describing key concepts, the study area, rationale for this research, and the overall thesis objectives. Chapters 2 and 3 are presented as separate research papers and written so that findings in Chapter 3 are dependent and enhanced upon by findings in Chapter 2 and vice versa. Both Chapters 2 and 3 contain an abstract, introduction, objectives, methods, description of results, discussion of findings, and a conclusion. Chapter 4 summarizes conclusions from Chapter 2 and 3 and provides suggestions for future work.

1.8 References

- Alley, R. B., Clark, P. U., Huybrechts, P., and Joughin, I., 2005, Ice-sheet and sea-level changes: *Science*, v. 310, no. 5747, p. 456-460.
- Appleby, P., 2001, Chronostratigraphic techniques in recent sediments, *Tracking environmental change using lake sediments*, Springer, p. 171-203.
- , 2008, Three decades of dating recent sediments by fallout radionuclides: a review: *The Holocene*, v. 18, no. 1, p. 83-93.
- Appleby, P., and Oldfield, F., 1992, Applications of lead-210 to sedimentation studies, *Uranium-series disequilibrium: applications to earth, marine, and environmental sciences*. 2. ed.
- Appleby, P. G., and Oldfield, F., 1978, The calculation of lead-210 dates assuming a constant rate of supply of unsupported ^{210}Pb to the sediment: *CATENA*, v. 5, no. 1, p. 1-8.
- Blair, N. E., and Aller, R. C., 2012, The fate of terrestrial organic carbon in the marine environment: *Annual Review of Marine Science*, v. 4, p. 401-423.
- Bobbitt, J., and Akenhead, S., 1982, Influence of controlled discharge from the Churchill River on the oceanography of Groswater Bay, Labrador: Research and Resource Services, Department of Fisheries and Oceans.

- Bogen, J., and Bønsnes, T. E., 2001, The impact of a hydroelectric power plant on the sediment load in downstream water bodies, Svartisen, northern Norway: *Science of The Total Environment*, v. 266, no. 1–3, p. 273-280.
- Boyer-Villemare, U., St-Onge, G., Bernatchez, P., Lajeunesse, P., and Labrie, J., 2013, High-resolution multiproxy records of sedimentological changes induced by dams in the Sept-Îles area (Gulf of St. Lawrence, Canada): *Marine Geology*, v. 338, p. 17-29.
- Brown, T., Reimer, K., Sheldon, T., Bell, T., Luque, B. S., Fisk, A., and Iverson, S., 2012, . A first look at Nunatsiavut Kangidualuk (‘fjord’) ecosystems: Nunavik and Nunatsiavut: From Science to Policy an Integrated Regional Impact Study (IRIS) of Climate Change and Modernization. ArcticNet Inc., Quebec City, Quebec, Canada.
- Bruland, K. W., Koide, M., and Goldberg, E. D., 1974, The comparative marine geochemistries of lead 210 and radium 226: *Journal of Geophysical Research*, v. 79, no. 21, p. 3083-3086.
- Burdige, D. J., 2005, Burial of terrestrial organic matter in marine sediments: A re-assessment: *Global Biogeochemical Cycles*, v. 19, no. 4.
- , 2007, Preservation of organic matter in marine sediments: controls, mechanisms, and an imbalance in sediment organic carbon budgets?: *Chemical reviews*, v. 107, no. 2, p. 467-485.
- Carpenter, M., 2012, Benthic habitats of a sub-arctic fiord: the case study of Okak Bay, Labrador: Memorial University of Newfoundland (M.Sc. Thesis).
- Carpenter, R., Bennett, J., and Peterson, M., 1981, 210 Pb activities in and fluxes to sediments of the Washington continental slope and shelf: *Geochimica et Cosmochimica Acta*, v. 45, no. 7, p. 1155-1172.
- Chaulk, K. G., Michelin, D., Williams, M., and Wolfrey, T., 2013, Community-Based Observations of Marine Mammal Occurrences in Groswater Bay, Labrador: *The Canadian Field-Naturalist*, v. 127, no. 1, p. 31-37.
- Cochran, J. K., McKibbin-Vaughan, T., Dornblaser, M. M., Hirschberg, D., Livingston, H. D., and Buesseler, K. O., 1990, 210 Pb scavenging in the North Atlantic and North Pacific oceans: *Earth and Planetary Science Letters*, v. 97, no. 3, p. 332-352.
- Déry, S. J., Mlynowski, T. J., Hernández-Henríquez, M. A., and Straneo, F., 2011, Interannual variability and interdecadal trends in Hudson Bay streamflow: *Journal of Marine Systems*, v. 88, no. 3, p. 341-351.
- Déry, S. J., Stieglitz, M., McKenna, E. C., and Wood, E. F., 2005, Characteristics and trends of river discharge into Hudson, James, and Ungava Bays, 1964-2000: *Journal of Climate*, v. 18, no. 14, p. 2540-2557.
- Dittmar, T., and Kattner, G., 2003, The biogeochemistry of the river and shelf ecosystem of the Arctic Ocean: a review: *Marine Chemistry*, v. 83, no. 3–4, p. 103-120.
- Fairbridge, R. W., 1968, *The encyclopedia of geomorphology*, Reinhold New York.
- Fang, Z., Yang, W., Zhang, X., Chen, M., Fan, D., Ma, Q., Zhang, R., Zheng, M., and Qiu, Y., 2013, Sedimentation and lateral transport of 210Pb over the East China Sea Shelf: *Journal of Radioanalytical and Nuclear Chemistry*, v. 298, no. 2, p. 739-748.
- Finkl, C. W., 2004, Coastal classification: systematic approaches to consider in the development of a comprehensive scheme: *Journal of Coastal research*, p. 166-213.
- Finnis, J., and Bell, T., 2015, An analysis of recent observed climate trends and variability in Labrador: *The Canadian Geographer/Le Géographe canadien*.

- Friedl, G., and Wüest, A., 2002, Disrupting biogeochemical cycles-Consequences of damming: *Aquatic Sciences*, v. 64, no. 1, p. 55-65.
- Gattuso, J.-P., Frankignoulle, M., and Wollast, R., 1998, Carbon and carbonate metabolism in coastal aquatic ecosystems: *Annual Review of Ecology and Systematics*, v. 29, no. 1, p. 405-434.
- Goldberg, E. D., 1963, *Geochronology with 210Pb: Radioactive dating*, p. 121-131.
- Gong, G. C., Chang, J., Chiang, K. P., Hsiung, T. M., Hung, C. C., Duan, S. W., and Codispoti, L., 2006, Reduction of primary production and changing of nutrient ratio in the East China Sea: Effect of the Three Gorges Dam?: *Geophysical Research Letters*, v. 33, no. 7.
- Gupta, H., Kao, S.-J., and Dai, M., 2012, The role of mega dams in reducing sediment fluxes: A case study of large Asian rivers: *Journal of Hydrology*, v. 464, p. 447-458.
- Hare, A. A., Stern, G. A., Kuzyk, Z. Z. A., Macdonald, R. W., Johannessen, S. C., and Wang, F., 2010, Natural and Anthropogenic Mercury Distribution in Marine Sediments from Hudson Bay, Canada: *Environmental Science & Technology*, v. 44, no. 15, p. 5805-5811.
- He, Q., and Walling, D., 1996, Interpreting particle size effects in the adsorption of 137 Cs and unsupported 210 Pb by mineral soils and sediments: *Journal of environmental radioactivity*, v. 30, no. 2, p. 117-137.
- Humborg, C., Conley, D. J., Rahm, L., Wulff, F., Cociasu, A., and Ittekkot, V., 2000, Silicon Retention in River Basins: Far-Reaching Effects on Biogeochemistry and Aquatic Food Webs in Coastal Marine Environments: *Ambio*, v. 29, no. 1, p. 45-50.
- Hutchison-Benson, E., Svoboda, J., and Taylor, H., 1985, The latitudinal inventory of 137Cs in vegetation and topsoil in northern Canada, 1980: *Canadian Journal of Botany*, v. 63, no. 4, p. 784-791.
- Johannessen, S., Macdonald, R., and Paton, D., 2003, A sediment and organic carbon budget for the greater Strait of Georgia: *Estuarine, Coastal and Shelf Science*, v. 56, no. 3, p. 845-860.
- Johannessen, S. C., and Macdonald, R. W., 2012, There is no 1954 in that core! Interpreting sedimentation rates and contaminant trends in marine sediment cores: *Marine Pollution Bulletin*, v. 64, no. 4, p. 675-678.
- Jones, B. M., Arp, C., Jorgenson, M., Hinkel, K. M., Schmutz, J., and Flint, P., 2009, Increase in the rate and uniformity of coastline erosion in Arctic Alaska: *Geophysical Research Letters*, v. 36, no. 3.
- Klages, M., Boetius, A., Christensen, J., Deubel, H., Piepenburg, D., Schewe, I., and Soltwedel, T., 2004, The benthos of Arctic seas and its role for the organic carbon cycle at the seafloor, *The Organic carbon cycle in the Arctic Ocean*, Springer, p. 139-167.
- Koide, M., Bruland, K. W., and Goldberg, E. D., 1973, Th-228/Th-232 and Pb-210 geochronologies in marine and lake sediments: *Geochimica et Cosmochimica Acta*, v. 37, no. 5, p. 1171-1187.
- Koide, M., Soutar, A., and Goldberg, E. D., 1972, Marine geochronology with 210 Pb: *Earth and Planetary Science Letters*, v. 14, no. 3, p. 442-446.
- Krishnaswami, S., and Cochran, J. K., 2011, U-Th series nuclides in aquatic systems, Elsevier.
- Krishnaswamy, S., Lal, D., Martin, J., and Meybeck, M., 1971, Geochronology of lake sediments: *Earth and Planetary Science Letters*, v. 11, no. 1, p. 407-414.
- Kuzyk, Z. Z. A., Gobeil, C., and Macdonald, R. W., 2013, 210Pb and 137Cs in margin sediments of the Arctic Ocean: Controls on boundary scavenging: *Global Biogeochemical Cycles*, v. 27, no. 2, p. 422-439.

- Kuzyk, Z. Z. A., Macdonald, R. W., Johannessen, S. C., Gobeil, C., and Stern, G. A., 2009, Towards a sediment and organic carbon budget for Hudson Bay: *Marine Geology*, v. 264, no. 3, p. 190-208.
- Kuzyk, Z. Z. A., Macdonald, R. W., Johannessen, S. C., 2015, Calculating Rates and Dates and Interpreting Contaminant Profiles in Biomixed Sediments *Environmental contaminants: Using natural archives to track sources and long-term trends of pollution.* : Dordrecht, Springer, p. 547.
- Lantuit, H., Overduin, P. P., Couture, N., Wetterich, S., Aré, F., Atkinson, D., Brown, J., Cherkashov, G., Drozdov, D., and Forbes, D. L., 2012, The Arctic coastal dynamics database: A new classification scheme and statistics on Arctic permafrost coastlines: *Estuaries and Coasts*, v. 35, no. 2, p. 383-400.
- Lantuit, H., and Pollard, W., 2008, Fifty years of coastal erosion and retrogressive thaw slump activity on Herschel Island, southern Beaufort Sea, Yukon Territory, Canada: *Geomorphology*, v. 95, no. 1, p. 84-102.
- Lavelle, J. W., Massoth, G. J., Crecelius, E. A., 1985, Sedimentation rates in Puget Sound from ²¹⁰Pb measurements: National Oceanic and Atmospheric Administration.
- Libes, S., 2011, Introduction to marine biogeochemistry, Academic Press.
- Lu, Z., DeYoung, B., and Foley, J., 2013, Analysis of physical oceanography data from Lake Melville, Labrador, July-September 2012: Department of Physics and Physical Oceanography, Memorial University of Newfoundland.
- Lujanienė, G., Beneš, P., Štamberg, K., Jokšas, K., Vopalka, D., Radžiūtė, E., Šilobritienė, B., and Šapolaitė, J., 2010, Experimental study and modelling of ¹³⁷Cs sorption behaviour in the Baltic Sea and the Curonian Lagoon: *Journal of Radioanalytical and Nuclear Chemistry*, v. 286, no. 2, p. 361-366.
- Macdonald, R., Solomon, S., Cranston, R., Welch, H., Yunker, M., and Gobeil, C., 1998, A sediment and organic carbon budget for the Canadian Beaufort Shelf: *Marine Geology*, v. 144, no. 4, p. 255-273.
- Macdonald, R. W., Macdonald, D. M., O'Brien, M. C., and Gobeil, C., 1991, Accumulation of heavy metals (Pb, Zn, Cu, Cd), carbon and nitrogen in sediments from Strait of Georgia, B.C., Canada: *Marine Chemistry*, v. 34, no. 1-2, p. 109-135.
- Madden, P., Organ, M., and Power, R., 2014, LCP Aquatic Environment Effects Monitorin Plan.
- McClelland, J. W., Déry, S. J., Peterson, B. J., Holmes, R. M., and Wood, E. F., 2006, A pan-arctic evaluation of changes in river discharge during the latter half of the 20th century: *Geophysical Research Letters*, v. 33, no. 6.
- Middelburg, J. J., Soetaert, K., and Herman, P. M., 1997, Empirical relationships for use in global diagenetic models: *Deep Sea Research Part I: Oceanographic Research Papers*, v. 44, no. 2, p. 327-344.
- Monetti, M. A., 1996, Worldwide deposition of strontium-90 through 1990: USDOE Environmental Measurements Lab., New York, NY (United States). Funding organisation: USDOE, Washington, DC (United States).
- Moore, W. S., and Dymondt, J., 1988, Correlation of ²¹⁰Pb removal with organic carbon fluxes in the Pacific Ocean: *Nature*, v. 331, no. 6154, p. 339-341.
- Muller-Karger, F. E., Varela, R., Thunell, R., Luerssen, R., Hu, C., and Walsh, J. J., 2005, The importance of continental margins in the global carbon cycle: *Geophysical Research Letters*, v. 32, no. 1.

- Oguri, K., Harada, N., and Tadai, O., 2012, Excess ^{210}Pb and ^{137}Cs concentrations, mass accumulation rates, and sedimentary processes on the Bering Sea continental shelf: *Deep Sea Research Part II: Topical Studies in Oceanography*, v. 61, p. 193-204.
- Oughton, D. H., Børretzen, P., Salbu, B., and Tronstad, E., 1997, Mobilisation of ^{137}Cs and ^{90}Sr from sediments: potential sources to arctic waters: *Science of the total environment*, v. 202, no. 1–3, p. 155-165.
- Payette, S., Delwaide, A., Caccianiga, M., and Beauchemin, M., 2004, Accelerated thawing of subarctic peatland permafrost over the last 50 years: *Geophysical Research Letters*, v. 31, no. 18.
- Perillo, G. M., 1995, Definitions and geomorphologic classifications of estuaries: *Geomorphology and sedimentology of estuaries. Developments in Sedimentology*, v. 53, p. 17-47.
- Peterson, B. J., Holmes, R. M., McClelland, J. W., Vörösmarty, C. J., Lammers, R. B., Shiklomanov, A. I., Shiklomanov, I. A., and Rahmstorf, S., 2002, Increasing river discharge to the Arctic Ocean: *Science*, v. 298, no. 5601, p. 2171-2173.
- Power, M. E., Dietrich, W. E., and Finlay, J. C., 1996, Dams and downstream aquatic biodiversity: potential food web consequences of hydrologic and geomorphic change: *Environmental Management*, v. 20, no. 6, p. 887-895.
- Rachold, V., Grigoriev, M. N., Are, F. E., Solomon, S., Reimnitz, E., Kassens, H., and Antonow, M., 2000, Coastal erosion vs riverine sediment discharge in the Arctic Shelf seas: *International Journal of Earth Sciences*, v. 89, no. 3, p. 450-460.
- Robbins, J. A., and Edgington, D. N., 1975, Determination of recent sedimentation rates in Lake Michigan using Pb-210 and Cs-137 : *Geochimica et Cosmochimica Acta*, v. 39, no. 3, p. 285-304.
- Roberts, J., Pryse-Phillips, A., and Snelgrove, K., 2012, Modeling the Potential Impacts of Climate Change on a Small Watershed in Labrador, Canada: *Canadian Water Resources Journal / Revue canadienne des ressources hydriques*, v. 37, no. 3, p. 231-251.
- Schäfer, J., Blanc, G., Lapaquellerie, Y., Maillet, N., Maneux, E., and Etcheber, H., 2002, Ten-year observation of the Gironde tributary fluvial system: fluxes of suspended matter, particulate organic carbon and cadmium: *Marine Chemistry*, v. 79, no. 3, p. 229-242.
- Schlünz, B., and Schneider, R., 2000, Transport of terrestrial organic carbon to the oceans by rivers: re-estimating flux-and burial rates: *International Journal of Earth Sciences*, v. 88, no. 4, p. 599-606.
- Shimmield, G. B., Ritchie, G. D., and Fileman, T. W., 1995, The impact of marginal ice zone processes on the distribution of ^{210}Pb , ^{210}Po and ^{234}Th and implications for new production in the Bellingshausen Sea, Antarctica: *Deep Sea Research Part II: Topical Studies in Oceanography*, v. 42, no. 4, p. 1313-1335.
- Sholkovitz, E. R., Cochran, J. K., and Carey, A. E., 1983, Laboratory studies of the diagenesis and mobility of $^{239,240}\text{Pu}$ and ^{137}Cs in nearshore sediments: *Geochimica et Cosmochimica Acta*, v. 47, no. 8, p. 1369-1379.
- Smith, J. N., 2001, Why should we believe ^{210}Pb sediment geochronologies?: *Journal of Environmental Radioactivity*, v. 55, no. 2, p. 121-123.
- Smith, L. M., Alexander, C., and Jennings, A. E., 2002, Accumulation in East Greenland Fjords and on the Continental Shelves Adjacent to the Denmark Strait over the Last Century Based on ^{210}Pb Geochronology: *Arctic*, p. 109-122.

- Smith, R. W., Bianchi, T. S., Allison, M., Savage, C., and Galy, V., 2015, High rates of organic carbon burial in fjord sediments globally: *Nature Geoscience*.
- Staunton, S., and Roubaud, M., 1997, Adsorption of ¹³⁷Cs on montmorillonite and illite: Effect of charge compensating cation, ionic strength, concentration of Cs, K and fulvic acid: *Clays and clay minerals*, v. 45, no. 2, p. 251-260.
- Stein, R., 1991, Accumulation of organic carbon in marine sediments, Springer Berlin Heidelberg, Lecture Notes in Earth Science, 85 p.:
- Stein, R., Macdonald, R., Naidu, A., Yunker, M., Gobeil, C., Cooper, L., Grebmeier, J., Whitley, T., Hameedi, M., and Petrova, V., 2004, Organic carbon in Arctic Ocean sediments: sources, variability, burial, and paleoenvironmental significance, *The Organic Carbon Cycle in the Arctic Ocean*, Springer, p. 169-314.
- Suess, E., 1980, Particulate organic carbon flux in the oceans—surface: *Nature*, v. 288, p. 261.
- Sugai, S., 1990, Transport and sediment accumulation of ²¹⁰Pb and ¹³⁷Cs in two Southeast Alaskan fjords: *Estuaries*, v. 13, no. 4, p. 380-392.
- Syvitski, J., Burrell, D., and Skei, J., 1987, *Fjords: Processes and Products*, New York, NY, Springer-Verlag, 379 p.:
- Syvitski, J. P., and Lee, H. J., 1997, Postglacial sequence stratigraphy of Lake Melville, Labrador: *Marine Geology*, v. 143, no. 1, p. 55-79.
- Syvitski, J. P., Vörösmarty, C. J., Kettner, A. J., and Green, P., 2005, Impact of humans on the flux of terrestrial sediment to the global coastal ocean: *Science*, v. 308, no. 5720, p. 376-380.
- Turekian, K. Y., Nozaki, Y., and Benninger, L. K., 1977, Geochemistry of atmospheric radon and radon products: *Annual Review of Earth and Planetary Sciences*, v. 5, p. 227.
- Vonk, J., Sánchez-García, L., van Dongen, B., Alling, V., Kosmach, D., Charkin, A., Semiletov, I., Dudarev, O., Shakhova, N., and Roos, P., 2012, Activation of old carbon by erosion of coastal and subsea permafrost in Arctic Siberia: *Nature*, v. 489, no. 7414, p. 137-140.
- Vörösmarty, C. J., Meybeck, M., Fekete, B., Sharma, K., Green, P., and Syvitski, J. P., 2003, Anthropogenic sediment retention: major global impact from registered river impoundments: *Global and Planetary Change*, v. 39, no. 1, p. 169-190.
- Walling, D., and He, Q., 2000, The global distribution of bomb-derived ¹³⁷Cs reference inventories: Final report on IAEA technical contract, v. 10361, p. 1-19.
- Wassmann, P., 1997, Retention versus export food chains: processes controlling sinking loss from marine pelagic systems: *Hydrobiologia*, v. 363, no. 1-3, p. 29-57.
- Wassmann, P., Bauerfeind, E., Fortier, M., Fukuchi, M., Hargrave, B., Moran, B., Noji, T., Nöthig, E.-M., Olli, K., and Peinert, R., 2004, Particulate organic carbon flux to the Arctic Ocean sea floor, *The organic carbon cycle in the Arctic Ocean*, Springer, p. 101-138.
- Way, R. G., and Viau, A. E., 2014, Natural and forced air temperature variability in the Labrador region of Canada during the past century: *Theoretical and Applied Climatology*, p. 1-12.
- Wei, C.-L., Lin, S.-Y., Sheu, D.-D., Chou, W.-C., Yi, M.-C., Santschi, P., and Wen, L.-S., 2011, Particle-reactive radionuclides (²³⁴Th, ²¹⁰Pb, ²¹⁰Po) as tracers for the estimation of export production in the South China Sea: *Biogeosciences*, v. 8, no. 12, p. 3793-3808.
- Wright, S., Howard, B., Strand, P., Nylén, T., and Sickel, M., 1999, Prediction of ¹³⁷Cs deposition from atmospheric nuclear weapons tests within the Arctic: *Environmental Pollution*, v. 104, no. 1, p. 131-1

Chapter 2 : Patterns and Sources of Sediment and Particulate Organic Carbon in Lake Melville, Labrador, Canada: Inferences from ^{210}Pb , ^{137}Cs , and $\delta^{13}\text{C}$

2.1 Abstract

Modern sedimentological processes, sources and distribution of sediment and organic carbon (OC) were investigated in recently deposited sediment from Lake Melville, Labrador to better understand the impacts of anthropogenic and climatic changes to the system over the last 100-150 years. Fifteen sediment cores collected across Lake Melville in 2013 and 2014 were analysed for ^{210}Pb and ^{137}Cs while stable isotope $\delta^{13}\text{C}_{\text{org}}$ and percentage OC were measured down select cores and surface sediment. Mass accumulation rates (MAR) were established by fitting $^{210}\text{Pb}_{\text{ex}}$ profiles to a two-layer advection diffusion model and validated with ^{137}Cs . MARs varied between 0.04 to 0.41 $\text{g cm}^{-2} \text{yr}^{-1}$, respectively. In general, MARs decreased with distance from the Churchill River, the greatest source of sediment to the system. In the west end of the Lake, near the outflow of the Kenamu River, MARs are greatest, reflecting the combined contributions of fine material carried eastward in the Churchill River plume and coarser particles from the Kenamu River. Comparing inventories of ^{137}Cs and excess ^{210}Pb ($^{210}\text{Pb}_{\text{ex}}$) to expected atmospheric inputs, suggest sediment in Lake Melville is largely sourced from the watershed. In the eastern end of Lake Melville, an elevated $^{210}\text{Pb}_{\text{ex}}$ inventory was associated with particle scavenging of dissolved ^{210}Pb from inflowing marine water and is likely linked to increased primary production in the area. Surface sediment $\delta^{13}\text{C}_{\text{org}}$ (mean = -26.2 ± 1.75 ‰) support a mixture of both terrestrial and marine organic carbon to the system. Using a transient tracer mixing model, the depth in each core corresponding to 90% sediment deposited pre and post

hydroelectric development at Churchill Falls (1970) was established and applied to profiles of $\delta^{13}\text{C}_{\text{org}}$. This approach revealed a significant increase of terrestrial OC to Lake Melville post 1970 which we interpret to reflect both change in climate and hydrology of the Churchill River.

2.2 Introduction

Coastal environments are considered the interface between land and the ocean and are often areas with high sedimentation rates, making them significant regions for the burial of organic carbon (OC) and thus, major sinks in the global carbon cycle (cf., Muller-Karger et al., 2005; Smith and Hollibaugh, 1993). Over the last century, increasing hydrological and climatic changes have resulted in shifts to the seasonality and magnitude of freshwater discharge to coastal environments (Déry et al., 2011; Déry and Wood, 2005; Lammers et al., 2001; Peterson et al., 2002; Vörösmarty et al., 2000). Consequently, the delivery of sediment and organic matter from riverine runoff to these environments has been altered in many regions of the world (Syvitski et al., 2005; Vörösmarty et al., 2003). Additionally, because of rising sea levels (Alley et al., 2005), loss of sea ice (Jones et al., 2009), and thawing permafrost (Lantuit and Pollard, 2008; Payette et al., 2004) in Arctic and sub-arctic regions, rates of coastal erosion have amplified the delivery of sediment and terrestrial organic carbon (OC) to coastal and marine environments (Rachold et al., 2000).

Northern fjords and fjards are particularly sensitive to changes in the delivery of sediment and OC because they are strongly linked to the surrounding land and the terrestrial environment through river runoff. Fjords and Fjards often have shallow sills at their mouth that restrict the circulation of water and transport of particulates to and from the adjacent marine continental shelf (Bentley et al., 2012; Syvitski, 1987). Consequently, fjords and fjards are considered major

repositories for sediment and OC (Smith et al., 2015). In these accumulating sediments, records of the environment from which the sediment and OC were sourced and deposited can be found. These records can be used to gain insight into change over the last century and a half, representing the period of greatest human influence to the environment (Gilbert, 2000). Moreover, provided that baseline data of the rates and mechanisms of sedimentation and sources and distribution of sediment and OC deposition have been obtained, sediment records can be used to quantify changes to these systems in the future as they undergo climate or hydrological change (Boyer-Villemaire et al., 2013).

In this study, we established sedimentation velocity and mass accumulation rates (MAR) based on ^{210}Pb (Appleby and Oldfield, 1992; Koide et al., 1972) and validated with a transient tracer, ^{137}Cs (Smith, 2001) from 15 box cores collected at various depths across Lake Melville, a fjard estuary in Labrador, Canada. Previous work on sediments and sedimentary OC in Lake Melville was conducted with a view to paleoenvironmental reconstructions through the Holocene (cf., Syvitski, 1993; Tan and Vilks, 1987), while few studies have focused on the more contemporary oceanography of the system (Bobbitt and Akenhead, 1982a; Coachman, 1953; Prinsenberg et al., 2011). We used the MARs developed here together with surficial and selected subsurface measurements of OC and $\delta^{13}\text{C}_{\text{org}}$ to evaluate the sources, distribution and accumulation rates of sediment and OC for the more contemporary (ca. 100 y BP) Lake Melville system. This investigation is timely because of the planned hydroelectric development of the Lower Churchill River, which is expected to begin altering river flow by 2016. The Churchill River, a major source of freshwater to the Lake Melville system, underwent hydroelectric development in its upper reaches in the 1970s, with largely unknown impacts on the downstream environment of Lake Melville. This study is one component of a larger interdisciplinary research

and monitoring program, Lake Melville: *Avativut, Kanuittailinnivut* (Our Environment, Our Health).

The specific objectives of this study presented here are to determine and evaluate the following:

- i) modern-day sedimentological processes within Lake Melville through the development and comparison of ^{210}Pb -based MARs, validated with ^{137}Cs ;
- ii) sources (i.e., terrigenous or marine) of OC reaching the sea floor; and
- iii) changes to sedimentary processes and delivery OC to the system over the last ca.100 years.

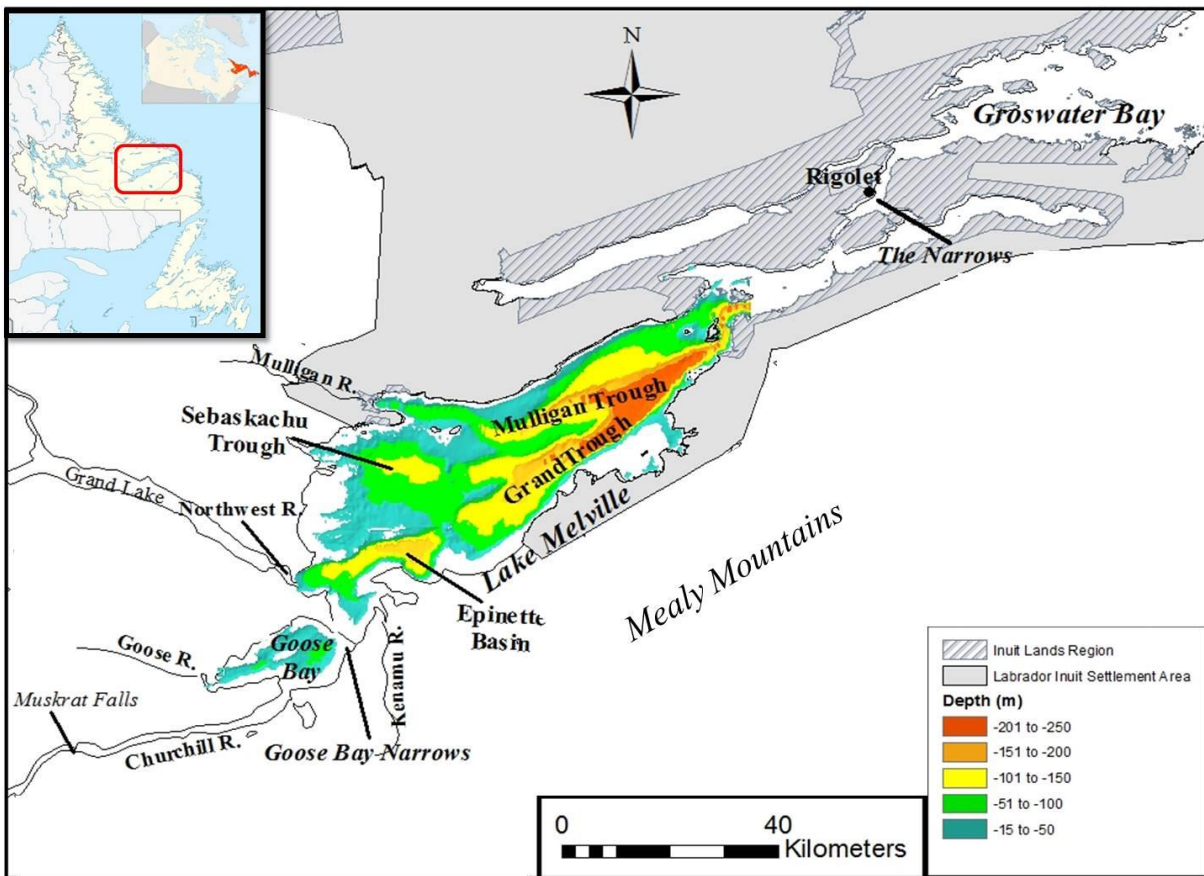
2.3 Study area

2.3.1 Overview

Lake Melville is a subarctic fjard estuary located within the boreal forest ecoregion of central Labrador, Canada ($53^{\circ}33'N$ and $59^{\circ}35'W$) (Roberts et al., 2006) (Figure 2-1). Lake Melville is part of the largest inlet on the Labrador coast (Hamilton Inlet), which extends landward 250 km from the coastline (Coachman, 1953; Syvitski and Lee, 1997). Hamilton Inlet comprises three connected water bodies including Groswater Bay, Lake Melville and Goose Bay (Figure 2-1). Groswater Bay extends from the Labrador Sea ca.50 km landward where it tapers into a 22 km long, narrow and shallow channel known as the Narrows. A sill located in the Narrows, south of the community of Rigolet, decreases water depth to 30 m and channel width to 2.8 km. Lake Melville extends ca.130 km from the Narrows westward to the mouth of Goose Bay, covering an area of $2,100 \text{ km}^2$ (Syvitski and Lee, 1997). The Lake is widest at 35 km in the

southwest end and deepest (ca. 250 m) in the southeast end of the basin. Goose Bay is a 25 km western extension of Lake Melville connected by a 2.5 km wide and 6 m deep shipping channel known as the Goose Bay Narrows. The water body extending eastward from these Goose Bay Narrows to the Narrows connecting Lake Melville to Groswater Bay is referred to hereafter as Lake Melville proper. Collectively Goose Bay and Lake Melville are referred to as the Lake Melville System (LMS).

Figure 2-1. Map of Hamilton Inlet including Groswater Bay, Lake Melville and Goose Bay, as well as major inflowing rivers (Churchill, Goose, Northwest, and Kenamu).



The Hamilton Inlet region is characterized by cold winters and short summers with mean annual precipitation ca.900-1000 mm (Macpherson and Macpherson, 1981). By late November,

saline land fast ice begins to form over Lake Melville with complete freeze up occurring by mid-December. Ice breakup usually takes place in late April to May while open water is generally present in the Narrows and Groswater Bay (ca. 50 km offshore) year round because of strong tidal currents (Prinsenberget al., 2011).

2.3.2 Geological Setting

Lake Melville lies within the Canadian Shield in the Grenville Province where flat lowlands dominate the landscape, apart from the Mealy Mountain plateaux, which border the southern shoreline of the Lake (Greene, 1974; Syvitski and Lee, 1997). Surficial geology in the region varies from very thick, well sorted fluvial and marine deposits of sand and clay in the west and northwest shorelines to basal till deposits (< 1 m thick) with minor components of colluvium and boulders along the southeastern shorelines (Fulton, 1981; Liverman, 1997). Fine grained marine deposits are found along the shores of Mulligan Bay, Eppinett Point and in the Churchill Valley near Muskrat Falls (Liverman, 1997).

Marine clay deposits in the western end of the Lake point to relative sea level decline of ca. 110-120 m since the retreat of the Laurentide Ice Sheet ca. 9000 y BP (Fitzhugh, 1973; Vilks et al., 1987). Sella et al. (2007) estimated a more contemporary isostatic uplift rate of approximately 1-2 mm yr⁻¹ within the Goose Bay area, corresponding to similar estimations by Henton et al. (2006).

During the late Wisconsinan period, the Laurentide ice sheet moved over Lake Melville, scouring and deepening the basin (Kindle, 1924; Syvitski and Lee, 1997). Lake Melville is thought of as an important calving ground during deglaciation (10 000 – 9000 BP), which resulted in thick deposits of glaciomarine sediments in the southeastern end of the basin (ca. >400 m of unconsolidated sediment (Syvitski and Lee, 1997)).

Today Lake Melville features two large troughs, Grand (maximum depth ca.250 m) and Mulligan, both ca. 4-5 km wide, and one smaller trough, Sebaskachu (Syvitski and Lee, 1997) (see Figure 1). Grand Trough is the largest of the three and runs parallel (east to west) to the southern shoreline. Mulligan Trough extends from Mulligan Bay on the northern shore and converges with Grand Trough in the eastern end of the basin. The LMS also hosts a number of basins in the west, including Sebaskachu (see Figure 2-1) that are separated by a sequence of shallow shoals, in some cases less than 10 m deep (Canadian Hydrologic Service, chart #5143). Syvitski (1990) describes a submarine channel ca.700 m wide and 6 km long that begins ca. 200 m off the Kenamu River delta and extends to ca. 85 m water depth where it meets up with Epinette Basin (also referred to as Kenamu Basin). The basin is about 160 m deep and ca. 5-9 km wide (Syvitski, 1990).

2.3.3 Hydrology and oceanography

Lake Melville is made up of a stratified water column with two distinct water masses: a brackish surface layer (top 10-20 m) from river runoff flowing seaward atop a saline bottom layer flowing landward from Groswater Bay (Cardoso and deYoung, 2002). On a yearly average Lake Melville receives ca. $3000 \text{ m}^3 \text{ s}^{-1}$ ($85 \text{ km}^3 \text{ yr}^{-1}$) of freshwater from four major rivers: Churchill, Goose, Kenamu, and Northwest (Bobbitt and Akenhead, 1982). Of these, the Churchill and Goose Rivers discharge into Goose Bay while the latter two rivers discharge directly into the western end of Lake Melville. The Churchill River is by far the largest with a watershed area and mean annual discharge of $92,500 \text{ km}^2$ and $1,700 \text{ m}^3 \text{ s}^{-1}$, respectively. Since 1972 the headwaters of the Churchill River have been controlled by the Churchill Falls hydroelectric generating station and Smallwood Reservoir (Bobbitt and Akenhead, 1982). The other three major rivers discharging into Lake Melville currently are not affected by reservoir

development, except perhaps Northwest River, which connects the large, deep Grand Lake to Lake Melville. To increase water capacity of the Smallwood reservoir, the Naskapi River, which originally drained into Grand Lake, was re-routed to the Reservoir. Impacts on Grand Lake and Lake Melville from the re-routing of the Naskapi River are not known.

Inflow of deep, cold saline water from Groswater Bay to Lake Melville is restricted within the Narrows by a shallow sill that reduces water depth to 30 m. At the same time, the Narrows facilitates turbulent mixing of the two water masses (Bobbitt and Akenhead, 1982). During spring, summer and winter, a strong density gradient (halocline), 5-20 m deep, limits entrainment of saline bottom water to the surface layer where salinities are typically <10, while bottom water salinities vary from about 20 to 28 (Cardoso and deYoung, 2002; Prinsenberg et al., 2011). In October, surface mixing and cooling temperatures increase surface water density, breaking down the halocline and allowing for mixing between the two water masses. This late fall-early winter mixing is recorded in the salinity of sea ice across Lake Melville (cf., Prinsenberg et al., 2011). Additionally, deep water exchange occurs during fall and early winter months, bringing with it oxygen to the deeper waters (Bobbitt and Akenhead, 1982). There are no reports of anoxic bottom waters having been found in Lake Melville.

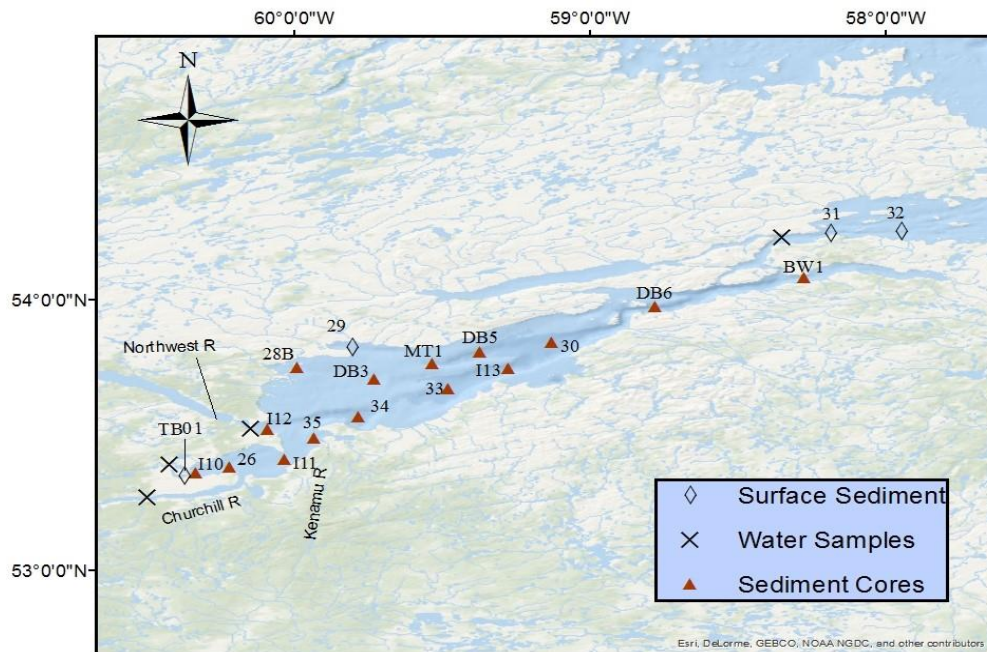
2.4 Methods

2.4.1 Sample collection

Box cores were collected 10-17 June 2013 and 17-22 October 2014 aboard *R/V Nuliajuk* and *M/V What's Happening*, respectively. Sediment core sites (Figure 2-2) were selected on the basis of Canadian Hydrographical Service nautical charts (4724, 4728, 5140, and 5143), multibeam bathymetric data collected and processed by the Ocean Mapping Group at the

University of New Brunswick in 2012 and 2013, and previously published literature, to obtain the best representation of the system. Areas of interest for sediment core collection included the deepest areas (>100 m) of the basins, where minimal mixing of deposited sediment was expected and near river mouths. Sediment cores were collected using two box corers; one supplied by the Nunatsiavut Government and used primarily in 2013 and one supplied by the University of Manitoba and used in 2013 and 2014. Successful retrieval of intact sediment was determined visually. If sediment appeared slumped, it was discarded and the box core was re-deployed. Upon successful collection of a box core, excess overlying water was siphoned off with care to ensure minimal disturbance to the sediment. A 10 cm diameter core tube was used to subsample the box core by pressing a tube slowly into the sediment ≥ 5 cm from the box edge and subsequently capping both ends. Within 12 hours, sediment cores were extruded and sectioned into 1 cm intervals, placed in whirl packs, homogenised by hand, and frozen (-20°C).

Figure 2-2. Locations where sediment cores and water samples were collected in 2013 and 2014.



Suspended particulate matter (SPM) was collected from the Churchill, Goose, and Northwest Rivers in June 2013 and October 2014 for the purpose of $\delta^{13}\text{C}_{\text{org}}$ analysis (Figure 2-2). From the shore, we pumped surface water (top ca. 0.25-0.5 m), using a submersible pump, for 0.5 to 1 hour. River water was pumped through a Teflon-lined hose that was connected to a stainless steel filter holder where solids were collected on pre-combusted Whatman® GF/F glass fiber filters (nominal pore size, 0.7 μm).

2.4.2 Radiochemical analysis

To estimate sedimentation rates, the activities of the radioisotopes ^{210}Pb and ^{137}Cs were counted in sediment core sections at the Environmental Radiochemistry Laboratory (ERL) at University of Manitoba. ^{210}Pb (half-life 22.3 years) is a naturally occurring radioisotope produced within the decay series of ^{238}U (Koide et al., 1973). ^{238}U is contained in minerals (i.e., rock and soil) and, through *in situ* decay, gives rise to ‘supported’ ^{210}Pb activities in soils and sediments. Unsupported or excess ^{210}Pb ($^{210}\text{Pb}_{\text{ex}}$) in soils or sediments originates from the decay of ^{222}Rn (half-life 3.8 days) in the atmosphere and from the *in situ* decay of dissolved ^{226}Ra within the water column (Cochran et al., 1990; Kuzyk, 2015). $^{210}\text{Pb}_{\text{ex}}$ is readily deposited by dry or wet fallout to the earth’s surface where it becomes linked to sedimentary processes (Appleby and Oldfield, 1978). Within the water column, $^{210}\text{Pb}_{\text{ex}}$ is rapidly scavenged by sediment particles. In each of our sediment sections, $^{210}\text{Pb}_{\text{ex}}$ was calculated by subtracting supported ^{210}Pb (estimated from the ^{226}Ra activity in the same section) from total ^{210}Pb . $^{210}\text{Pb}_{\text{ex}}$ was then date corrected to the time of sampling. Radioisotope ^{137}Cs (half-life 30.7 years), a product of nuclear fission, is widely used and recommended as a transient tracer for validating ^{210}Pb -derived sedimentation rates (cf., Smith et al., 2001). The release of ^{137}Cs into the environment occurred

primarily from 1952 to 1962 from nuclear weapons testing; atmospheric deposition peaked ca. 1963 (Wright et al., 1999).

Prior to analysis of radioisotopes, sediment samples were thawed, re-homogenised by hand, sub-sampled, refrozen, and freeze dried at -55°C for approximately 3-4 days at the Centre for Earth Observation Science (CEOS) and at the Freshwater Institute in Winnipeg, Manitoba. Wet and dry weights were recorded for each sub-sample. Weight lost on drying was used to calculate porosity and correct for salt according to bottom water conditions at the time of sampling (cf., Appendix I of Lavelle, 1985). Freeze dried samples were then ground using a pestle and mortar and sealed within 50 x 9 mm Petri dishes for ≥ 20 days to prevent the escape of ^{222}Rn and allow secular equilibrium between supported ^{210}Pb and ^{226}Ra (Murray et al., 1987).

Weighed and sealed samples were measured for total ^{210}Pb and ^{137}Cs by counting gamma emissions at 46.5 and 661 keV, respectively. Activities of ^{226}Ra were estimated by counting its granddaughter isotope, ^{214}Pb , at 352keV. Activities were counted for 24-48 hours on a CANBERRA® Broad Energy Germanium (BEGe) P-type detector (model BE3830). Known energy peaks were analysed with Genie 2000® software. Detector efficiency and self-absorption were corrected by counting reference material distributed by the International Atomic Energy Agency (IAEA) within the same geometry (i.e. petri dish). The reproducibility errors, determined by counting the same sample four times, were 5.7, 8.8, and 3.8%, for ^{210}Pb , ^{137}Cs , and ^{226}Ra , respectively.

Alpha counting methods (hereafter referred to as alpha) for ^{210}Pb were used much more commonly in the past (Zaborska et al., 2007) but are still generally regarded as superior to gamma methods because of their very low detection limits (ca.0.0004 Bq) (Robbins, 1978). To assess the appropriateness of counting total ^{210}Pb directly by gamma emission in Lake Melville

sediment samples, four sediment cores (26, I13, DB3, MT1) were subjected to the alpha technique. In this method, ^{210}Pb is measured indirectly via its ^{210}Po daughter (half-life 138 days). Samples were prepared by chemically separating ^{210}Po from 0.5 to 1.2 g of sample using 30 mL of 6N HCl on a hot plate (180°C for 5 hours). Since the activity of ^{210}Po is based on chemical separation during the digestion stage, 200 μL ^{209}Po tracer was added and used to compare the activity of measured ^{210}Po with that of known absolute activities of the tracer (Zaborska et al., 2007). After cooling, the clear liquid (digest) was decanted into 50 mL deionized water and 5 mL 10% ascorbic acid. A 25 mm silver disk was dropped into this solution. The beaker of solution and silver disk were placed on a hot plate at 80°C overnight to allow spontaneous deposition of ^{210}Po onto the disk (Flynn, 1968). The disk was removed from the solution, rinsed with deionized water, allowed to air dry, and subsequently counted for ^{210}Po and ^{209}Po over a period of 6 days using an alpha spectrometer. The tracer was calibrated against a ^{210}Po standard solution that is NIST traceable (Isotope Product Laboratories, product # 6310, Source No.: 1130-1). The reproducibility error, determined by counting the same sample four times, was less than 1%.

2.4.3 Calculation of sedimentation and mass accumulation rates

Sediment velocities were estimated by least-squares fitting the natural log of $^{210}\text{Pb}_{\text{ex}}$ profiles to outputs of a one dimensional two-layer advection diffusion model that accounts for both biomixing and compaction with depth (Eq. 1) (Kuzyk, 2015; Lavelle, 1985; Robbins, 1978):

$$\omega_s(\delta C/\delta z) - (\delta/\delta z)*K_b(\delta C/\delta z) = -\lambda C \quad \text{Eq. 1}$$

where ω_s is the constant sediment velocity (cm yr^{-1}), C is the $^{210}\text{Pb}_{\text{ex}}$ activity (dpm cm^{-3}), z is depth (positive downward in cm), K_b is the diffusion coefficient or mixing rate ($\text{cm}^2 \text{yr}^{-1}$), and λ

is the radioisotope decay constant (0.03114 yr^{-1}). The sediment profile is treated as a two layer system with a surface mixed layer (SML) influenced by bioturbation (K_{b1}) overlaying a deeper sediments layer with minimal mixing ($K_{b2} = 0.01 \text{ cm}^2 \text{ yr}^{-1}$). The SML depths were assigned visually by choosing inflection points down the core profiles where $^{210}\text{Pb}_{\text{ex}}$ activity transitioned from a homogenized profile near the surface to an observed exponential decrease with depth (Bentley et al., 2012; Kuzyk et al., 2009; Lavelle, 1985). Assuming constant rate of supply, sediment velocities (Eq 2) were calculated by manually adjusting values of K_{b1} , C_0 (surface activity, dpm cm^{-3}) and slope (m) of $\ln ^{210}\text{Pb}_{\text{ex}}$ below the SML according to equations outlined by Lavelle (1985):

$$\omega_s = -\lambda / m \quad \text{Eq. 2}$$

From ω_s , the mass accumulation rate (MAR, $\text{g cm}^{-2} \text{ yr}^{-1}$) was calculated as follows:

$$\text{MAR} = \rho_s (1-\Phi) * \omega_s \quad \text{Eq. 3}$$

where ρ_s is the dry sediment density (estimated at 2.65 g cm^3 , the density of quartz and commonly applied to marine sediment (Berner, 1971) and $1-\Phi$ is the volume fraction of sediment particles (Burdige, 2006).

MARs were validated by applying a numerical advection-diffusion model to corresponding ^{137}Cs (dpm g^{-1}) activities using parameters (ω_s , SML, K_{b1} , and C_0) derived from $^{210}\text{Pb}_{\text{ex}}$ profiles. On the basis of historical ^{137}Cs fallout an input function was developed and compared to measured values of ^{137}Cs (cf., Kuzyk et al., 2013). Following similar temporal variations of ^{137}Cs atmospheric fallout outlined by Monetti (1996) and Wright et al. (1999), the input function for ^{137}Cs included zero activity for 3 years (1951-1954) followed by a constant pulse of 8.2 dpm g^{-1} of ^{137}Cs for 9 years (1954-1963) and a reduction to 1.2 dpm g^{-1} for 35 years

(1963-1998). To account for plausible delayed inputs from drainage basins (Walling and Qingping, 1992), post depositional remobilization (i.e. bioturbation and molecular diffusion (Robbins and Edgington, 1975)) and/or sediment focusing and resuspension of deposited sediment (Crusius and Anderson, 1995), the input function was held constant towards the surface of the cores at 0.2 dpm g^{-1} for 15 years (1998-2013). The model was run using MATLAB® software and accounted for loss of ^{137}Cs through radio-decay (0.0231 yr^{-1}). The best fit between simulated and measured profiles was determined visually by comparing the onset, depth of penetration, and peak location of ^{137}Cs (cf., Johannessen et al., 2003; Kuzyk et al., 2013; Kuzyk, 2015). Sediment velocities were adjusted, within 95% confidence limits, to give the best fit for both $^{210}\text{Pb}_{\text{ex}}$ and ^{137}Cs . Adjustments were applied to all cores apart from cores 33, DB6, and 30 because parameters were in good agreement for both $^{210}\text{Pb}_{\text{ex}}$ and ^{137}Cs profiles. Due to homogenized ^{137}Cs profiles, validation of $^{210}\text{Pb}_{\text{ex}}$ derived sedimentation rates was not possible for cores I10, 26, I11 and 35.

2.4.4 $^{210}\text{Pb}_{\text{ex}}$ and ^{137}Cs inventories

Inventories (Eq. 4) of $^{210}\text{Pb}_{\text{ex}}$ and ^{137}Cs were calculated by summing the mass-depth activities (C_i , dpm g^{-1}) down-core until activity was no longer detected (Kuzyk et al., 2009):

$$I = \sum C_i m_i \quad \text{Eq. 4}$$

where C_i (dpm g^{-1}) is activity at depth and m_i is the mass-depth increment (g cm^{-2}) corresponding to the depth interval. Mass-depth was calculated as:

$$\text{Mass-Depth} = \rho_s * (1 - \Phi) * \Delta_z \quad \text{Eq. 5}$$

where Δ_z is the thickness of sediment core interval (cm).

Inventories within 30% of estimated surface fluxes ($\text{dpm cm}^{-2} \text{ yr}^{-1}$, Eq 6) were used to check sediment velocities and MARs.

$$\text{Surface Flux} = \omega_s * C_0 \quad \text{Eq. 6}$$

Since $^{210}\text{Pb}_{\text{ex}}$ is a steady-state tracer, the $^{210}\text{Pb}_{\text{ex}}$ activity profile of core 26 was extrapolated to reach background levels. This resulted in a 3.5% increase in its inventory from 20.8 to 21.6 dpm cm^{-2} . Whereas core 26 showed exponential decay in the bottom three slices, core I11 was completely homogenized and extrapolating $^{210}\text{Pb}_{\text{ex}}$ activity to background levels was not possible. Since ^{137}Cs is a time-dependant tracer it was impossible to extrapolate to background levels for both cores I11 and 26. Because of these mixed ^{137}Cs profiles, cores I11 and I12 are not included in our comparison of ^{137}Cs inventories.

Since our study region is relatively small, it is reasonable to assume that the expected inventories from direct $^{210}\text{Pb}_{\text{ex}}$ and ^{137}Cs atmospheric fallout would be uniform (within expected uncertainty) across the LMS. The inventory from atmospheric ^{210}Pb was estimated as 23.6 dpm cm^{-2} across the LMS. This was calculated by dividing the expected atmospheric flux of 0.732 $\text{dpm cm}^{-2} \text{ y}^{-1}$, established by Appleby and Oldfield (1992) from direct measurements of $^{210}\text{Pb}_{\text{ex}}$ in rainfall across eastern North America, by the decay rate of ^{210}Pb , 0.03114 y^{-1} .

The expected ^{137}Cs inventory (ca.1.5 dpm cm^{-2} for 2013 and 2014) from direct atmospheric fallout was estimated using a numerical model developed by Walling and He (2000). This model was established using direct measurements of bomb-derived ^{90}Sr fallout from across the globe and employing the known fission ratio of 1.60 between ^{90}Sr and ^{137}Cs . Included in the model was latitude, longitude, and because ^{137}Cs fallout is associated with precipitation,

the mean yearly precipitation obtained from Environment Canada records (1105.2 mm from 1952 to 2013) for Lake Melville was included.

2.4.5 Organic carbon and $\delta^{13}\text{C}_{\text{org}}$ measurements

Total organic carbon (TOC) content and $\delta^{13}\text{C}_{\text{org}}$ were measured on surface sediment (ca. 0-1 cm) and down ten cores, at the University of Manitoba's Stable Isotope for Innovative Research Laboratory (SIFIR). TOC was derived from the difference between total carbon (TC) and carbonate carbon (inorganic carbon, IC). Both TC and IC were measured from pre-weighed dried sediment subsamples. TC was measured by combusting the subsample at ca. 1400°C and analysing using an elemental analyser. IC was measured by removing inorganic carbon (decarbonation) from the subsample with 20% HCl and immediately analysing the gas released from the sample using a CO₂ coulometer. Replicate analysis of QC standards B2150 (TC) and AR1034 (IC) indicate a propagated precision for OC of $\pm 0.1\%$.

Organic carbon isotope composition (‰ relative to VPDB) was measured by an elemental analyser isotope-ratio mass spectrometer (EA-IRMS) at SIFIR. Prior to analysis, dried samples were decarbonated with 6M HCl and re-dried in an oven for about three days. To ensure quality of sample (decarbonation) and analysis performance, an international standard, USGS Green River shale SGR-1b, was treated and analysed along with samples. Replicate samples of SGR-1b (n=21) yielded a precision of $\pm 0.1\%$.

2.4.6 Calculation of the percentage of terrestrial and marine organic carbon

The percentage of terrigenous OC and, by difference, marine OC were calculated for each core and surface sediment by applying a simple two-endmember mixing model along with corresponding $\delta^{13}\text{C}_{\text{org}}$ values as outlined in (Stein and Macdonald, 2004a):

$$OC_{terr}(\%) = (\delta^{13}C_{sample} - \delta^{13}C_{mar}) / (\delta^{13}C_{terr} - \delta^{13}C_{mar}) \times 100\% \quad \text{Eq. 8}$$

where $\delta^{13}C_{sample}$ is the measured $\delta^{13}C_{org}$ (‰) of the sediment sample and $\delta^{13}C_{mar}$ and $\delta^{13}C_{terr}$ are the marine and terrestrial end-members, estimated at -21.3 ± 0.32 ‰ (n=5) and -31.2 ± 1.66 ‰ (n=6) (mean $\pm 1\sigma$, relative to VPDB), respectively. The terrestrial end-member was established from the analyses of $\delta^{13}C_{org}$ in SPM filtered from the Churchill, Northwest, and Goose Rivers. -31.2 ± 1.66 ‰ represents the discharge-weighted mean from all three rivers, including both spring (June) and autumn (October) data. Because of mixing between fresh and marine water in the Narrows, the marine end-member was more difficult to establish. We used the mean and standard deviation of previously published data of $\delta^{13}C$ signatures from surficial sediment in Groswater Bay reported by Tan and Vilks (1987). Similar signatures were also reported by Muzuka and Hillaire-Marcel (1999) for surficial sediment just east of Groswater Bay.

3.4.7 Modelling of organic carbon

The occurrence of a SML in each core indicates mixing between newly deposited sediment and sediment deposited at a previous time. As such, it is impossible to assign specific ages to sediment core slices (Johannessen and Macdonald, 2012; Kuzyk, 2015). Following Bailey et al. (2013), we applied a transient tracer method developed by Johannessen et al. (2005) to core profiles and estimated the region of the core that was deposited before and after the development of the Smallwood Reservoir and Churchill Falls generating station (pre- and post-1970). The sections of each core that represents $\geq 90\%$ of sediment deposited pre- and post-1970 was modelled in MATLAB® using the numerical model outlined by Johannessen et al. (2005). This model included SML depth, mixing coefficient (Kb_1), and sediment velocities established from modeling $^{210}Pb_{ex}$. The transient tracer was turned on in 1970 and allowed to run until date of collection (2013 and 2014) without any correction for decay. The tracer concentration within

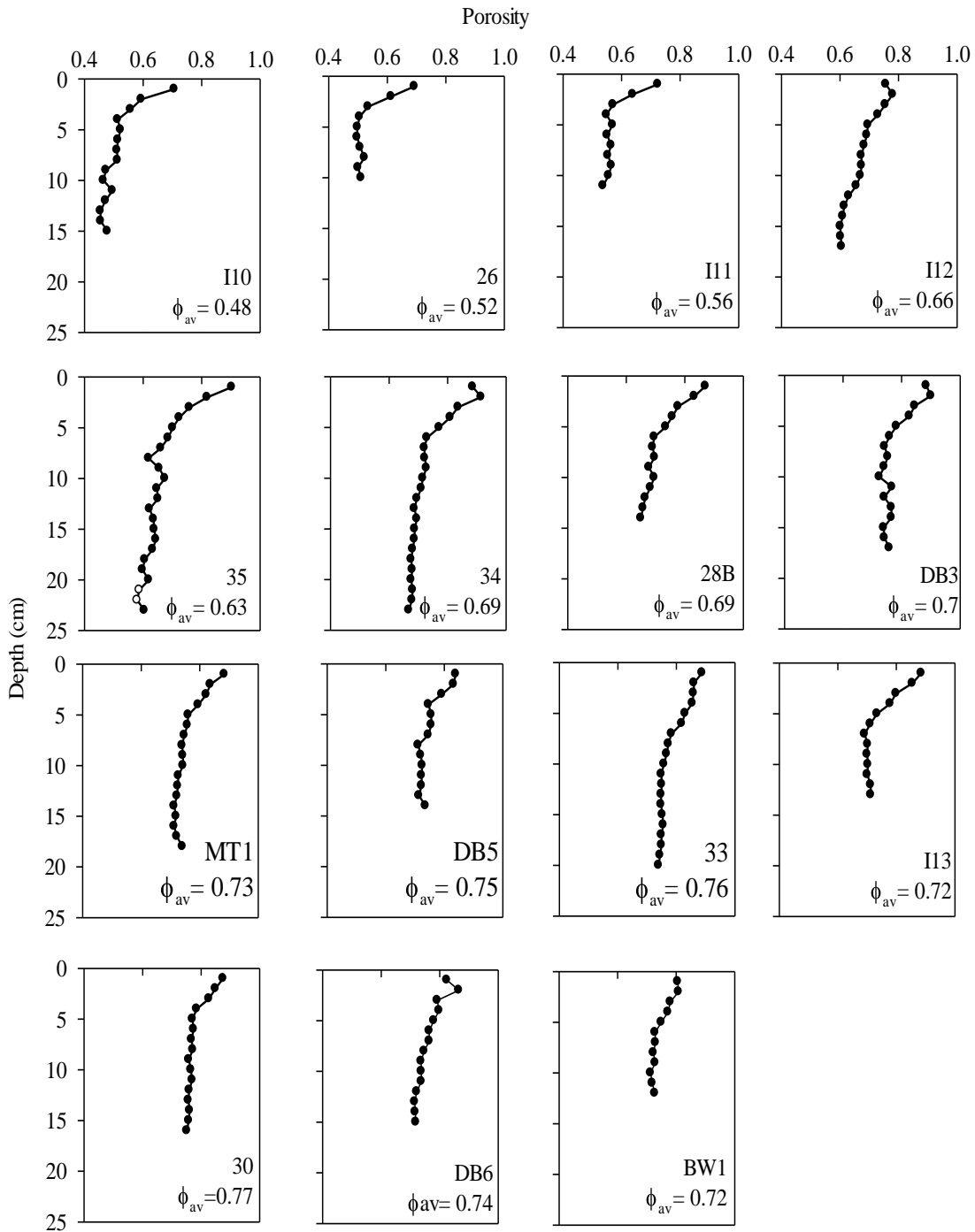
each sediment slice was obtained and the percentage of pre-and post-1970 sediment was determined from the known tracer concentration.

2.5 Results

2.5.1 Porosity profiles

In most cores, profiles of porosity (the ratio of water filled void spaces to the total volume of sediment) decrease smoothly downwards to depths just below the SML, followed by relatively constant porosity for the remainder of the core (Figure 2-3). An exception to this is core 35, where shifts in porosity below 7 cm correspond to coarser particles observed during sectioning (Figure 2-3).

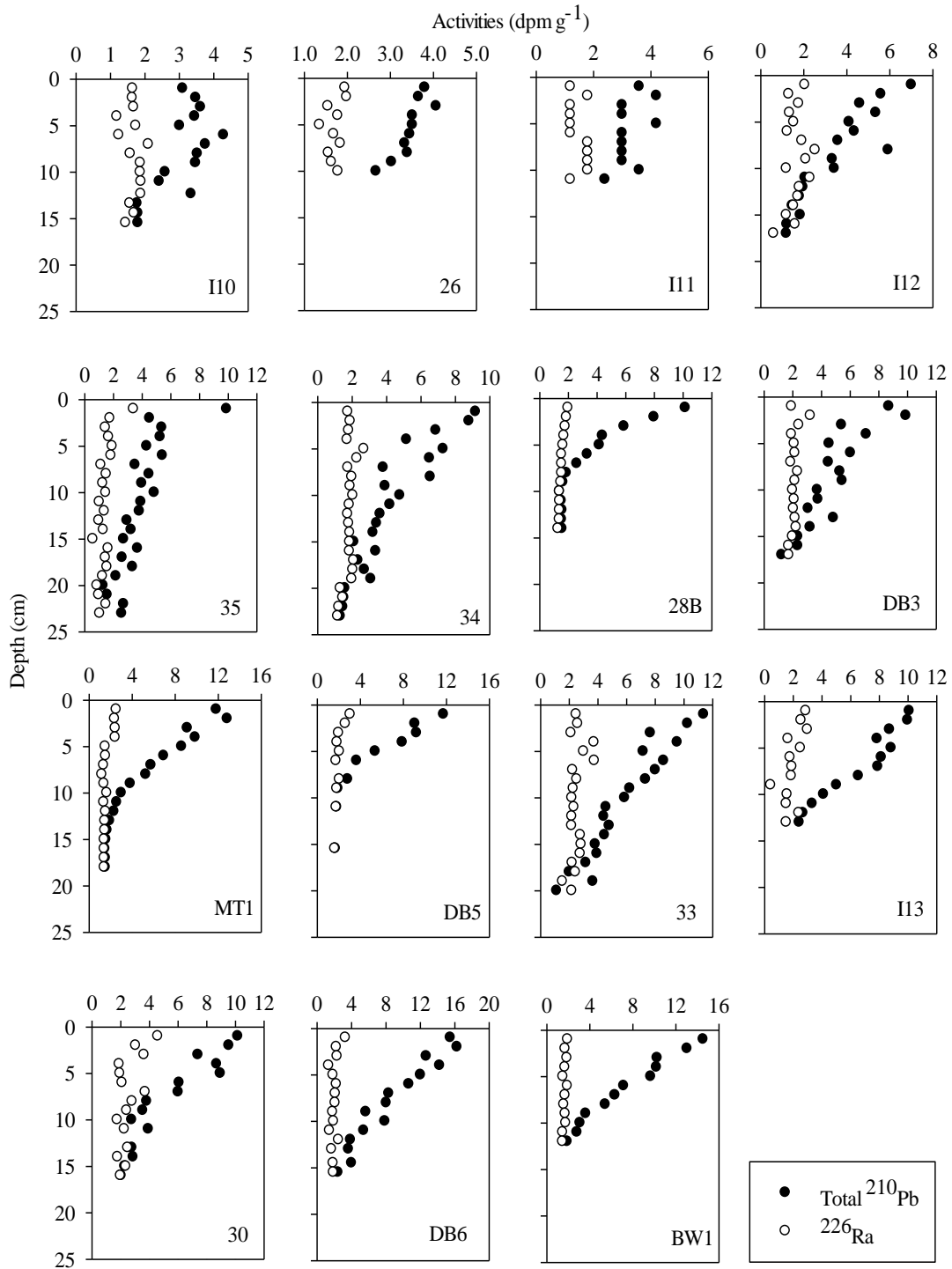
Figure 2-3. Porosity profiles of sediment cores. Observed coarse particles in slice 20 and 21 cm of core 35 are shown as open dots. These sections had unusually low ^{210}Pb activities and were omitted from modelling.



2.5.2 ^{210}Pb , ^{226}Ra , and ^{137}Cs radiochemistry

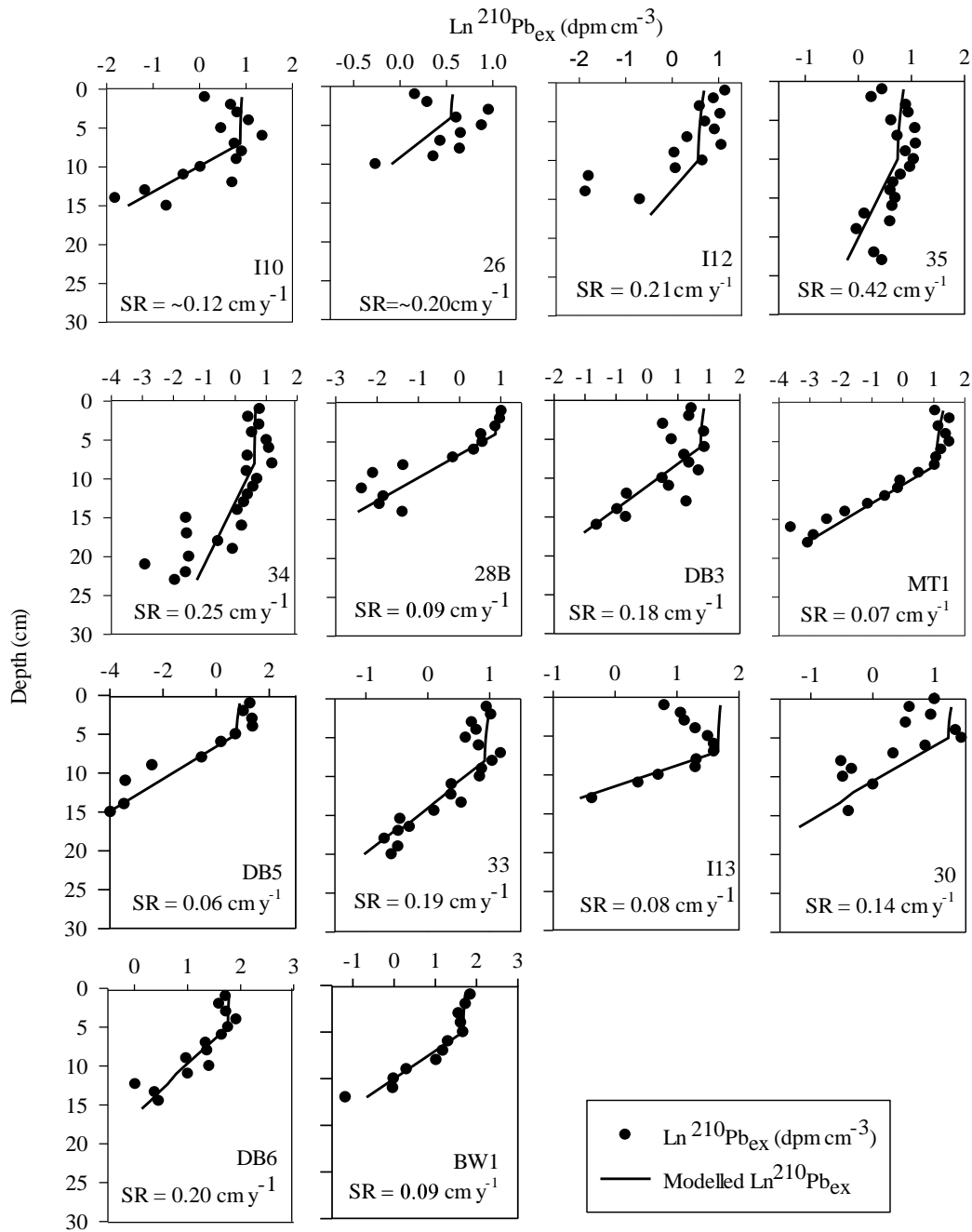
Activities of ^{210}Pb , ^{226}Ra , and ^{137}Cs were counted down fifteen sediment cores collected throughout Lake Melville in 2013 and 2014. In most cores, total ^{210}Pb decreased downwards until background levels of supported ^{210}Pb (determined from the grandparent radionuclide, ^{226}Ra) were reached; after which total ^{210}Pb remained relatively constant with depth (Figure 2-4). Background levels of supported ^{210}Pb in all cores were ca. 1.5-3 dpm g⁻¹ (decays per minute per gram of dry sediment) and were reached at depths ranging from 8 to 20 cm. Total ^{210}Pb profiles in cores 26 and I11, both collected in Goose Bay, did not reach background levels (Figure 2-4). While total ^{210}Pb in core 26 began displaying an exponential profile below 8 cm, activity in core I11 was nearly constant throughout the length of the core. With the exception of the surface activity, total ^{210}Pb in core 35 was also fairly uniform, decreasing only slightly from 5.4 dpm g⁻¹ at 3 cm to 3.2 dpm g⁻¹ at 20 cm; not quite reaching background levels. Core I13 scarcely reached levels similar to supported ^{210}Pb in the bottom slice (13 cm) (Figure 2-4).

Figure 2-4. Profiles of total ^{210}Pb (black dot) and ^{226}Ra (open dot) activities for cores collected in 2013 and 2014. Total ^{210}Pb activities in cores 26, I13, and MT1 were counted indirectly by alpha.



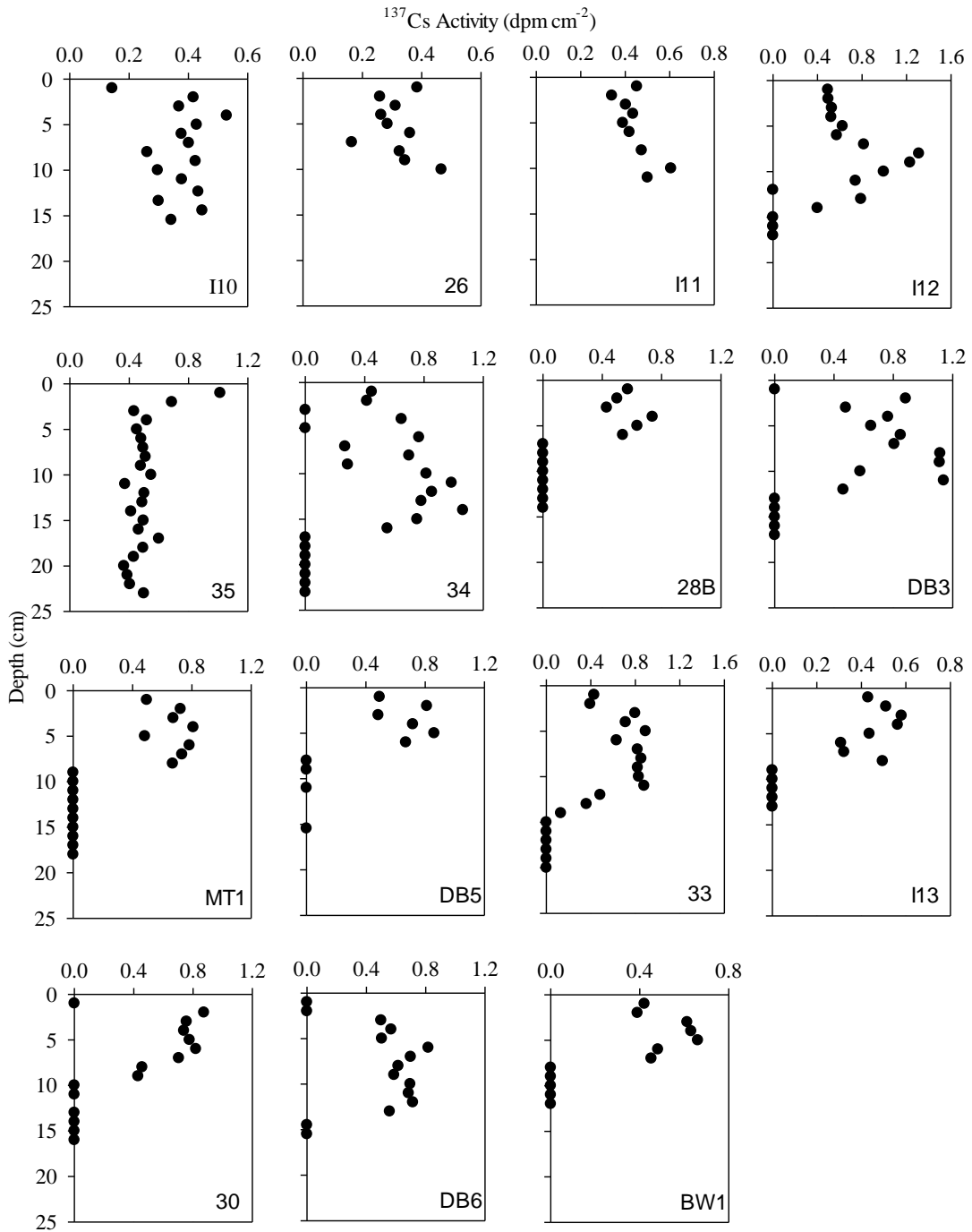
$^{210}\text{Pb}_{\text{ex}}$ exhibited a general profile of uniform activity at the surface, corresponding to the SML. Below the SML, $^{210}\text{Pb}_{\text{ex}}$ decreased exponentially, suggesting negligible mixing at depth (Figure 2-5). The thickness of the SML ranged between 4-9 cm with a mean thickness of 5.5 ± 1.8 cm (mean $\pm 1\sigma$ n=14).

Figure 2-5. Profiles of measured (black point) and modelled (line) natural log $^{210}\text{Pb}_{\text{ex}}$ activity. Sedimentation rates beginning with “~” could not be validated using ^{137}Cs profiles and should be interpreted cautiously. Coarse grained material observed at depths of 20 and 21 cm in core 35 resulted in abnormally low activities, thus these sections were excluded from the modelling. Irregularly low $^{210}\text{Pb}_{\text{ex}}$ activities at depths 16 and 17 cm in core I12 were also excluded from the modelling. ^{210}Pb activities in core 26 were measured by alpha method.



In most cores, activity profiles of ^{137}Cs displayed a general shape that included no activity at the bottom of the core, peak activity between 4 and 14 cm and decreasing activity upwards (Figure 2-6). The deepest occurrences of ^{137}Cs activity are interpreted as corresponding to the onset of nuclear weapons testing. Subsurface peaks of ^{137}Cs ranged in activity between 0.7 and 1.3 dpm g^{-1} . Activities in cores DB6 and DB3 reached levels below detection limit at the surface. The vertical distribution of ^{137}Cs was homogeneous and penetrated deeper than expected from ^{210}Pb in cores I10 and 35. Due to the proximity of these cores to sources of freshwater (Goose and Kenamu River) ^{137}Cs profiles could be displaying post-depositional re-mobilization (cf., Oughton et al., 1997). Profiles of ^{137}Cs were also homogeneous in cores 26 and I11. Since background levels of supported ^{210}Pb were not reached in those cores, we assume the onset of ^{137}Cs was deeper than the length of the cores.

Figure 2-6. Down-core profiles of ^{137}Cs .



2.5.3 Sedimentation and Mass Accumulation Rates

Sediment velocities and MARs rates exhibited greater than five-fold variability across Lake Melville, ranging between 0.06-0.42 cm y⁻¹ and 0.04-0.41 g cm⁻² y⁻¹, respectively (Figure 2-7 and Table 2-1). Sediment velocities and MARs were highest in the western end of the LMS, in shallow waters (49 m) near the mouth of the Kenamu River (core 35, 0.42 cm y⁻¹) and in nearby deeper waters (161 m) in Epinette Basin (core 34, 0.25 cm y⁻¹), with corresponding MARs of 0.41 and 0.20 g cm⁻² y⁻¹, respectively. In deep waters (217 m and 213 m) of eastern Lake Melville, in Mulligan and Grand Trough, core DB5 and I13 had the lowest sediment velocities and MARs at 0.06 and 0.08 cm y⁻¹ and 0.04 and 0.06 g cm⁻² y⁻¹, respectively (Figure 2-7).

The average sediment velocity and MAR in Grand Trough (0.13 cm yr⁻¹ and 0.08 g cm⁻² y⁻¹, n=2) is nearly double that found in Mulligan Trough (0.07 cm y⁻¹ and 0.04 g cm⁻² y⁻¹, n=2). In Goose Bay, sediment velocity and MARs are higher than in Lake Melville proper, with averages of 0.16 cm y⁻¹ and 0.21 g cm⁻² y⁻¹ (n=2), respectively. A higher sediment velocity and MAR was found near the mouth of the Churchill River (ca.0.20 cm y⁻¹ and ca.0.27 g cm⁻² y⁻¹) than near the mouth of the Goose River (ca. 0.12 cm y⁻¹ and ca. 0.16 g cm⁻² y⁻¹). Due to homogenised profiles, it was not possible to establish MARs for core I11. Since ¹³⁷Cs profiles in cores I10 and 26 were homogenized, the sedimentation and MARs for these cores were not validated and should be viewed with caution.

Figure 2-7. ^{210}Pb -derived sedimentation (cm y^{-1}) and mass accumulation rates ($\text{g cm}^{-2} \text{y}^{-1}$) across Lake Melville.

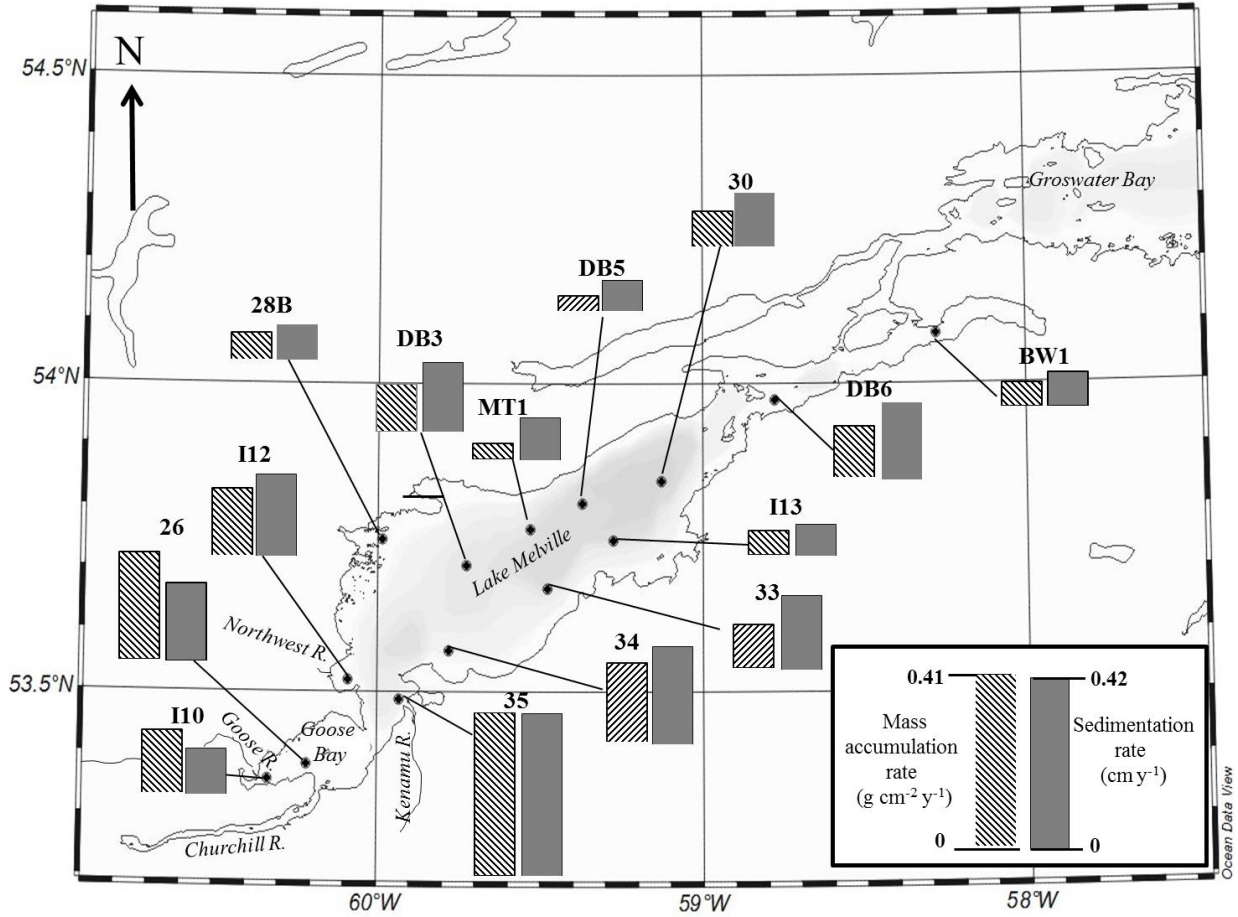


Table 2-1. Sediment core properties and sedimentation rates and parameters.

Core	Core Length (cm)	Water Depth (m)	Φ_{av}	SML (cm)	C_0 (dpm cm ⁻³)	K_{b1} (cm ² yr ⁻¹)	ω_s (cm yr ⁻¹)	MAR (g cm ⁻² yr ⁻¹)	$\Sigma^{210}\text{Pb}_{ex}$ (dpm cm ⁻²)	$\Sigma^{137}\text{Cs}$ (dpm cm ⁻²)	Comments
I10 ²	15	25.5	0.48	6	7	15	~0.12	~0.16	25.5±3.2	7.4±0.3	
26 ^{1,2,3}	10	49	0.52	7	5	8	~0.2	~0.27	21.6±1.3		¹³⁷ Cs not reached.
I12	17	48	0.66	9	10	9	0.21	0.17	23.3±2.6	6.8±0.3	Adjusted according to ¹³⁷ Cs onset.
35 ^{2,4}	23	47	0.63	9	5.5	14	0.42	0.41	36.7±1.5	9.6±0.2	Mixed core.
34	23	161	0.69	5	3.5	19	0.25	0.20	30.7±2.1	7.2±0.3	Adjusted according to onset of ¹³⁷ Cs.
28B	14	50	0.69	4	10.5	3	0.09	0.07	13.8±1.2	1.9±0.4	¹³⁷ Cs in top 6 cm.
DB3	17	126	0.70	5	4.5	6	0.18	0.12	25.3±5.2	5.4±0.6	Adjusted according to onset of ¹³⁷ Cs.
MT1	18	149	0.73	7	10	3	0.07	0.05	31.0±0.9	2.9±0.1	¹³⁷ Cs deeper than predicted.
DB5	14	217	0.74	4	8	3	0.06	0.04	19.0±2.0	2.3±0.3	¹³⁷ Cs deeper than predicted.
33	20	175	0.76	7	5	8.5	0.19	0.11	34.1±1.9	4.9±0.2	SR gives good fit to ¹³⁷ Cs onset
I13 ¹	13	213	0.7	6	18	10	0.08	0.06	37.2±0.9	1.5±0.2	Low ¹³⁷ Cs activity.
30	16	220	0.77	4	6.5	5	0.14	0.09	21.9±1.9	3.0±0.2	Wide range.
DB6	15	196	0.74	4	9.7	13	0.20	0.13	55.9±2.1	4.7±0.2	ω gives good fit to ¹³⁷ Cs onset.
BW1	12	98	0.73	4	10	5	0.09	0.06	40.7±1.2	2.2±0.3	ω in agreement with ¹³⁷ Cs.

Note: SML= surface mixed layer; Φ_{av} = average porosity below SML; $C_0 = ^{210}\text{Pb}_{ex}$ activity at the sediment-water interface; K_{b1} = upper layer mixing rate (mixing below K_{b1} , defined by K_{b2} (not shown), was 0.01 cm² yr⁻¹ for all cores); ω_s = sedimentation rate; MAR=mass accumulation rate; $\Sigma^{210}\text{Pb}_{ex}$ and $\Sigma^{137}\text{Cs}$ = sediment inventories ± propagated uncertainty. ¹The ²¹⁰Pb activities were determined by alpha method; ²Unable to validate core due to incomplete or uniform ¹³⁷Cs profile; ³Background levels were not reached within the length of the core. ⁴ The sedimentation rate is likely underestimated because ²¹⁰Pb activities at depth were variable, probably reflecting dilution from coarser grained particles.

2.5.4 Inventories of $^{210}\text{Pb}_{\text{ex}}$ and ^{137}Cs

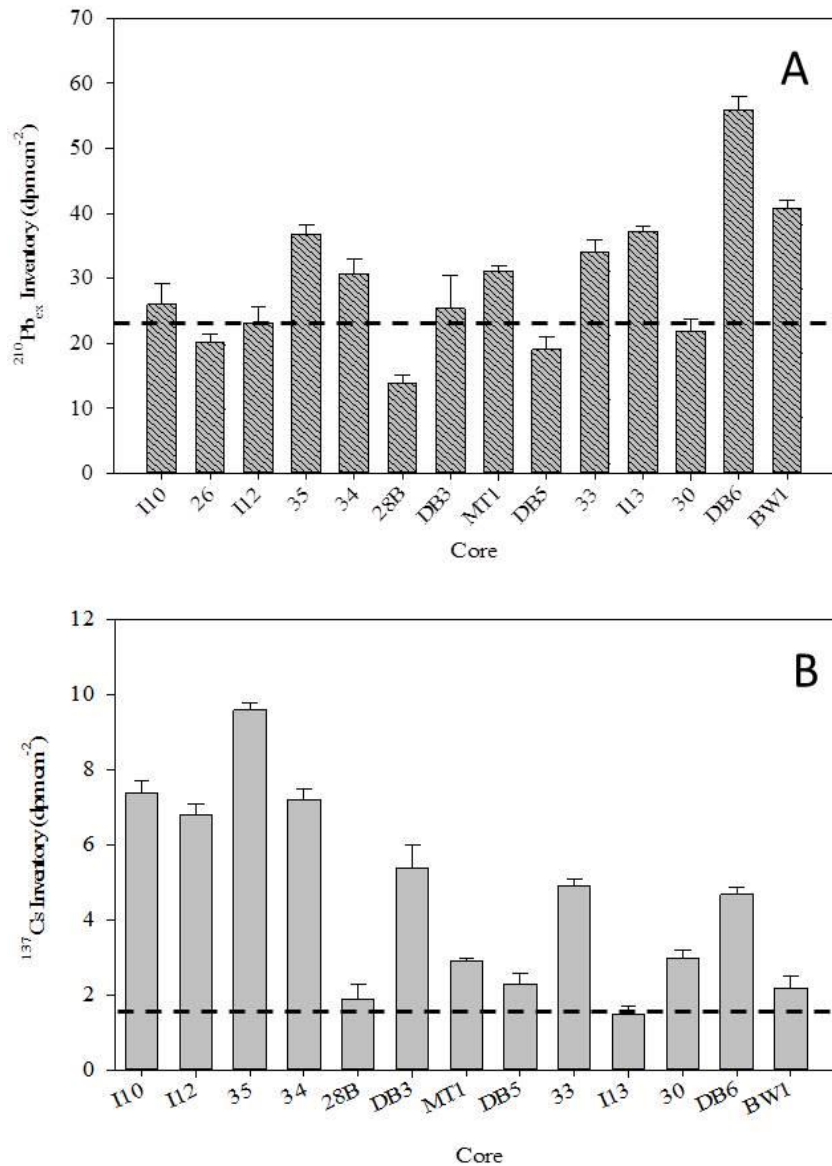
Average inventories of $^{210}\text{Pb}_{\text{ex}}$ and ^{137}Cs in Lake Melville are 29.4 ± 9.9 (n=15) and 4.8 ± 1.7 dpm cm^{-2} (n=14), respectively. Generally, $^{210}\text{Pb}_{\text{ex}}$ inventories are lower in the shallow western regions of Lake Melville and higher in the deeper eastern end of the basin (Figure 2-8 and Table 2-1). For example, near the outflows of the Goose (core I10), Northwest (core I12) and, particularly the Sebaskachu (core 28B) Rivers, where water depths are ≤ 50 m, $^{210}\text{Pb}_{\text{ex}}$ inventories are 26.0 ± 3.2 , 23.1 ± 2.6 , and 13.8 ± 1.2 dpm cm^{-2} , respectively. In contrast, cores DB6 and BW1, collected from greater depths in the eastern end of the LMS, support the greatest $^{210}\text{Pb}_{\text{ex}}$ inventories at 55.9 ± 2.1 and 40.7 ± 1.2 dpm cm^{-2} , respectively, exceeding expected inventory from direct atmospheric fallout (23.6 dpm g^{-1} , Figure 2-8a). Some exceptions to this trend (i.e., higher $^{210}\text{Pb}_{\text{ex}}$ inventories in the deeper eastern end of the basin) include core DB5, collected from a water depth of 217 m in the Mulligan Trough, which maintains one of the lowest $^{210}\text{Pb}_{\text{ex}}$ inventories (19.0 ± 2.0 dpm cm^{-2}), while a nearby core (MT1) has a $^{210}\text{Pb}_{\text{ex}}$ inventory of 31.0 ± 0.9 dpm cm^{-2} . ^{137}Cs inventories are similar in these two cores (2.3 ± 0.3 and 2.9 ± 0.1 , respectively), and similar to the average ^{137}Cs inventory (3.1 dpm cm^{-2} , n = 2) found in the Grand Trough. In addition to variability between $^{210}\text{Pb}_{\text{ex}}$ and ^{137}Cs inventories, $^{210}\text{Pb}_{\text{ex}}$ inventories meet, exceed or fall below expected inventory from direct atmospheric fallout (Figure 2-8a), implying something inconsistent in the $^{210}\text{Pb}_{\text{ex}}$ supply, specifically to site DB5.

In all cores, ^{137}Cs inventories either meet or exceed the expected inventory from direct atmospheric fallout (ca. 1.5 dpm cm^{-2}) (Figure 2-8b). In the western end of the LMS, near river mouths, ^{137}Cs inventories are greatest. For example, near the mouths of the Goose, Northwest, and Kenamu Rivers, ^{137}Cs inventories are higher than anywhere else in the LMS (7.4 ± 0.3 , 6.8 ± 0.3 , and 9.6 ± 0.2 dpm cm^{-2} , respectively). Whereas, in the eastern end of the LMS, ^{137}Cs

inventories are lower than the overall average for sediment in the Lake (i.e., 2.2 ± 0.3 and 4.7 ± 0.2 dpm cm^{-2} , cores BW1 and DB6, respectively) but are still greater than expected from

atmospheric deposition (Figure 8b)

Figure 2-8. $^{210}\text{Pb}_{\text{ex}}$ (A) and ^{137}Cs (B) inventories are compared to the expected inventory from direct atmospheric fallout (1.5 and 23.6 dpm cm^{-2} , respectively) (dashed horizontal line). Inventories are arranged along a west (Goose Bay) to east (Lake Melville) axis. The inventory of ^{137}Cs in core 26 was not available because background levels were not reached within the length of the core. $^{210}\text{Pb}_{\text{ex}}$ inventory in core 26 was estimated by extrapolating the $^{210}\text{Pb}_{\text{ex}}$ activity downwards to background levels.



2.5.5 Distribution and profiles of organic carbon and $\delta^{13}\text{C}$

Average TOC in surficial sediment across Hamilton Inlet was $1.1 \pm 0.31\%$ (n=13) (including surface samples from Groswater Bay). Overall, percentage of TOC in surficial sediment (ca. 0-2 cm) ranged from $0.3 \pm 0.1\%$ to $1.7 \pm 0.1\%$ across Lake Melville and Goose Bay with TOC in Groswater Bay of $1.4 \pm 0.1\%$ (Figure 2-9). In Goose Bay, TOC varied from $0.9 \pm 0.1\%$ near the mouth of the Goose River (I10) to $0.4 \pm 0.1\%$ near the mouth of the Churchill River. West of Goose Bay Narrows, TOC was only $0.5 \pm 0.1\%$ (I11), while a nearby site (35), east of Goose Bay Narrows, TOC was $1.6 \pm 0.1\%$, similar to surficial sediment from the constricted eastern end of Lake Melville (core DB6, $1.7 \pm 0.10\%$). TOC was comparable between Mulligan ($1.3 \pm 0.10\%$, n=1), Grand ($1.1 \pm 0.14\%$, n=2) and Sebaskachu ($1.1 \pm 0.10\%$, n=1) Troughs. $\delta^{13}\text{C}_{\text{org}}$ values in surficial sediment range from $-27.9 \pm 0.1 \text{‰}$ in Goose Bay (I10) to $-24.2 \pm 0.1 \text{‰}$ in the constricted region of Lake Melville (DB6). In Groswater Bay $\delta^{13}\text{C}_{\text{org}}$ was $-22.4 \pm 0.1\text{‰}$ for surficial sediment (Figure 2-10).

Figure 2-9. A thematic map showing organic carbon content in surface sediment (0-1 cm) across Lake Melville.

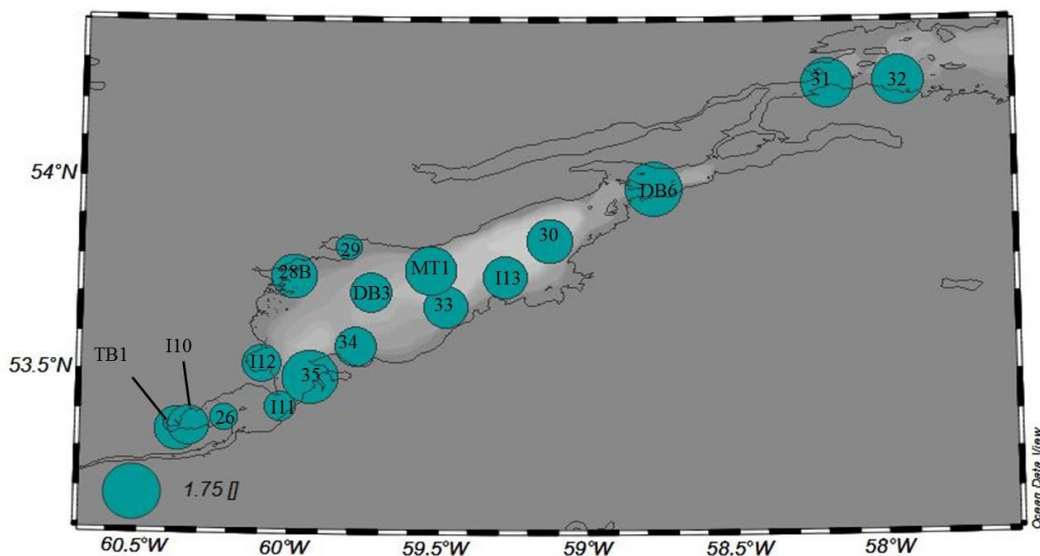
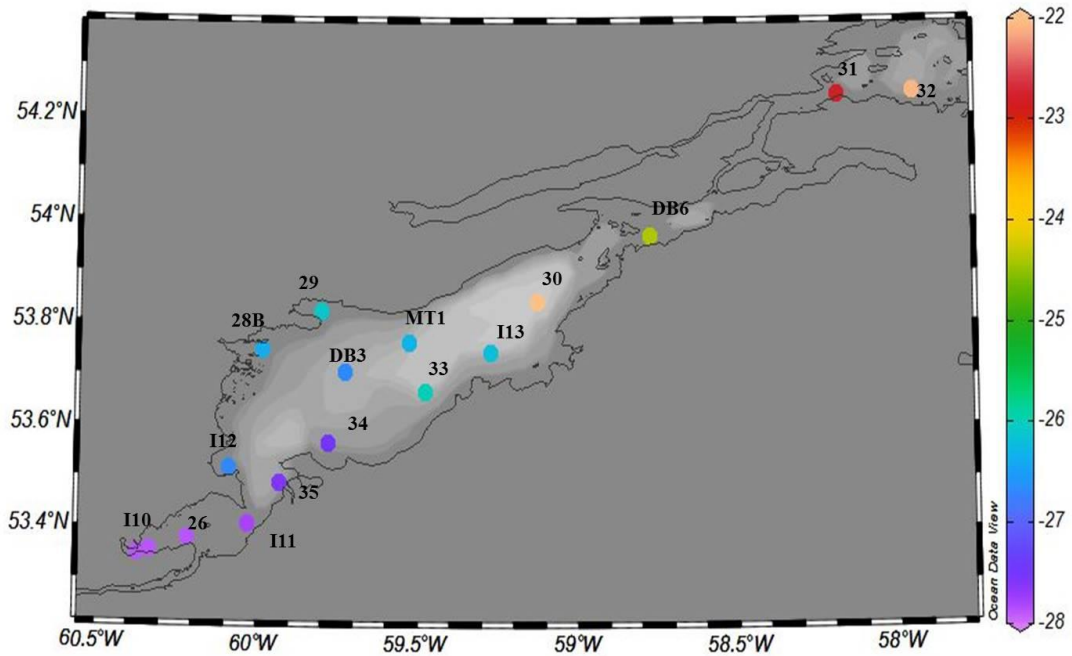
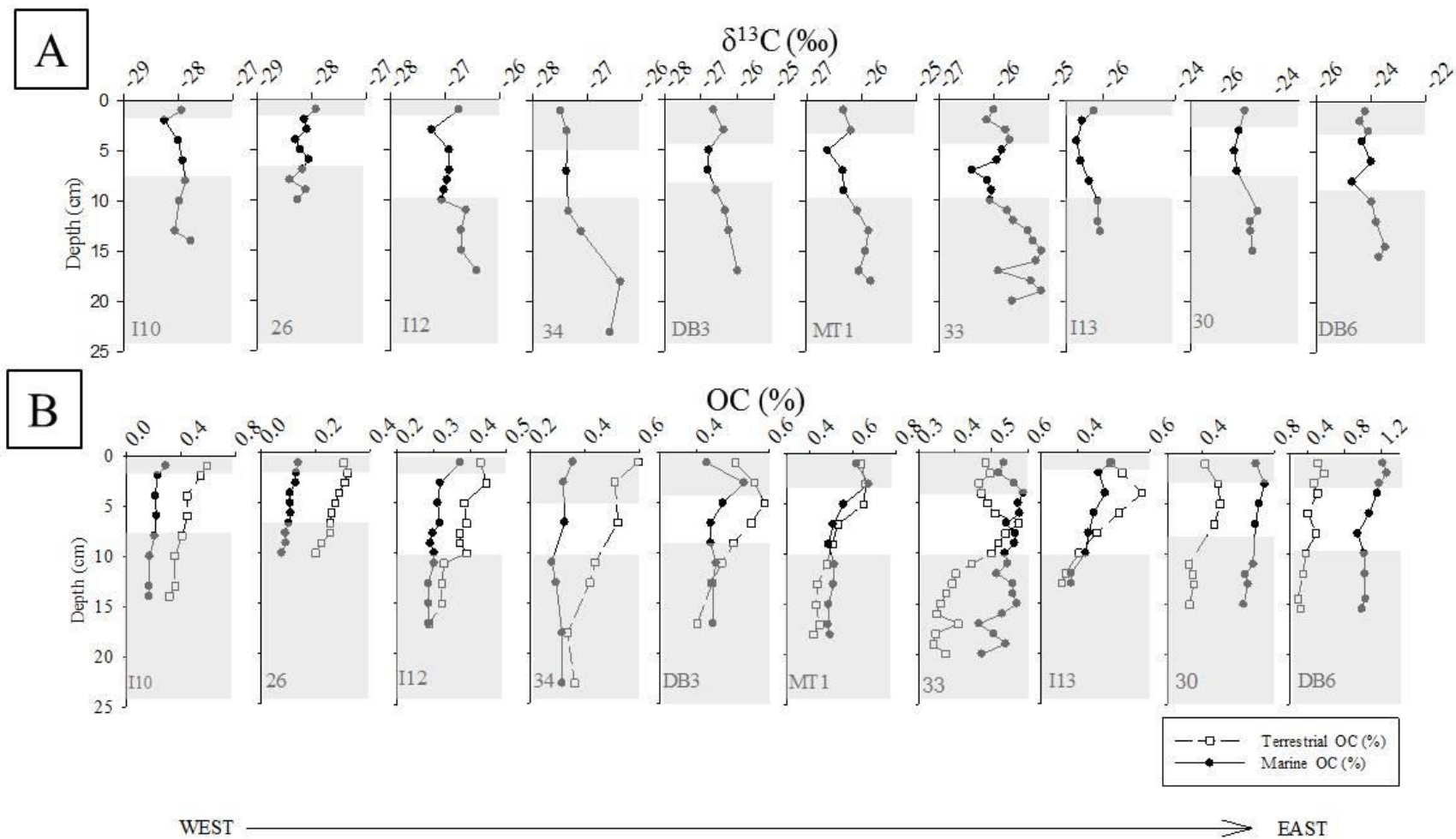


Figure 2-10. Surface sedimentary $\delta^{13}\text{C}_{\text{org}}$ values (‰ relative to VPDB) across Lake Melville.



Profiles of $\delta^{13}\text{C}_{\text{org}}$ and percentage of OC_{terr} and OC_{mar} are compared in Figure 2-11. In cores collected across Lake Melville (I12, 34, DB3, MT1, 33, I13 30, DB6) $\delta^{13}\text{C}_{\text{org}}$ becomes heavier down-core and display a con-cave like shape. Cores I10 and 26, collected from Goose Bay, remain relatively constant (see Figure 2-11a). The greatest decrease in $\delta^{13}\text{C}_{\text{org}}$ is in core 34 which decreases by 0.9‰ from sediment deposited pre-development (bottom of core, 23 cm) to the most recently deposited sediment (post-development) (Figure 2-11b)

Figure 2-11. Profiles $\delta^{13}\text{C}_{\text{org}}$ (A) and percent contribution of terrestrial- and marine-type OC (B). Shading represents sediment containing 90% pre-1970 (surface) and post-1970 (bottom) while non-shaded areas are a mixture of both.



2.6 Discussion

2.6.1 Overview

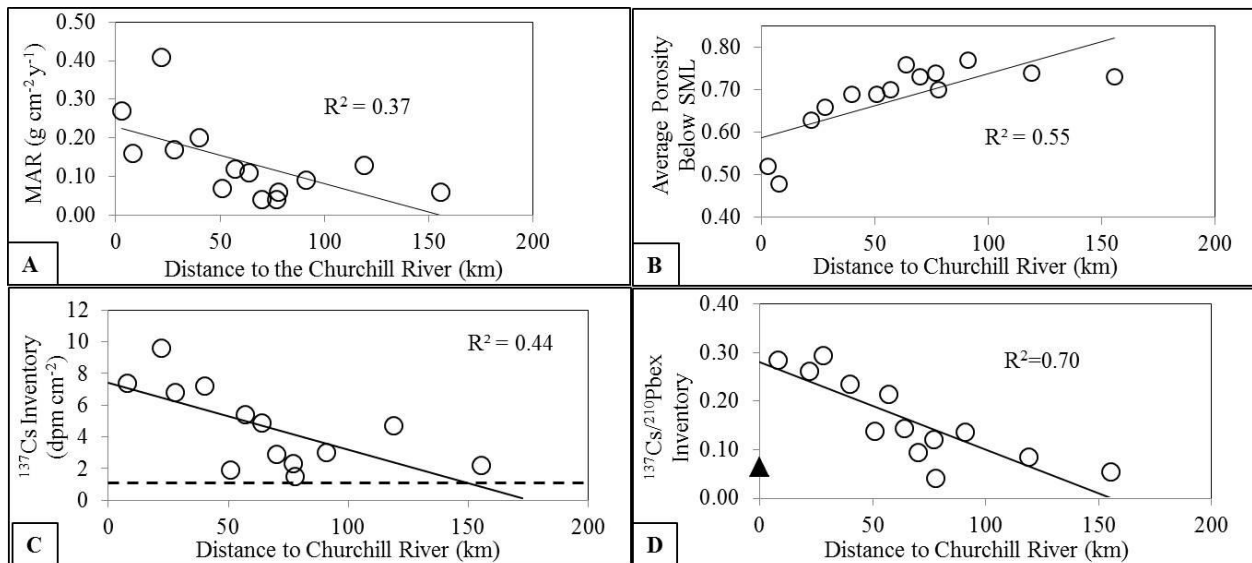
The average MAR based on ^{210}Pb and validated with ^{137}Cs (where possible) in Lake Melville sediments resembles other subarctic regions characterised by mostly flat lowland shorelines that are largely influenced by river runoff. Similarly, many of the sedimentary parameters examined here show strong relationships with distance to major freshwater sources (i.e., the Churchill River and other rivers), while no statistically significant relationships to water depth were found. From the distributions of MARs, inventories of ^{137}Cs and $^{210}\text{Pb}_{\text{ex}}$, and taking ^{137}Cs in this environment as primarily sourced from land-derived particles (cf., Baskaran and Naidu, 1995; Smith and Ellis, 1982; Smith et al., 2002), we conclude that sediment is primarily brought into this system from river runoff. $\delta^{13}\text{C}_{\text{org}}$ values, which are relatively low, also point to rivers as major sources of the OC captured in surface sediment. The bulk organic $\delta^{13}\text{C}_{\text{org}}$ composition of sediment, however, becomes increasingly heavier eastward indicating more marine OM toward the east and the two-layer estuarine circulation of Lake Melville (i.e., inflow of marine-derived materials at its eastern end). Over the time period represented in these cores, $\delta^{13}\text{C}_{\text{org}}$ is statistically lighter in sediment deposited after 1970, consistent with greater contributions of terrestrial OC across the Lake. Given the expected preferential “burn-down” of labile marine OM at the sediment surface, it is not likely that the $\delta^{13}\text{C}_{\text{org}}$ profile is produced by loss of marine OM but rather than an increase in terrestrial OM.

2.6.2 Inputs of riverine sediment inferred from mass accumulation rates

Our results show that distance from the mouth of the Churchill River, an expected major source of sediment, strongly influences the sediment composition and MAR, which decreases

significantly with distance from the Churchill River mouth ($R^2=0.37$, $p<0.05$, $n=14$) (Figure 2-12a). In Lake Melville, average porosity below SML is also significantly associated with distance to the Churchill River ($R^2=0.55$, $p<0.05$, $n=14$) (Figure 2-12b). In Goose Bay, closer to the outflow of the Churchill River, mean porosity below SML is lowest at ca. 0.50, increasing eastward to ca. 0.73 near the centre of the LMS and remaining relatively constant throughout Lake Melville proper (see Figure 2-12b). There is no significant spatial trend in surficial grain size data collected by colleagues in 2012 ($R^2=0.02$, $p>0.05$, $n=42$, not shown).

Figure 2-12. Mass accumulation rates (MAR, $\text{g cm}^{-2} \text{y}^{-1}$) (A), average porosity below the surface mixed layer (SML) (B), ^{137}Cs inventories (dpm cm^{-2}) (C), and ratio of ^{137}Cs to $^{210}\text{Pb}_{\text{ex}}$ inventories (D) plotted as a function of distance to the Churchill River. In C, the dashed line represents the expected ^{137}Cs inventory from direct atmospheric fallout. In D, the filled triangle represents the expected $^{137}\text{Cs}/^{210}\text{Pb}_{\text{ex}}$ inventory from direct atmospheric fallout.



A complication in the overall spatial pattern is the supply of sediment from smaller rivers, in addition to the Churchill River. Our results show that the highest MAR occurs near the mouth of the Kenamu River (core 35, $0.42 \text{ g cm}^{-2} \text{y}^{-1}$, respectively) (see Figure 2-7 and Table 2-

1). The MAR here is almost two times greater than in Goose Bay (core 26, $0.27 \text{ g cm}^{-2} \text{ y}^{-1}$, respectively). This difference is surprising given that Goose Bay is near the outflow of the Churchill River, which has a considerably larger discharge rate (ca.2000 versus ca.100 $\text{m}^3 \text{ sec}^{-1}$) and drainage basin (92 500 versus 4403 km^2) than the Kenamu River (Anderson, 1985; Bobbitt and Akenhead, 1982a).

The greater MAR calculated for core 35 is probably, a result of sediment being transported in suspension eastward in the Churchill River plume through the shallow (ca. 6 m deep and ca. 0.8 km wide) Goose Bay Narrows. In these Narrows, surface water flows eastward, both during ebb and flood tides with currents up to ca. 5 m sec^{-1} (Syvitski, 1990). Therefore, this area would not be conducive for deposition. The effects of strong currents on sediment deposition (i.e., mixing and resuspension) are reflected in both the low and homogenised radioisotope profiles of core I11 (see Figures 2-4, 2-5, 2-6) and in the exceptionally low TOC in surface sediment from this location (0.5% TOC). East of Goose Bay Narrows, however, where the Kenamu River discharges into Lake Melville, the Lake widens and deepens allowing water velocity to decrease and particles to settle out. At this site (core 35) TOC in surficial sediment was three times greater than core I11 at 1.5% TOC. This spatial pattern suggests that fine particles are carried eastward through Goose Bay Narrows and deposited on the east side where the Lake widens. This can be observed in MODIS images, which show the Churchill River plume extending into this region during spring freshet and, because of its size, the plume likely contributes fine grained material to Epinette Basin (core 34). This basin is the first deep basin east of Goose Bay. Here the MAR is higher than anywhere else in Lake Melville proper at $0.20 \text{ g cm}^{-2} \text{ y}^{-1}$.

Supply of sediment from the Kenamu River likely also contributes to the MAR in core 35. Coarser particles were observed at depth (below 7 cm) while sectioning core 35. These coarse particles are also reflected in the porosity profiles (Figure 2-3) and surficial grain size (not shown), and are more likely to have come from the nearby Kenamu River (2 km) than the more distant Churchill River (22 km). Syvitski (1990) suggested that the Kenamu River carries a larger fraction of bedload material than suspended sediment to its delta, which is consistent with supply of coarse-grained sediment and a rapid progradation ($10 - 30 \text{ m yr}^{-1}$) of the delta. Furthermore, turbidity currents are common in this area, which would transport coarser particles from the delta to the deeper basin. These factors all imply that the Kenamu River contributes at least a moderate amount of sediment to the system even though it drains an area $<5\%$ of that drained by the Churchill River (Anderson, 1985).

The difference in river morphology between the Kenamu and Churchill Rivers could explain the variation in MARs and coarse-grained sediment supply. In an analysis of 280 rivers draining into the world's seas, Milliman and Syvitski (1992) concluded that sediment discharge is controlled primarily by the topographical relief and size of the drainage basin. The authors found that small mountainous (maximum elevation of 1,000-3,000 m) rivers with drainage basins $\leq 10,000 \text{ km}^2$ discharge disproportionately more sediment (including bedload) than larger rivers because of their steeper gradient and proneness to flooding, which favours erosion.

Although the maximum basin relief of the Kenamu River is only ca. 305 m, its meandering channel is prone to flooding in spring and during storm events in late summer and autumn (Syvitski, 1990). Also, tributaries of the Kenamu River drain some of the west side of the Mealy Mountains, the only mountain range in the otherwise flat lowland shoreline of Lake Melville (Anderson, 1985). In contrast, the Churchill River flows through a complex range of

conditions that govern its sediment load. Lakes above Muskrat Falls would expectedly trap sediment, while the River transitions from a meandering to a braided channel in the last 40 km from Muskrat Falls to its mouth (Amec, 2008b; Anderson, 1985). In this lower reach, sand bars are abundant and would accumulate coarse material (Amec, 2008b).

2.6.3 Indications of riverine inputs, focusing, and boundary scavenging from ^{137}Cs and $^{210}\text{Pb}_{\text{ex}}$ inventories

To discern the contribution of riverine sediment to Lake Melville, inventories of ^{137}Cs were compared across the Lake and to the expected inventory from direct atmospheric fallout (ca. 1.5 dpm cm^{-2}) (see Figure 8). Unlike in marine water where ^{137}Cs is less particle reactive and exhibits conservative behaviour (Mackenzie et al., 1979), in terrestrial and freshwater environments, ^{137}Cs binds almost irreversibly to clay particles by means of ion exchange (Jenne and Wahlberg, 1968; Smith and Ellis, 1982; Smith et al., 1987). Thus, in a system like Lake Melville, which receives both freshwater from river runoff and inflowing seawater, inventories of ^{137}Cs provide a useful proxy for interpreting sources of sediment (e.g., Smith et al., 2002).

In Lake Melville, ^{137}Cs inventories either meet or exceed the estimated inventory from direct atmospheric fallout (Figure 2-8b), consistent with additional terrestrial contributions. The spatial patterns reflect major inputs from the Churchill River ($R^2=0.45$, $p<0.05$, $n=13$) (Figure 2-12c). Similar to MAR, an exceptionally high ^{137}Cs inventory (six times greater than expected from direct atmospheric fallout) was calculated for core 35 (9.6 dpm cm^{-2}) near the mouth of the Kenamu River. In this core, background levels of ^{137}Cs were not reached and it is possible that the inventory of 9.6 dpm cm^{-2} is underestimated. Nevertheless, the large inventory at this location integrates the combined contribution of fine material transported in suspension by the Churchill

River plume, inputs from the Kenamu River (as discussed in the preceding section), and direct deposition onto the Lake surface.

A relatively high ^{137}Cs inventory was observed near the outflows of the Northwest (I12) River. Here, the ^{137}Cs inventory was ca. 4.5 times greater than in the eastern end of the Lake (compare to core I13, 1.5 dpm cm^{-2} in Figure 2-8b). This suggests that the Northwest River has at least a local influence on sediment input to this system, but the spatial extent of influence is difficult to discern because of overlap with sediment from the Churchill River plume.

Nevertheless, Vilks et al. (1987), described a rise in the sea floor and sediment strata from Epinette Basin towards the Northwest River delta, and inferred this river to be a source of fine grained sediment to Epinette Basin, likely in addition to the Churchill River.

The distribution of radioisotope inventories in estuarine and shelf environments can also be affected by sediment focusing, the lateral transport of fine grained material from shallow to deeper water (cf., Crusius and Anderson, 1995). This process may explain the relatively high ^{137}Cs inventories in some isolated basins (i.e., Sebaskachu Basin) of Lake Melville proper.

As outlined by Kuzyk et al. (2013), focusing, boundary scavenging of $^{210}\text{Pb}_{\text{ex}}$ and sources of sediment were investigated by comparing inventories of ^{137}Cs and $^{210}\text{Pb}_{\text{ex}}$ and their ratios, to the estimated ratio of $^{210}\text{Pb}_{\text{ex}}/^{137}\text{Cs}$ inventories in terrestrial soil for this region (ca. 15.7) (Figure 2-13). In contrast to ^{137}Cs , $^{210}\text{Pb}_{\text{ex}}$ binds rapidly and almost irreversibly to suspended particles, which then settle to the seafloor (i.e., *scavenging*) (cf., Fang et al., 2013). This difference in particle reactivity between $^{210}\text{Pb}_{\text{ex}}$ and ^{137}Cs in marine environments tends to increase $^{210}\text{Pb}_{\text{ex}}$ inventories, while inventories of ^{137}Cs remain relatively unchanged (Oguri et al., 2012). Focusing of sediment is expected to increase both ^{137}Cs and $^{210}\text{Pb}_{\text{ex}}$ inventories simultaneously while maintaining their relative ratio similar to that expected in terrestrial soil (Kuzyk et al., 2013). In

contrast, terrestrial inputs from rivers and coastal erosion tend to increase ^{137}Cs inventories, while inventories of $^{210}\text{Pb}_{\text{ex}}$ remain relatively unaffected (Sugai, 1990b).

Figure 2-13. Inventories of $^{210}\text{Pb}_{\text{ex}}$ and ^{137}Cs , and their ratios are compared across Lake Melville, and to the expected ratio in local soil from direct atmospheric fallout (shaded area). Cores with $^{210}\text{Pb}/^{137}\text{Cs}$ ratios that fall within the shaded area (i.e. high ^{137}Cs inventories), suggest additional terrigenous particles. Cores with $^{210}\text{Pb}/^{137}\text{Cs}$ ratios similar to soil (15.9), implies sediment focusing (black arrow), cores above the black arrow indicate an additional source of $^{210}\text{Pb}_{\text{ex}}$.

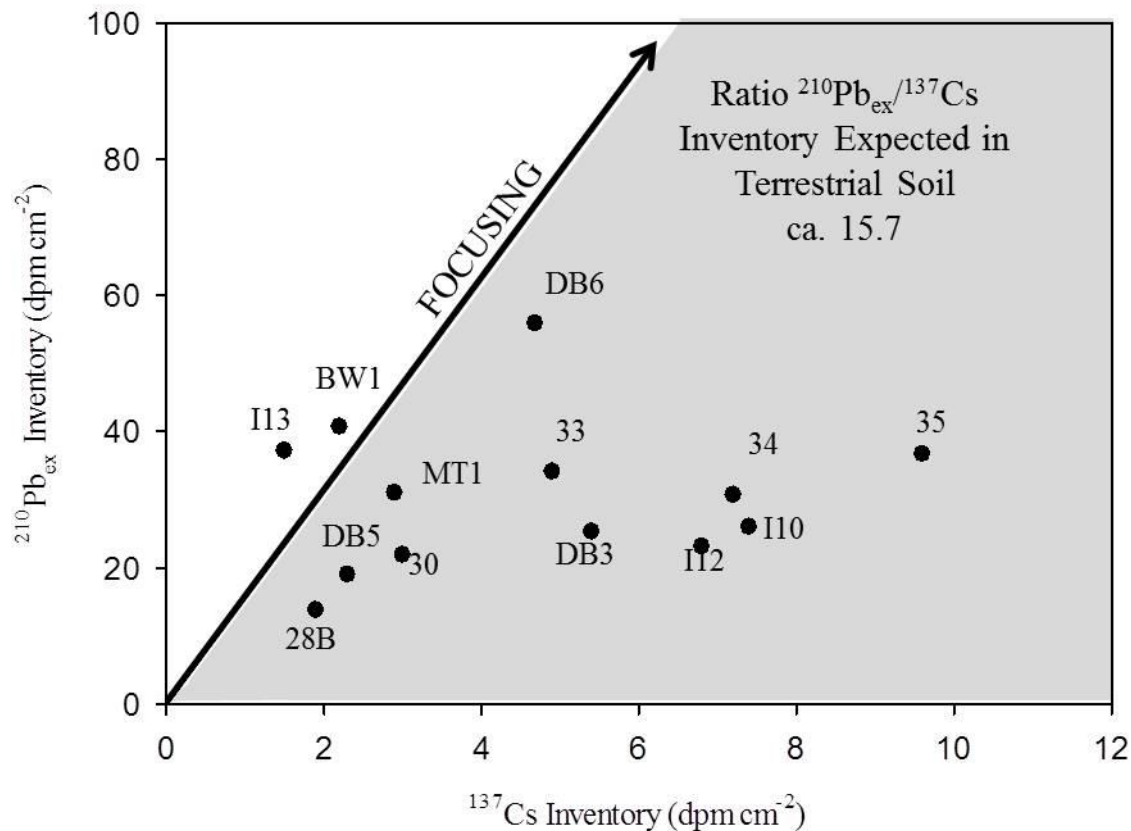
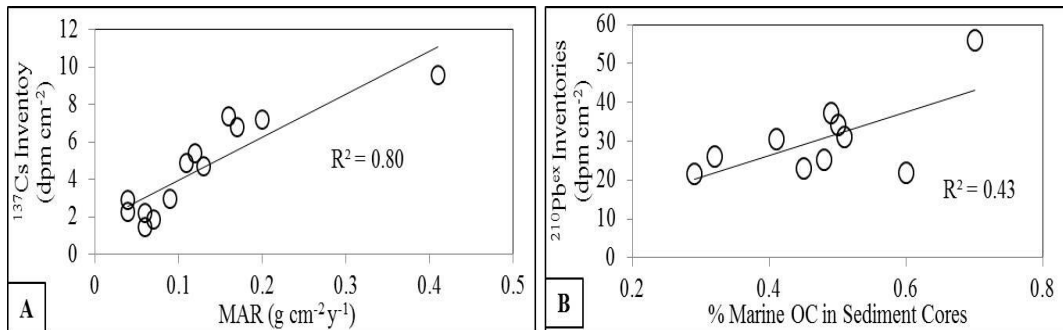


Figure 2-13 shows that the majority of cores fall below the expected $^{210}\text{Pb}_{\text{ex}}/^{137}\text{Cs}$ inventory ratio in terrestrial soils. Most cores have $^{210}\text{Pb}_{\text{ex}}$ inventories scattered about the expected $^{210}\text{Pb}_{\text{ex}}$ inventory from atmospheric fallout (23.6 dpm cm⁻²). A larger variance is evident in ^{137}Cs inventories, with high inventories resulting in low $^{210}\text{Pb}_{\text{ex}}/^{137}\text{Cs}$ ratios. We can infer that ^{137}Cs affixed to particles from rivers and coastal erosion contributes considerably to the

sediment in this system. This conclusion is further supported by the strong linear relationship between ^{137}Cs inventories and MARs ($R^2=0.80$, $p<0.05$, $n=13$) (Figure 2-14a). From Figure 2-13, focusing does not appear to be a major process in this system, at least not in the western end. However, because of the large imprint by the Churchill River, the process of focusing could be obscured. Our results show that the ratio of $^{210}\text{Pb}_{\text{ex}}/^{137}\text{Cs}$ inventories is inversely associated with distance to the Churchill River ($R^2=0.70$, $p<0.05$, $n=13$) (Figure 2-12d), suggesting the Churchill River is a major source of particulate ^{137}Cs .

Figure 2-14. Relationships between ^{137}Cs inventories (dpm cm^{-2}) and mass accumulation rates (MAR, $\text{g cm}^{-2} \text{y}^{-1}$) (A) and $^{210}\text{Pb}_{\text{ex}}$ inventories (dpm cm^{-2}) and the percentage of marine OC within cores (B).



Cores collected from the eastern end of the basin (DB6, BW1, and I13) fall closest to the estimated terrestrial ratio (Figure 2-13), with comparable ratios of 11.9, 18.5, and 24.8, respectively. The nearness of these cores to the expected ratio in soil implies focusing of sediment in the eastern end of the basin. On the other hand, $^{210}\text{Pb}_{\text{ex}}$ inventories generally increase eastward from the Churchill River ($R^2=0.27$, $p=0.06$, $n=14$). In view of the proximity of these sites to inflowing seawater from Groswater Bay, the increased $^{210}\text{Pb}_{\text{ex}}$ inventories in the most eastern cores could reflect scavenging of $^{210}\text{Pb}_{\text{ex}}$ from the landward flowing seawater (cf., Radakovitch et al., 2003; Smoak et al., 1996).

It is well known that $^{210}\text{Pb}_{\text{ex}}$ is more effectively scavenged by particulate organic matter than fine lithogenic particles (i.e. clay) (cf., Moore and Dymondt, 1988; Oguri et al., 2012; Robbins and Edgington, 1975; Yang et al., 2015). Thus, the higher $^{210}\text{Pb}_{\text{ex}}$ inventories in the eastern end of the LMS could also reflect higher primary production. In August 2012, Lu et al. (2013) recorded an upwelling event east of the sill in the Narrows. This renewal of deep, cold water to the eastern end of the Lake, driven partly by estuarine entrainment, could provide a sustained delivery of nutrients to the surface waters and support increased primary production.

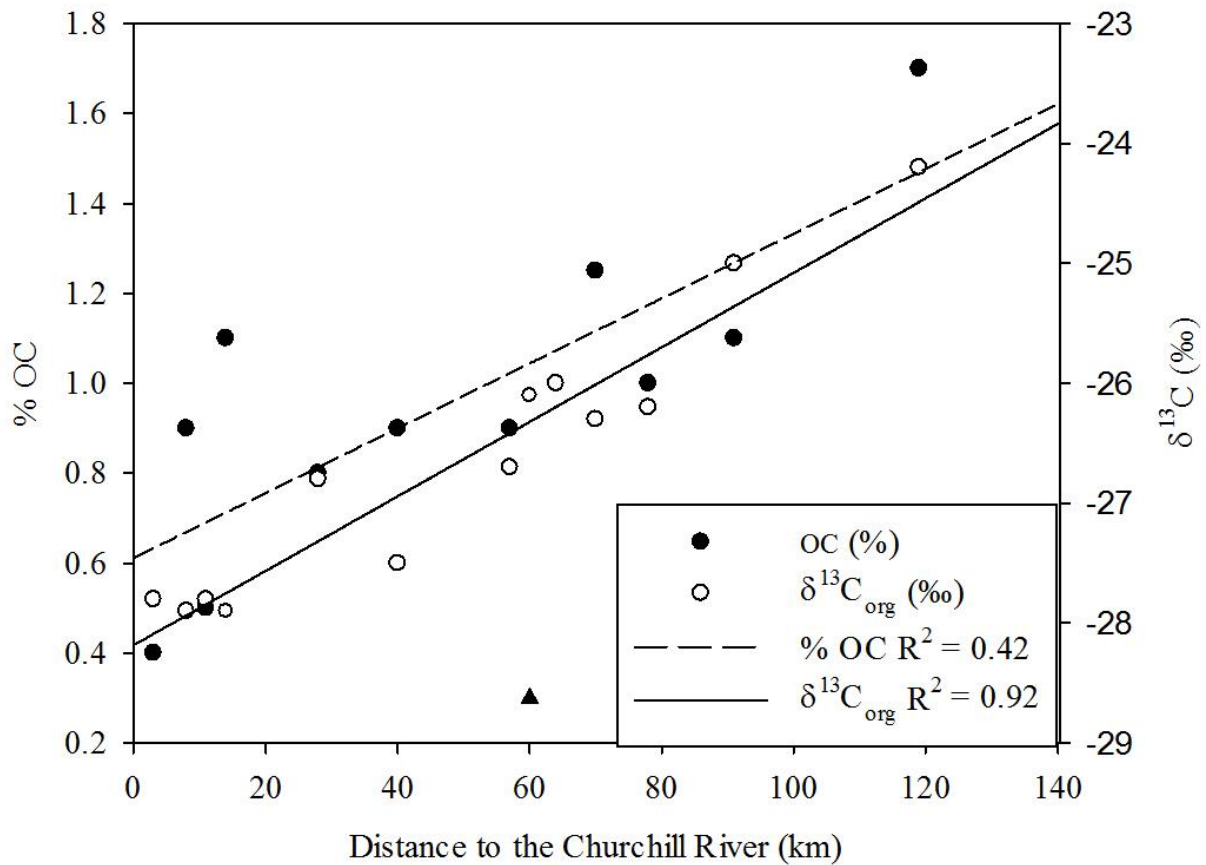
In the constricted eastern end of the Lake Melville proper (core DB6), where $^{210}\text{Pb}_{\text{ex}}$ inventory is greatest (core DB6, 55.9 ± 2.1 dpm cm^{-2}), the corresponding TOC (%) in surface sediment is greater than anywhere else in the LMS ($1.7 \pm 0.01\%$) (see Figure 2-9). Furthermore, in this area 70% of the TOC is OC_{mar} , which is more than double that in Goose Bay cores. More compelling, is the positive linear relationship between percentage of OC_{mar} in sediment cores and $^{210}\text{Pb}_{\text{ex}}$ inventories ($R^2=0.43$, $p<0.05$, $n=10$) (Figure 2-14b).

2.6.4 Terrestrial and marine influence on sediment composition inferred from $\delta^{13}\text{C}_{\text{org}}$

The two-layer estuarine circulation of the LMS strongly influences the distribution and composition of particulates across the system. Comparable to findings by Tan and Vilks (1987), $\delta^{13}\text{C}_{\text{org}}$ values and percentage of TOC in surficial sediment are significantly correlated with distance to the mouth of the Churchill River ($R^2=0.92$, $p<0.05$, $n=13$; $R^2=0.42$, $p<0.05$, $n=12$, respectively; Figure 2-15). The effect of strong terrigenous sources to the west and strong marine sources to the east are reflected in the relative proportions of the two OC sources in sediments at any given site. In Goose Bay, $\delta^{13}\text{C}_{\text{org}}$ and OC (%) are lowest (i.e., -27.8 ‰ and 0.4, respectively at site 26), reflecting the sites proximity to the major sources of terrestrial organic material and lithogenic material which would dilute the percentage of OC. The $\delta^{13}\text{C}_{\text{org}}$ values in Goose Bay (-

27.9 ‰) however, are slightly heavier (3.3 ‰) than the terrestrial endmember, -31.2 ± 1.66 ‰ (n=6) suggesting some degree of marine-derived OC in the western-most region of the Lake.

Figure 2-15. $\delta^{13}\text{C}$ (open dot) and OC content (black dot) plotted as a function of distance from the Churchill River. Site 29 (black triangle) was excluded from the OC regression analysis because this site is not considered a depositional area.



In Groswater Bay, east of the Narrows, $\delta^{13}\text{C}_{\text{org}}$ values in surface sediment reflect closely (-22.6 ± 0.28 ‰), albeit slightly light, the expected marine endmember of -21.3 ± 0.32 ‰. Tan and Vilks (1987) found that $\delta^{13}\text{C}_{\text{org}}$ values in the POC of the surface water remained relatively depleted across the lake, and similar to terrestrial OC. Thus, this slightly lighter $\delta^{13}\text{C}_{\text{org}}$ in surface sediment in Groswater Bay could reflect some inputs of OC_{terr} carried in the fresh surface water

of Lake Melville and deposited east of the Narrows where fresh surface water is mixed with saline water (Lu et al., 2013).

2.6.5 Inferences of Change from Profiles of $\delta^{13}C_{org}$ and OC

To investigate changes in the source and delivery of OC to the seafloor since the development of the Smallwood Reservoir and generating station at Churchill Falls, we used a transient tracer mixing model to establish the depth of sediment cores predominantly (90%) deposited pre- and post-development (1970) and compared average $\delta^{13}C_{org}$ signatures from the two time periods (see Figure 2-11a). In general, the average sedimentary $\delta^{13}C_{org}$ was heavier in sediments deposited before 1970 (mean = -26.2, SD = 1.3 ‰) and lighter after 1970 (mean = -26.5, SD = 1.3 ‰) with a small but significant difference between the two time periods ($t(9) = -4.9, p < 0.001$). The greatest difference, 0.7 ‰, in sediment deposited pre- and post-1970 was in Epinette Basin (core 34) and in the eastern most core (DB6) while the average difference across the Lake was 0.3 ‰.

Comparing profiles of OC_{mar} and OC_{terr} (%) in each of the ten cores (see Figure 2-11b) revealed that OC_{mar} is relatively invariant with some degree of burn down while OC_{terr} is more variable. The consistency of this change across the system, implies an increase in the delivery of OC_{terr} to the LMS rather than a change to the OC_{mar} after 1970. The most obvious changes in OC_{terr} are observed in cores 34, DB3, 33, and I13, all of which were collected from Lake Melville proper. For example, over the length of core 34, OC_{terr} decreased by about 0.18% with depth while OC_{mar} decreased by only about 0.01% between 7 and 18 cm. Similarly, in core 33, OC_{terr} decreased by 0.20% between 7 and 18 cm, while OC_{mar} fluctuated slightly but overall did not change.

Based solely on our data, we cannot determine the exact reason(s) for this lighter $\delta^{13}\text{C}_{\text{org}}$ signature and presumably greater OC_{terr} deposited in years after 1970. However, by combining our results with known historical development in the region and previously published findings, we propose possible explanations.

- 1) The Churchill River is the major source of sediment to Goose Bay and Lake Melville, it is reasonable to assume it is also a major supplier of OC_{terr} . Therefore, changes to the river could influence the delivery and type (i.e., soil organic material, fossil organic matter, fresh terrestrial plant material, and freshwater algae) of particulate OC_{terr} downstream (e.g., Kendall et al., 2001). Following the development of the Churchill Falls Generating Station and Smallwood Reservoir in the early 1970's, the mean annual discharge of the Churchill River increased by about $500 \text{ m}^3 \text{ y}^{-1}$ with the greatest increase (ca. $1000 \text{ m}^3 \text{ y}^{-1}$) taking place December to March (Bobbitt and Akenhead, 1982a; Syvitski, 1987). This increased discharge and change to seasonal runoff could have amplified OC_{terr} inputs to the system.
- 2) Records also show that atmospheric warming in the Labrador region has been ongoing since ca. 1998 (cf., Finnis and Bell, 2015; Way and Viau, 2014). Warming could contribute to accelerated contributions of POC_{terr} since 1970. For example, a warming atmosphere has been linked to changes in the type of OC delivered to coastal Arctic and sub-arctic environments over the last few decades through: i) alteration in river hydrology (e.g., Lammers et al., 2001; Roberts et al., 2012); ii) thawing of permafrost (e.g., Goni et al., 2005; Mann et al., 2015); and iii) longer open water season that favour greater fetch and storm surges (Lantuit et al., 2012), all of which could increase coastal and river bank erosion.

Due to the remoteness of Lake Melville, long term monitoring of this system is essentially non-existent. Therefore, it is difficult to conclude, with confidence, the reason(s) for

the observed increase in OC_{terr} after 1970. In light of this observed increase in OC_{terr} , the expected completion of the Lower Churchill Hydroelectric Project in 2017, and continuing climate change, long term monitoring of freshwater runoff, OC composition (POC and DOC), and coastal erosion is needed for assessing any biogeochemical changes to this system in the future.

2.7 Conclusion

Many of the parameters examined in this study are associated with distance to the Churchill River, which is seen as gradients along a west to east axis across the LMS. MARs are significantly associated with distance to the Churchill River with the greatest MAR found outside of Goose Bay near the mouth of the Kenamu River. Variation in MARs across the Lake axis can be attributed to three main factors: 1) additional inputs from smaller rivers, particularly the Kenamu River, whose channel morphology (meandering), proneness to flooding, and tributaries which drain the Mealy Mountains, all favour disproportionate contributions to the sediment supply and; 2) local topographic lows (troughs, basins, shoals, and shallow narrow channels) that affect waves, tides and currents, thus influencing the distribution of sediment.

Inventories of ^{137}Cs also decreased with distance from the mouth of Churchill River. From all cores, inventories of ^{137}Cs either met or exceeded the estimated inventory from direct atmospheric deposition implying additional inputs of ^{137}Cs from terrestrial sources (i.e., through river runoff or coastal erosion). We compared inventories of $^{210}Pb_{ex}$ to corresponding ^{137}Cs and the expected ratio in terrestrial soil. This comparison revealed that the majority of cores reflect terrestrial inputs. Patterns of $^{210}Pb_{ex}$ inventories however, generally oppose those of ^{137}Cs , suggesting an additional source of $^{210}Pb_{ex}$ in the eastern end of the Lake. This additional input of

$^{210}\text{Pb}_{\text{ex}}$ is most likely a reflection of boundary scavenging of dissolved $^{210}\text{Pb}_{\text{ex}}$ from landward flowing seawater.

Across the LMS, the distribution of $\delta^{13}\text{C}_{\text{org}}$ in surficial sediments indicates a mix of both terrestrial and marine OC, reflecting the two-layer water estuarine circulation of this system. Similar to findings by Tan and Vilks (1987), $\delta^{13}\text{C}_{\text{org}}$ values from surficial sediment across Lake Melville revealed a strong correlation with distance to the Churchill River. Down-core profiles of $\delta^{13}\text{C}_{\text{org}}$ revealed a small, but significant decrease in $\delta^{13}\text{C}_{\text{org}}$ between sediment deposited predominately before and after 1970. A comparison of profiles of OC_{terr} and OC_{mar} (%) revealed that the portion of OC_{terr} increased over time while OC_{mar} remained relatively consistent down-core, suggesting an increase in the supply of OC_{terr} rather than a decline in OC_{mar} over the last 43-44 years.

In seeking reasons for the increase in POC_{terr} , it is likely that the strongest source of POC_{terr} would be involved. Specifically, changes in the flow and drainage area of the Churchill River because of hydroelectric development of Churchill Falls in the 1970's would have released POC_{terr} (cf., Houel et al., 2006), thus likely increasing the delivery of such POC to Lake Melville, at least for some period until the system readjusted (cf., Newbury and McCullough, 1984). Climate warming could also lead to an increase in freshwater runoff to the LMS while at the same time, a shorter season of sea ice cover and greater storm events could increase coastal erosion and the delivery of OC_{terr} .

Acknowledgments

Funding was provided by ArcticNet NCE program and NSERC CERC. Support was provided by the Centre for Earth Observation Science at the University of Manitoba. Additional funding was

provided by the Northern Scientific Training Program. Grain size analyses was conducted by Helen Gillespie, Research Laboratory Co-ordinator Earth Sciences, Memorial University of Newfoundland.

2.8 References

- Alley, R. B., Clark, P. U., Huybrechts, P., and Joughin, I., 2005, Ice-sheet and sea-level changes: *Science*, v. 310, no. 5747, p. 456-460.
- Amec, 2008, Lower Churchill Hydroelectric Generation Project: Sedimentation and Morphodynamics Study
- Anderson, T., 1985, Rivers of Labrador: Canadian Special Publication of Fisheries and Aquatic Sciences 81, Ottawa 1985. 389.
- Appleby, P., and Oldfield, F., 1992, Applications of lead-210 to sedimentation studies, Uranium-series disequilibrium: applications to earth, marine, and environmental sciences. 2. ed.
- Appleby, P. G., and Oldfield, F., 1978, The calculation of lead-210 dates assuming a constant rate of supply of unsupported 210Pb to the sediment: *CATENA*, v. 5, no. 1, p. 1-8.
- Bailey, J. N.-L., Macdonald, R. W., Sanei, H., Outridge, P. M., Johannessen, S. C., Hochheim, K., Barber, D., and Stern, G. A., 2013, Change at the margin of the North Water Polynya, Baffin Bay, inferred from organic matter records in dated sediment cores: *Marine Geology*, v. 341, p. 1-13.
- Baskaran, M., and Naidu, A., 1995, 210 Pb-derived chronology and the fluxes of 210 Pb and 137 Cs isotopes into continental shelf sediments, East Chukchi Sea, Alaskan Arctic: *Geochimica et Cosmochimica Acta*, v. 59, no. 21, p. 4435-4448.
- Bentley, S. J., Kahlmeyer, E., and Bustin, M. R., 2012, Patterns and mechanisms of fluvial sediment flux and accumulation in two subarctic fjords: Nachvak and Saglek Fjords, Nunatsiavut, Canada: *Canadian Journal of Earth Sciences*, v. 49, no. 10, p. 1200-1215.
- Berner, R. A., 1971, Principles of chemical sedimentology NY, McGraw-Hill.
- Bobbitt, J., and Akenhead, S., 1982, Influence of controlled discharge from the Churchill River on Oceanography of Groswater Bay, Labrador.
- Boyer-Villemare, U., St-Onge, G., Bernatchez, P., Lajeunesse, P., and Labrie, J., 2013, High-resolution multiproxy records of sedimentological changes induced by dams in the Sept-Îles area (Gulf of St. Lawrence, Canada): *Marine Geology*, v. 338, p. 17-29.
- Burdige, D. J., 2006, Geochemistry of marine sediments, Princeton University Press Princeton.
- Canada, G. S. o., 1979, Surficial Material: Lake Melville, Newfoundland: Geological Survey of Canada, scale 1:250 000.
- Cardoso, D., and deYoung, B., 2002, Historical Hydrographic Data from Goose Bay, Lake Melville, and Groswater Bay, Labrador: 1950-1997.
- Coachman, L. K., 1953, River flow and winter hydrographic structure of the Hamilton Inlet-Lake Melville Estuary of Labrador, p. 21.
- Cochran, J. K., McKibbin-Vaughan, T., Dornblaser, M. M., Hirschberg, D., Livingston, H. D., and Buessler, K. O., 1990, 210 Pb scavenging in the North Atlantic and North Pacific oceans: *Earth and Planetary Science Letters*, v. 97, no. 3, p. 332-352.

- Crusius, J., and Anderson, R. F., 1995, Sediment focusing in six small lakes inferred from radionuclide profiles: *Journal of Paleolimnology*, v. 13, no. 2, p. 143-155.
- Déry, S. J., Mlynowski, T. J., Hernández-Henríquez, M. A., and Straneo, F., 2011, Interannual variability and interdecadal trends in Hudson Bay streamflow: *Journal of Marine Systems*, v. 88, no. 3, p. 341-351.
- Déry, S. J., and Wood, E., 2005, Decreasing river discharge in northern Canada: *Geophysical Research Letters*, v. 32, no. 10.
- Fang, Z., Yang, W., Zhang, X., Chen, M., Fan, D., Ma, Q., Zhang, R., Zheng, M., and Qiu, Y., 2013, Sedimentation and lateral transport of ²¹⁰Pb over the East China Sea Shelf: *Journal of Radioanalytical and Nuclear Chemistry*, v. 298, no. 2, p. 739-748.
- Finnis, J., and Bell, T., 2015, An analysis of recent observed climate trends and variability in Labrador: *The Canadian Geographer/Le Géographe canadien*.
- Fitzhugh, W., 1973, Environmental Approaches to the Prehistory of the North: *J. Wash. Acad. Sci*, v. 63, no. 2, p. 40.
- Flynn, W., 1968, The determination of low levels of polonium-210 in environmental materials: *Analytica chimica acta*, v. 43, p. 221-227.
- Fulton, R. J., Hodgson, D.A., Minning, G.V., 1981, Surficial Materials, Lake Melville, Newfoundland.
- Gilbert, R., 2000, Environmental assessment from the sedimentary record of high-latitude fiords: *Geomorphology*, v. 32, no. 3-4, p. 295-314.
- Goni, M. A., Yunker, M. B., Macdonald, R. W., and Eglinton, T. I., 2005, The supply and preservation of ancient and modern components of organic carbon in the Canadian Beaufort Shelf of the Arctic Ocean: *Marine Chemistry*, v. 93, no. 1, p. 53-73.
- Greene, B. A., 1974, *An Outline of the Geology of Labrador: 1974*.
- Henton, J. A., Craymer, M. R., Dragert, H., Mazzotti, S., Ferland, R., and Forbes, D. L., 2006, Crustal motion and deformation monitoring of the Canadian landmass: *Geomatica*, v. 60, no. 2, p. 173-191.
- Houel, S., Louchouart, P., Lucotte, M., Canuel, R., and Ghaleb, B., 2006, Translocation of soil organic matter following reservoir impoundment in boreal systems: Implications for in situ productivity: *Limnology and oceanography*, v. 51, no. 3, p. 1497-1513.
- Jenne, E. A., and Wahlberg, J., 1968, Role of certain stream-sediment components in radioion sorption, 2330-7102.
- Johannessen, S., Macdonald, R., and Paton, D., 2003, A sediment and organic carbon budget for the greater Strait of Georgia: *Estuarine, Coastal and Shelf Science*, v. 56, no. 3, p. 845-860.
- Johannessen, S. C., and Macdonald, R. W., 2012, There is no 1954 in that core! Interpreting sedimentation rates and contaminant trends in marine sediment cores: *Marine Pollution Bulletin*, v. 64, no. 4, p. 675-678.
- Johannessen, S. C., Macdonald, R. W., and Eek, K. M., 2005, Historical Trends in Mercury Sedimentation and Mixing in the Strait of Georgia, Canada: *Environmental Science & Technology*, v. 39, no. 12, p. 4361-4368.
- Jones, B. M., Arp, C., Jorgenson, M., Hinkel, K. M., Schmutz, J., and Flint, P., 2009, Increase in the rate and uniformity of coastline erosion in Arctic Alaska: *Geophysical Research Letters*, v. 36, no. 3.

- Kendall, C., Silva, S. R., and Kelly, V. J., 2001, Carbon and nitrogen isotopic compositions of particulate organic matter in four large river systems across the United States: *Hydrological Processes*, v. 15, no. 7, p. 1301-1346.
- Koide, M., Bruland, K. W., and Goldberg, E. D., 1973, Th-228/Th-232 and Pb-210 geochronologies in marine and lake sediments: *Geochimica et Cosmochimica Acta*, v. 37, no. 5, p. 1171-1187.
- Koide, M., Soutar, A., and Goldberg, E. D., 1972, Marine geochronology with 210 Pb: *Earth and Planetary Science Letters*, v. 14, no. 3, p. 442-446.
- Kuzyk, Z. Z. A., Gobeil, C., and Macdonald, R. W., 2013, 210Pb and 137Cs in margin sediments of the Arctic Ocean: Controls on boundary scavenging: *Global Biogeochemical Cycles*, v. 27, no. 2, p. 422-439.
- Kuzyk, Z. Z. A., Macdonald, R. W., Johannessen, S. C., Gobeil, C., and Stern, G. A., 2009, Towards a sediment and organic carbon budget for Hudson Bay: *Marine Geology*, v. 264, no. 3, p. 190-208.
- Kuzyk, Z. Z. A., Macdonald, R. W., Johannessen, S. C., 2015, Calculating Rates and Dates and Interpreting Contaminant Profiles in Biomixed Sediments *Environmental contaminants: Using natural archives to track sources and long-term trends of pollution.* : Dordrecht, Springer, p. 547.
- Lammers, R. B., Shiklomanov, A. I., Vörösmarty, C. J., Fekete, B. M., and Peterson, B. J., 2001, Assessment of contemporary Arctic river runoff based on observational discharge records: *Journal of Geophysical Research: Atmospheres* (1984–2012), v. 106, no. D4, p. 3321-3334.
- Lantuit, H., Overduin, P. P., Couture, N., Wetterich, S., Aré, F., Atkinson, D., Brown, J., Cherkashov, G., Drozdov, D., and Forbes, D. L., 2012, The Arctic coastal dynamics database: A new classification scheme and statistics on Arctic permafrost coastlines: *Estuaries and Coasts*, v. 35, no. 2, p. 383-400.
- Lantuit, H., and Pollard, W., 2008, Fifty years of coastal erosion and retrogressive thaw slump activity on Herschel Island, southern Beaufort Sea, Yukon Territory, Canada: *Geomorphology*, v. 95, no. 1, p. 84-102.
- Lavelle, J. W., Massoth, G. J., Crecelius, E. A., 1985, Sedimentation rates in Puget Sound from 210Pb measurements: National Oceanic and Atmospheric Administration.
- Liverman, D. G., 1997, Quaternary Geology of the Goose Bay area: Current Research. Newfoundland and Labrador Department of Mines and Energy, Geological Survey, Report, p. 97-91.
- Lu, Z., DeYoung, B., and Foley, J., 2013, Analysis of physical oceanography data from Lake Melville, Labrador, July-September 2012: Department of Physics and Physical Oceanography, Memorial University of Newfoundland.
- Mackenzie, A., Baxter, M., Mckinley, I., Swan, D., and Jack, W., 1979, The determination of 134Cs, 137Cs, 210Pb, 226Ra and 228Ra concentrations in nearshore marine sediments and seawater: *Journal of Radioanalytical and Nuclear Chemistry*, v. 48, no. 1-2, p. 29-47.
- Macpherson, A. G., and Macpherson, J. B., 1981, The natural environment of Newfoundland, past and present, Department of Geography, Memorial University of Newfoundland.
- Mann, P. J., Eglinton, T. I., McIntyre, C. P., Zimov, N., Davydova, A., Vonk, J. E., Holmes, R. M., and Spencer, R. G. M., 2015, Utilization of ancient permafrost carbon in headwaters of Arctic fluvial networks: *Nat Commun*, v. 6.

- Milliman, J. D., and Syvitski, J. P., 1992, Geomorphic/tectonic control of sediment discharge to the ocean: the importance of small mountainous rivers: *The Journal of Geology*, p. 525-544.
- Monetti, M. A., 1996, Worldwide deposition of strontium-90 through 1990: USDOE Environmental Measurements Lab., New York, NY (United States). Funding organisation: USDOE, Washington, DC (United States).
- Moore, W. S., and Dymondt, J., 1988, Correlation of ²¹⁰Pb removal with organic carbon fluxes in the Pacific Ocean: *Nature*, v. 331, no. 6154, p. 339-341.
- Muller-Karger, F. E., Varela, R., Thunell, R., Luerssen, R., Hu, C., and Walsh, J. J., 2005, The importance of continental margins in the global carbon cycle: *Geophysical Research Letters*, v. 32, no. 1.
- Murray, A. S., Marten, R., Johnston, A., and Martin, P., 1987, Analysis for naturally occurring radionuclides at environmental concentrations by gamma spectrometry: *Journal of Radioanalytical and Nuclear Chemistry*, v. 115, no. 2, p. 263-288.
- Muzuka, A. N., and Hillaire-Marcel, C., 1999, Burial rates of organic matter along the eastern Canadian margin and stable isotope constraints on its origin and diagenetic evolution: *Marine Geology*, v. 160, no. 3, p. 251-270.
- Newbury, R., and McCullough, G., 1984, Shoreline erosion and restabilization in the Southern Indian Lake reservoir: *Canadian Journal of Fisheries and Aquatic Sciences*, v. 41, no. 4, p. 558-566.
- Oguri, K., Harada, N., and Tadai, O., 2012, Excess ²¹⁰Pb and ¹³⁷Cs concentrations, mass accumulation rates, and sedimentary processes on the Bering Sea continental shelf: *Deep Sea Research Part II: Topical Studies in Oceanography*, v. 61, p. 193-204.
- Oughton, D. H., Børretzen, P., Salbu, B., and Tronstad, E., 1997, Mobilisation of ¹³⁷Cs and ⁹⁰Sr from sediments: potential sources to arctic waters: *Science of the total environment*, v. 202, no. 1-3, p. 155-165.
- Payette, S., Delwaide, A., Caccianiga, M., and Beauchemin, M., 2004, Accelerated thawing of subarctic peatland permafrost over the last 50 years: *Geophysical Research Letters*, v. 31, no. 18.
- Peterson, B. J., Holmes, R. M., McClelland, J. W., Vörösmarty, C. J., Lammers, R. B., Shiklomanov, A. I., Shiklomanov, I. A., and Rahmstorf, S., 2002, Increasing river discharge to the Arctic Ocean: *Science*, v. 298, no. 5601, p. 2171-2173.
- Prinsenber, S., Peterson, I., Holladay, J., and Lalumiere, L., Snow and Ice Thickness Properties of Lake Melville, a Canadian Fjord Located along the Labrador Coast, *in Proceedings The Twenty-first International Offshore and Polar Engineering Conference 2011*, International Society of Offshore and Polar Engineers.
- Rachold, V., Grigoriev, M. N., Are, F. E., Solomon, S., Reimnitz, E., Kassens, H., and Antonow, M., 2000, Coastal erosion vs riverine sediment discharge in the Arctic Shelf seas: *International Journal of Earth Sciences*, v. 89, no. 3, p. 450-460.
- Radakovitch, O., Sanchez-Cabeza, J. A., Abassi, A., Masqué, P., and Heussner, S., 2003, Meso and small-scale variations of ²¹⁰Pb fluxes on the Northwestern Mediterranean continental margins: *Continental Shelf Research*, v. 23, no. 7, p. 693-715.
- Robbins, J. A., 1978, The biogeochemistry of lead in the environment, *in* JO, N., ed.: Amsterdam, Elsevier/North-Holland Biomedical Press, p. 285-393.

- Robbins, J. A., and Edgington, D. N., 1975, Determination of recent sedimentation rates in Lake Michigan using Pb-210 and Cs-137: *Geochimica et Cosmochimica Acta*, v. 39, no. 3, p. 285-304.
- Roberts, B. A., Simon, N. P. P., and Deering, K. W., 2006, The forests and woodlands of Labrador, Canada: ecology, distribution and future management: *Ecological Research*, v. 21, no. 6, p. 868-880.
- Roberts, J., Pryse-Phillips, A., and Snelgrove, K., 2012, Modeling the Potential Impacts of Climate Change on a Small Watershed in Labrador, Canada: *Canadian Water Resources Journal / Revue canadienne des ressources hydriques*, v. 37, no. 3, p. 231-251.
- Sella, G. F., Stein, S., Dixon, T. H., Craymer, M., James, T. S., Mazzotti, S., and Dokka, R. K., 2007, Observation of glacial isostatic adjustment in “stable” North America with GPS: *Geophysical Research Letters*, v. 34, no. 2.
- Smith, J., and Ellis, K., 1982, Transport mechanism for Pb-210, Cs-137 and Pu fallout radionuclides through fluvial-marine systems: *Geochimica et Cosmochimica Acta*, v. 46, no. 6, p. 941-954.
- Smith, J. N., 2001, Why should we believe ^{210}Pb sediment geochronologies?: *Journal of Environmental Radioactivity*, v. 55, no. 2, p. 121-123.
- Smith, J. N., Ellis, K. M., and Nelson, D. M., 1987, Time-dependent modeling of fallout radionuclide transport in a drainage basin: Significance of “slow” erosional and “fast” hydrological components: *Chemical Geology*, v. 63, no. 1–2, p. 157-180.
- Smith, L. M., Alexander, C., and Jennings, A. E., 2002, Accumulation in East Greenland Fjords and on the Continental Shelves Adjacent to the Denmark Strait over the Last Century Based on ^{210}Pb Geochronology: *Arctic*, p. 109-122.
- Smith, R. W., Bianchi, T. S., Allison, M., Savage, C., and Galy, V., 2015, High rates of organic carbon burial in fjord sediments globally: *Nature Geoscience*.
- Smith, S., and Hollibaugh, J., 1993, Coastal metabolism and the oceanic organic carbon balance: *Reviews of Geophysics*, v. 31, no. 1, p. 75-89.
- Smoak, J. M., DeMaster, D. J., Kuehl, S. A., Pope, R. H., and McKee, B. A., 1996, The behavior of particle-reactive tracers in a high turbidity environment: ^{234}Th and ^{210}Pb on the Amazon continental shelf: *Geochimica et Cosmochimica Acta*, v. 60, no. 12, p. 2123-2137.
- Stein, R., and Macdonald, R., 2004, Geochemical proxies used for organic carbon source identification in Arctic Ocean sediments: In: Stein, R. and Macdonald, RW (Eds.), *The Organic Carbon Cycle in the Arctic Ocean*. Springer-Verlag, Berlin, p. 24-32.
- Sugai, S. F., 1990, Transport and sediment accumulation of ^{210}Pb and ^{137}Cs in two Southeast Alaskan fjords: *Estuaries*, v. 13, no. 4, p. 380-392.
- Syvitski, J., Burrell, D., and Skei, J., 1987, *Fjords: Processes and Products*, New York, NY, Springer-Verlag, 379 p.:
- Syvitski, J., Hinds, S.J., Burns, J.A., 1993, *Marine geology of Lake Melville (Labrador)*, scale 1:100,000.
- Syvitski, J., Schafer, C., 1990, *ADFEX Environmental Impact Statement (EIS)*.
- Syvitski, J. P., and Lee, H. J., 1997, Postglacial sequence stratigraphy of Lake Melville, Labrador: *Marine Geology*, v. 143, no. 1, p. 55-79.
- Syvitski, J. P., Vörösmarty, C. J., Kettner, A. J., and Green, P., 2005, Impact of humans on the flux of terrestrial sediment to the global coastal ocean: *Science*, v. 308, no. 5720, p. 376-380.

- Tan, F., and Vilks, G., 1987, Organic carbon isotope ratios and paleoenvironmental implications for Holocene sediments in Lake Melville, southeastern Labrador: *Canadian Journal of Earth Sciences*, v. 24, no. 10, p. 1994-2003.
- Vilks, G., Deonarine, B., and Winters, G., 1987, Late Quaternary Marine Geology of Lake Melville, Labrador: Geological Survey of Canada.
- Vörösmarty, C. J., Green, P., Salisbury, J., and Lammers, R. B., 2000, Global water resources: vulnerability from climate change and population growth: *Science*, v. 289, no. 5477, p. 284-288.
- Vörösmarty, C. J., Meybeck, M., Fekete, B., Sharma, K., Green, P., and Syvitski, J. P., 2003, Anthropogenic sediment retention: major global impact from registered river impoundments: *Global and Planetary Change*, v. 39, no. 1, p. 169-190.
- Walling, D., and He, Q., 2000, The global distribution of bomb-derived ¹³⁷Cs reference inventories: Final report on IAEA technical contract, v. 10361, p. 1-19.
- Walling, D., and Qingping, H., 1992, Interpretation of caesium-137 profiles in lacustrine and other sediments: the role of catchment-derived inputs: *Hydrobiologia*, v. 235, no. 1, p. 219-230.
- Way, R. G., and Viau, A. E., 2014, Natural and forced air temperature variability in the Labrador region of Canada during the past century: *Theoretical and Applied Climatology*, p. 1-12.
- Wright, S., Howard, B., Strand, P., Nylén, T., and Sickel, M., 1999, Prediction of ¹³⁷Cs deposition from atmospheric nuclear weapons tests within the Arctic: *Environmental Pollution*, v. 104, no. 1, p. 131-143.
- Yang, W., Guo, L., Chuang, C.-Y., Santschi, P. H., Schumann, D., and Ayrano, M., 2015, Influence of organic matter on the adsorption of ²¹⁰Pb, ²¹⁰Po and ⁷Be and their fractionation on nanoparticles in seawater: *Earth and Planetary Science Letters*, v. 423, p. 193-201.
- Zaborska, A., Carroll, J., Papucci, C., and Pempkowiak, J., 2007, Intercomparison of alpha and gamma spectrometry techniques used in ²¹⁰Pb geochronology: *Journal of environmental radioactivity*, v. 93, no. 1, p. 38-50.

Chapter 3 : Sediment and particulate organic carbon budgets of Lake Melville, Labrador

3.1 Abstract

In this study, sediment and terrestrial and marine particulate organic carbon (POC) budgets were constructed for the Lake Melville system, a large fjard estuary that receives runoff from the Churchill River in central Labrador. To estimate the exchange between Goose Bay, a western extension of Lake Melville that receives the majority of river runoff, and Lake Melville proper, the system was divided into two compartments. The sources, sinks, and losses of sediment and organic carbon were quantified using previously published data and new unpublished data. ^{210}Pb -based sedimentation rates, a $\delta^{13}\text{C}_{\text{org}}$ two-endmember mixing model and down-core profiles of organic carbon (%), were applied to a first-order degradation model to establish surface sediment flux and rates of burial and oxidation of marine and terrestrial OC in eight sediment cores collected in 2013 and 2014.

The Churchill River is the major source of sediment and terrestrial POC (POC_{terr}), contributing 74% of the total $34.0 \times 10^8 \text{ kg sediment yr}^{-1}$ and 53% of the total $34.7 \times 10^6 \text{ kg POC}_{\text{terr yr}^{-1}}$ input to the Lake Melville system. Although the Churchill River drains directly into Goose Bay, 76% and 95% of its sediment and POC_{terr} inputs are transported to Lake Melville, respectively. Goose Bay captures only 6% of the $20.2 \times 10^8 \text{ kg POC}_{\text{terr yr}^{-1}}$ input from the Churchill and Goose Rivers. Lake Melville buries 25% of the $32.1 \times 10^6 \text{ kg yr}^{-1}$ of the total POC_{terr} inputs .

Rates of new OC production (i.e., primary production), estimated by applying fluxes of marine OC at the sediment surface to a regression equation, revealed a “hotspot” of primary production ($165.6 \text{ g OC}_{\text{mar}} \text{ m}^{-2} \text{ yr}^{-1}$) in the eastern end of Lake Melville. This area, considered non-representative of the rest of the fjord (median = $42.5 \text{ g C m}^{-2} \text{ yr}^{-1}$), is associated with increased nutrients due to upwelling and a deeper euphotic zone. About 64% of the total primary production ($100.1 \times 10^6 \text{ kg yr}^{-1}$) in Goose Bay and Lake Melville is oxidized within the water column and at the sediment surface while 13% is buried. Exports of suspended sediment from Lake Melville to Groswater Bay are estimated at $4.7 \times 10^8 \text{ kg yr}^{-1}$ or 21% of total inputs. Assuming POC_{terr} and POC_{mar} parallels suspended sediment, $6.2 \times 10^6 \text{ kg POC}_{\text{terr}} \text{ yr}^{-1}$ and $19.5 \times 10^6 \text{ kg POC}_{\text{mar}} \text{ yr}^{-1}$ is lost to Groswater Bay.

We conclude that the supply and distribution of sediment and POC in Goose Bay and Lake Melville is dominated by the Churchill River. The runoff from the Churchill River probably has a major influence on primary production by reducing light penetration through its turbid discharge and driving estuarine circulation. In light of a new hydroelectric project on the Lower Churchill River, we estimate a doubling of sediment ($49.5 \times 10^8 \text{ kg yr}^{-1}$) and POC_{terr} ($24.3 \times 10^8 \text{ kg yr}^{-1}$) inputs from the Churchill River to the downstream environment in the first 2 years after impoundment.

3.2 Introduction

The development of sediment and organic carbon (OC) budgets are important for elucidating sources, sinks, and losses of particulates in marine systems. Simultaneously, sediment and OC budgets provide a means to quantify fundamental processes (i.e., inputs, remineralization, burial, export) which are essential to understanding elemental (Hare et al.,

2008) and biogeochemical cycling in marine environments (cf., Stein and Macdonald, 2004b and references within). The development of sediment and OC budgets of coastal environments are particularly crucial because these, often productive hotspots, are important regions for the transfer of sediment and nutrients between land and the open ocean.

Often, coastal environments like estuaries and fjords have high sedimentation and OC burial rates making them important sinks in the global carbon budget (Zhu and Olsen, 2013). Recently, Smith et al. (2015) highlighted the important role of high latitude fjords in regulating global atmospheric CO₂ levels over glacial-interglacial time scale by efficiently burying carbon. The capacity of fjords to sequester carbon is, however, under increasing pressure from hydroelectric and reservoir development upstream which traps sediment (cf., Brandt, 2000; Williams and Wolman, 1984, and references within). Because of the retention of sediment within reservoirs the sediment flux to coastal environments has decreased by approximately $1.4 \pm 0.3 \text{ Gt yr}^{-1}$ to $4\text{-}5 \text{ Gt yr}^{-1}$ globally (Syvitski et al., 2005; Vörösmarty et al., 2003). In contrast, a warming climate can increase sediment input and terrigenous OC by accelerating coastal erosion (Jones et al., 2009; Lantuit and Pollard, 2008; Payette et al., 2004). By developing sediment and OC budgets, an understanding of the processes most sensitive to future changes can be recognized (Johannessen et al., 2003; Kuzyk et al., 2009) and used to mitigate possible impacts to people and communities most directly connected to these environments (Barrie et al., 1992; Mason et al., 2012).

Lake Melville is a subarctic fjard estuary in central Labrador, the eastern half of which lies within the Nunatsiavut Inuit Settlement Area and is used extensively for fishing, hunting, and travelling by local Inuit people. Lake Melville is classified as a “fjard” because of its low-lying shoreline and irregular basins consisting of a series of troughs, shoals, sills, and narrows (see Brown et al., 2012; Carpenter, 2012). Lake Melville receives saline bottom water from the Labrador Sea through a shallow and long passageway known as the Narrows while processing

about 45% of the total surface runoff of Labrador. Therefore, Lake Melville is influenced by both the Labrador Sea and the interior hydrology and land-use practices within its watershed.

Since the early 1970s the headwaters of the Churchill River, the largest source of freshwater to Lake Melville, has been regulated by the Churchill Falls power generating station and Smallwood Reservoir. Impacts to the downstream environment from this past development on the Upper Churchill River are largely unknown because almost no previous work has studied the system. As such, primary productivity, the basis of the food chain and the link between the inorganic and organic carbon cycle, remains largely unknown. Schartup et al. (2015) stated that Lake Melville is oligotrophic, suggesting low productivity. However, the combination of large river runoff (ca. $3000 \text{ m}^3 \text{ sec}^{-1}$) and upwelling on the seaward side of the Narrows (Lu et al., 2013), points to a greater flux of nutrients. High nutrient fluxes should translate to net phytoplankton production and increased growth and productivity in higher trophic species (Cloern et al., 2014). Then again, large river runoff could limit primary production by increasing turbidity in surface water and thus, inhibit light penetration and restrict euphotic zone depth (Granskog et al., 2007; Uncles and Cloern, 1987).

The new hydroelectric project on the Lower Churchill River will begin to alter river flow in 2016 by flooding 41 km^2 of land behind Muskrat Falls; the generation of power will begin in 2017-18. This new development is located only 40 km from Goose Bay. Although the Churchill River is the main source of freshwater to Lake Melville, the downstream environment was not fully assessed. In addition to future hydrologic changes, the Lake Melville region has experienced warm winter anomalies events the late 1990's (Finnis and Bell, 2015). Here, sediment and OC budgets are developed for Goose Bay and Lake Melville to provide a base to assess changes to Lake Melville in the future. The budgets were constructed from previously

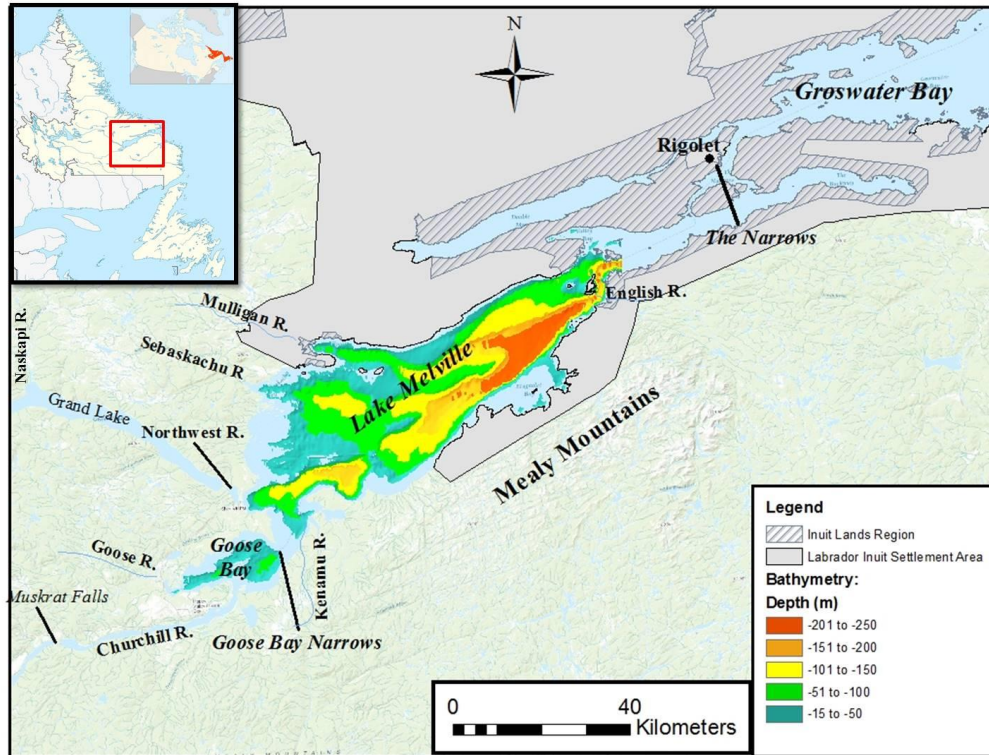
published literature and newly collected sediment boxcore and suspended particulate data. The objectives of this study are:

- 1) to apply newly acquired sedimentation rates to corresponding profiles of sedimentary organic carbon (OC) to estimate sediment fluxes and determine rates of OC burial and oxidation in the sediments of Lake Melville;
- 2) to develop contemporary box-models that incorporate the inputs, outputs and sinks of sediment and terrestrial and marine OC in Lake Melville so that these values can be used to assess potential changes to the system in the future.

3.3 Study Area

Lake Melville is a subarctic, fjard estuary, located partly in the Nunatsiavut Inuit land claim region of central Labrador, Canada at 53.55°N and 59.58°W (Figure 3-1). The fjard lies within the boreal forest ecoregion and is characterized by cold winters and short summers. By late November, saline land fast ice begins to form over Lake Melville with complete freeze up by mid-December and breakup in late April to May. Geologically, the area represents the northern extent of the Grenville Province, a subdivision of the Precambrian Canadian Shield, comprised of metamorphic gneiss rock overlain by extensive marine, glacial fluvial and alluvial deposits (Greene, 1974; Wardle, 1997). Flat lowlands surround the fjard, except along the southern shore where the Mealy Mountain range rises to a maximum altitude of 1,200 m a.s.l. (Gray, 1969).

Figure 3-1. Map of Hamilton Inlet, major inflowing rivers (Churchill, Goose, Northwest, and Kenamu), smaller rivers (Sebaskachu, Mulligan and English) and Inuit lands, settlement, and community (Rigolet).

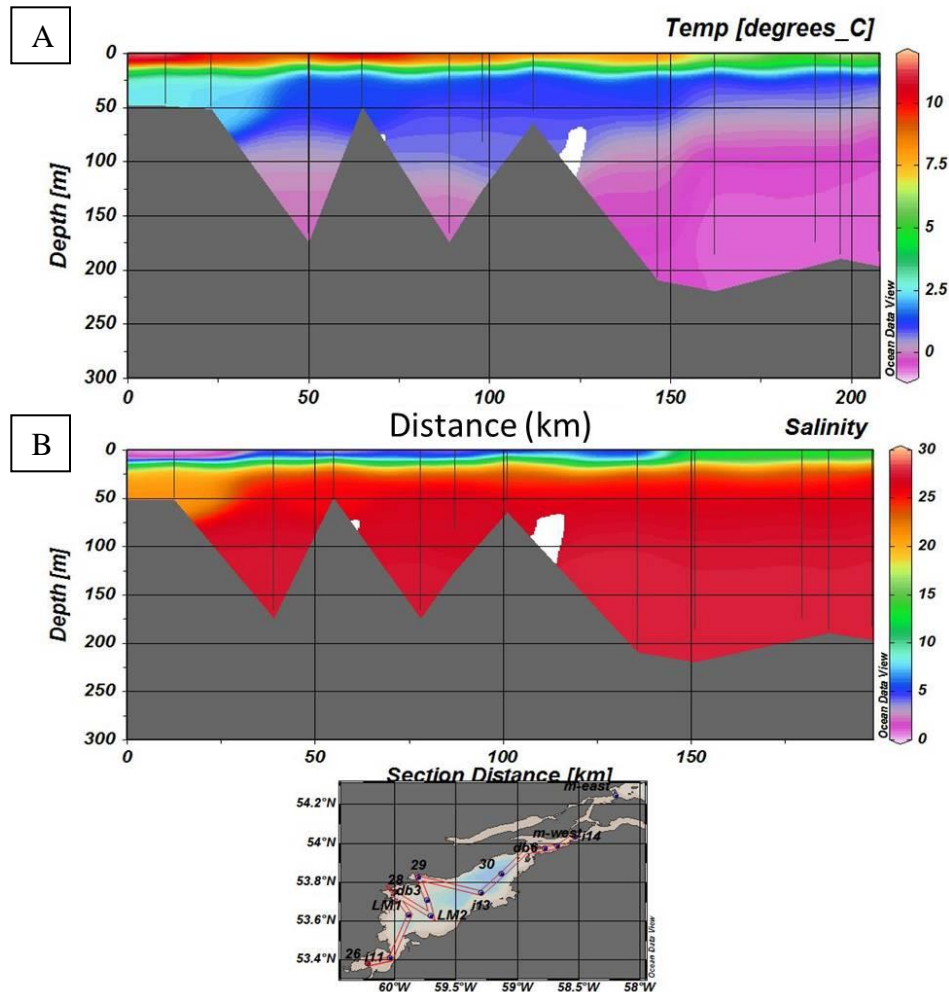


As part of Hamilton Inlet, the largest inlet on the Labrador coast, Lake Melville is connected to Groswater Bay and the Labrador Sea through a narrow (2.8 km) and shallow channel known as the Narrows. Near the community of Rigolet, a sill decreases water depth to 30 m, restricting exchange of seawater between Lake Melville and Groswater Bay. The Narrows dampens the tidal range from 1.3-3.0 m in Groswater Bay to 0.2-0.7 m in Lake Melville (Bobbitt and Ackenhead, 1982). Lake Melville itself extends from the Narrows westward ca.130 km to the mouth of Goose Bay where a shallow (8 m) and narrow (2.5 km) shipping channel, known as Goose Bay Narrows, connects Lake Melville and Goose Bay. Similar to the Narrows connecting Lake Melville to Groswater Bay, the Goose Bay Narrows dampens tidal range in Goose Bay to ≤

0.3 m (Amec and BAE-Newplan., 2001). Lake Melville and Goose Bay are referred to collectively as the Lake Melville System (LMS).

The oceanography of Goose Bay and Lake Melville is dominated by estuarine circulation, with fresh surface water flowing seaward over saline bottom water that flows landward (Figure 3-2). The fresh surface water primarily originates from four major rivers, Churchill, Goose, Northwest (NW), and Kenamu. These main rivers drain into Goose Bay and the western end of Lake Melville while smaller rivers (Mulligan, Sebaskachu, and English) drain into the north and south shoreline (Table 3-1). The Churchill River is the largest river in Labrador with a mean discharge of ca. $1,700 \text{ m}^3 \text{ sec}^{-1}$ and drainage area of $92,500 \text{ km}^2$ (Bobbitt and Ackenhead, 1982). Since 1972 the headwaters of the Churchill River have been regulated by the Churchill Falls hydroelectric generating station and Smallwood Reservoir. This regulation of the Upper Churchill River has tripled base flow in wintertime and decreased flow by about 30% in summer (Bobbitt and Ackenhead, 1982). At the same time, hydrological variation has been dampened by the controlled discharge at the Churchill Falls generating station. For example, prior to regulation discharge increased from winter to spring freshet (May to June) by ca. $1,200 \text{ m}^3 \text{ s}^{-1}$ while regulation reduced fluctuations between wintertime and springtime so that flow increases by only about $500 \text{ m}^3 \text{ s}^{-1}$ (Syvitski, 1987).

Figure 3-2. June 2013 temperature (A) and salinity (B) distribution of the water column of Goose Bay and Lake Melville.



The landward flowing saline bottom waters of Lake Melville and Goose Bay originate from Groswater Bay where salinity at sill depth is greater (ca. 33) than at comparable depth inside Lake Melville. Bobbitt and Akenhead (1982) suggest that, to create the bottom water mass in Lake Melville, landward flowing sea water is cooled and mixed to some degree in the Narrows, thus reducing bottom water salinity to ca. 24-28 in Lake Melville. Within Goose Bay and Lake Melville, the two water masses are separated by a halocline at 10-20 m with little evidence of entrainment of saline bottom water into the surface water (Bobbitt and Akenhead, 1982). The bottom water remains oxidic year round.

Table 3-1. Properties of rivers draining into Lake Melville.

Rivers	Watershed Area (km ²) ¹	Basin Relief (m) ²	Mean Annual Discharge (m ³ s ⁻¹)	Particulate Matter $\delta^{13}\text{C}_{\text{org}}$ (‰) ³
Churchill	92 500		1769	-31.6
Northwest				-31.1
Kenamu	4400	305	266 ⁴	
Goose	3432	610	204 ⁴	-27.1
Mulligan	1062	366		
English	640	1037		
Sebaskachu	580	211		

¹Anderson (1985). ²Environment Canada Water Survey (station 03OE001). ³Averaged from particulate matter collection in June 2013 and October 2014. ⁴Coachman (1953).

3.4 Methods

3.4.1 General approach

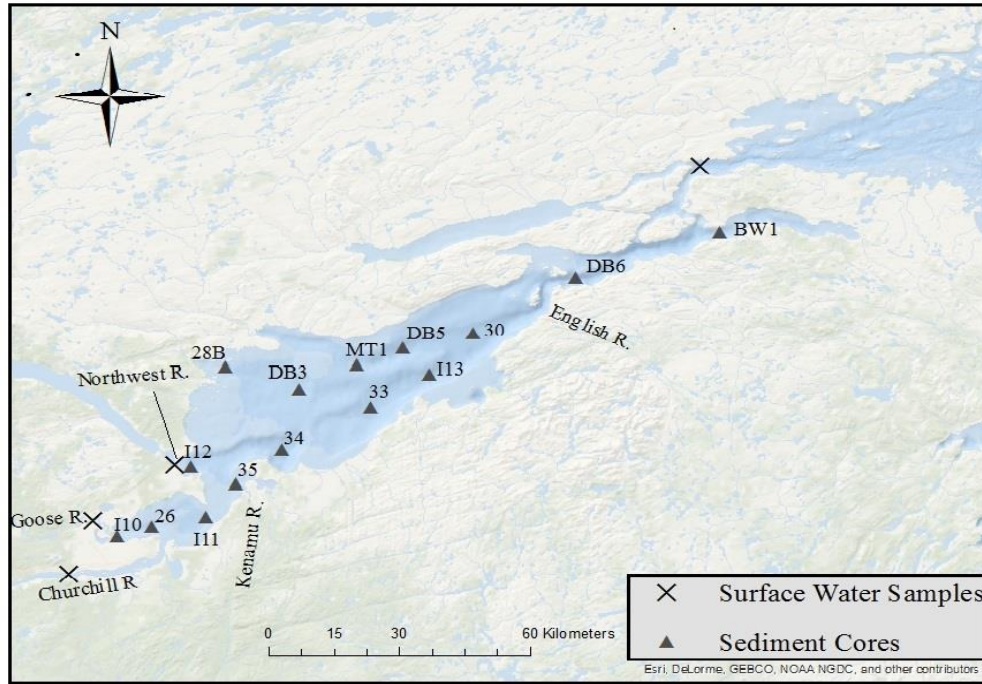
A mass balance box-model of the sources, sinks, and losses of sediment and particulate organic carbon (POC) in Goose Bay and Lake Melville was constructed from previously published literature and newly collected data (10-17 June 2013 and 17-22 October 2014). The box-model was set up by dividing the system into two boxes, Goose Bay and Lake Melville. This division was made because the shallow (8 m) Goose Bay Narrows is expected to restrict passage between Goose Bay and Lake Melville proper. Also, by compartmentalizing the system in this way, the amount of sediment and POC from the Churchill River transported into Lake Melville proper could be quantified. Sinks were estimated using hypsometry data and newly acquired ²¹⁰Pb_{ex}-based sedimentation rates (validated with ¹³⁷Cs). Sediment core profiles of marine and terrestrial OC were modelled to establish OC fluxes, and rates of burial and oxidation. The supplies of sediment and POC from river runoff were estimated from total suspended solids

(TSS) and POC data obtained in 2013 and 2014 and from limited published data (i.e., discharge rates, TSS data).

3.4.2 Sample collection

Sediment core collection is described in Chapter 2. In brief, 15 sediment box cores were collected from water depths of 25 to 220 m across Lake Melville in 10-17 June 2013 and 17-22 October 2014 from aboard *R/V Nuliak* and *M/V What's Happening*, respectively (Figure 3-3). Upon successful retrieval of the box core (i.e., water sealed and sediment undisturbed), surface water was carefully siphoned off and a 10 cm diameter core tube was pushed slowly into the sediment and capped at both ends. Within 12 hours of collection, sediment cores were sectioned into 1 cm intervals, placed in whirl packs, homogenized by hand and kept frozen while transported to U of M.

Figure 3-3. Map of sample locations. All sediment cores were used to establish mass accumulation rates and the size of the sediment sink except core I11, which was mixed throughout.



Near the mouths of the Churchill, Goose, and Northwest Rivers, a submersible pump was placed ca. 0.5 m below the water surface and, for approximately 0.5 to 1 hour, water was pumped through a Teflon-lined hose. The hose was connected to a stainless steel filter holder where suspended particulate matter (SPM) was collected on pre-combusted (ca. 550°C) Whatman® GF/F (nominal pore size, 0.7µm). Following collection (2013 and 2014), filters were wrapped in pre-combusted tinfoil and kept frozen until further analysis. Bulk water was also collected near the surface at several locations for subsequent filtration and analyses of TSS and POC. The bulk water was kept cool during transport to U of M. Then, in the lab, after inverting the container three times, 500 mL of water was vacuum filtered through pre-weighed Whatman GF/C filters. Filters were dried overnight at 105°C, cooled in a desiccator for ≥5 hours and re-

weighed. TSS was calculated from the difference of the pre and post filter weight and blank corrected.

3.4.3 Radioisotope analysis and calculation of sedimentation rates

As described in detail in the Chapter 2, activities of radioisotopes ^{210}Pb , ^{137}Cs , and ^{226}Ra were counted down 15 sediment cores by gamma ray spectrometry at the Environmental Radiochemistry Laboratory (ERL) at U of M. Activities of ^{226}Ra were determined indirectly by counting ^{214}Pb , its granddaughter isotope, at 352 keV. Total ^{210}Pb and ^{137}Cs were counted at 47 and 661 keV, respectively. Prior to analysis, subsamples of sediment slices were freeze dried at -50°C , homogenised using a pestle and mortar, and sealed in 50 x 9 mm Petri dishes for a minimum of three weeks. Porosity was calculated from the difference between wet and dry weights and were corrected for salt content assuming a density of 2.65 g cm^{-2} , which is considered typical for marine sediment (cf., Burdige, 2006). Radioisotope activities were corrected for sample weight and geometry (i.e., Petri dishes). Activities of $^{210}\text{Pb}_{\text{ex}}$ were calculated by subtracting activities of ^{226}Ra from total ^{210}Pb . To assess the appropriateness of using gamma to measure ^{210}Pb in sediment from Lake Melville, we followed the recommendation of Zaborska et al. (2007) and subjected cores 26, DB3, MT1, and I13 to alpha ray spectrometry using a similar method outlined by Flynn (1968). Sedimentation velocity and mass accumulation rates (MAR) were established by fitting the down core profile of $\ln ^{210}\text{Pb}_{\text{ex}}$ to a two-layer advection diffusion model (cf., Lavelle, 1985). As recommended by Smith (2001), sediment velocity and MARs were validated using a separate transient tracer, ^{137}Cs . Using a transient tracer model that included mixing (cf., Johannessen et al., 2005; Kuzyk et al., 2013), we applied an input function to fit the onset of ^{137}Cs observed in our cores. This model, performed in MATLAB®, included zero activity for 3 years (1951-1954), 8.2 dpm g^{-1} for 9 years (1954-

1963), 1.2 dpm g⁻¹ for 35 years (1963-1998), and 0.2 dpm g⁻¹ for 15 years (1998-2013). Included in the model was the mixing rate, sediment velocity, and flux at the sediment-water interface estimated from modelling ²¹⁰Pb_{ex}.

3.4.4 Stable Isotope and bulk organic carbon analysis

Total organic carbon content (OC) and stable carbon isotope ratios of organic carbon ($\delta^{13}\text{C}_{\text{org}}$) were measured down ten sediment cores (I10, 26, I12, 34, DB3, MT1, 33, I13, 30, DB6) from across Lake Melville at the Stable Isotope for Innovative Research Laboratory (SIFIR) at U of M. The OC content was calculated from the difference between total carbon (TC) and inorganic carbon (IC). Both TC and IC were measured on dried, pre-weighed sediment samples using an elemental analyser. Replicate analyses of QC standards B2150 (TC) and AR1034 (IC) indicate a propagated precision for OC of $\pm 0.1\%$. $\delta^{13}\text{C}_{\text{org}}$ (‰ relative to VPDB) was measured using an elemental analyser isotope-ratio mass spectrometer (EA-IRMS). Before analysis, dried samples were decarbonated with 6M HCl and re-dried in an oven for about three days. The international standard, USGS Green River shale SGR-1b, was treated and analysed along with samples and yielded a precision of $\pm 0.1\%$ (n=21). Particulate material collected on filters was measured for bulk POC and $\delta^{13}\text{C}_{\text{org}}$ at the University of British Columbia. The analyses were conducted on acid de-carbonated filters using a Carlo Erba NA-1500 Elemental Analyzer and in-line isotope ratio mass spectrometer.

3.4.5 Calculations for organic carbon surface flux, burial and oxidation rates

Profiles of OC content in the cores together with mass accumulation rates (MARs) were used to estimate the surface OC flux to the seafloor and rates of OC burial and oxidation (remineralisation). Assuming steady state conditions, negligible bioturbation effects (relative to oxidation), and only one type of reactive organic matter, a simple first-order degradation model

was fitted to profiles of the natural log of OC concentration (g OC per g sediment) versus cumulative mass to depth (g cm^{-2}) (cf., Burdige, 2006; Johannessen et al., 2003; Kuzyk et al., 2009) (Eq 1):

$$\text{OC}(m) = \text{OC}(m=0) * \exp(-km/\text{MAR}) \quad \text{Eq. 1}$$

where m is mass-depth (g cm^{-2}), k is oxidation rate constant (yr^{-1}), and MAR is sediment mass accumulation rate ($\text{g cm}^{-2} \text{ yr}^{-1}$). k was estimated by multiplying the MAR by the slope of $\ln \text{OC}$ versus mass-depth (above burial depth). Burial depths were visually determined as the depth where exponential decay of OC was no longer observed in the profile. The rate of burial was calculated as:

$$\text{Burial Rate} = \text{Average}(\text{OC below burial depth}) * \text{MAR} \quad \text{Eq. 2}$$

Assuming reactive (or metabolizable) OC degrades with first-order kinetics, only one boundary condition, the OC flux at the sediment surface ($\text{OC}_{m=0}$) (Eq. 3), was applied:

$$\text{Surface Flux} = \ln \text{OC}_{(m=0)} * \text{MAR} \quad \text{Eq. 3}$$

where $\ln \text{OC}_{(m=0)}$ was established from the intercept of $\ln \text{OC}$ ($\text{g OC g sediment}^{-1}$) at mass-depth = 0 g cm^{-2} . The oxidation rate was determined as the difference between the surface flux of OC and the burial rate.

The proportions of marine OC (OC_{mar}) and terrigenous OC (OC_{terr}), in the sediment cores, and their surface fluxes, burial and oxidation rates, were estimated using a two endmember mixing model and corresponding profiles of $\delta^{13}\text{C}_{\text{org}}$ (Kuzyk et al., 2009):

$$\delta^{13}\text{C}_{\text{org}} = (F_{\text{mar}})(\delta^{13}\text{C}_{\text{mar}}) + (1 - F_{\text{mar}})(\delta^{13}\text{C}_{\text{terr}}) \quad \text{Eq. 4}$$

where $\delta^{13}\text{C}_{\text{org}}$ is the measured $\delta^{13}\text{C}_{\text{org}}$ (‰) of the sediment sample, F_{mar} is the fraction of OC_{mar} , and $\delta^{13}\text{C}_{\text{mar}}$ and $\delta^{13}\text{C}_{\text{terr}}$ are the marine and terrestrial end-members, estimated at -21.3 ± 0.32 ‰ (n=5) and -31.2 ± 1.66 ‰ (n=6) (mean $\pm 1\sigma$), respectively. The terrestrial endmember was estimated using the discharge-weighted mean of $\delta^{13}\text{C}_{\text{org}}$ determined for suspended particulate matter (SPM) in the Churchill, Goose, and Northwest Rivers. Previously published $\delta^{13}\text{C}_{\text{org}}$ values from surficial sediment in Groswater Bay (cf., Tan and Vilks, 1987) was used to constrain the marine $\delta^{13}\text{C}_{\text{org}}$ endmember. The selected marine endmember is similar to $\delta^{13}\text{C}$ in surficial sediment of the Labrador Sea, reported by Muzuka and Hillaire-Marcel (1999).

3.5 Results and Discussion

3.5.1 Sediment sinks

In Lake Melville proper, sediment cores (n=14) were collected from various depths (47 to 222 m), providing good spatial coverage of the LMS and the heterogeneous seafloor and shoreline morphology (i.e., troughs, shoals, bays, and open water). This heterogeneity is reflected in the wide range of MARs (0.04 to 0.41 g cm⁻² yr⁻¹). Across the system, MARs are significantly associated with distance from the Churchill River ($R^2 = 0.37$, $p < 0.05$, n=14) with no statistical association to depth (see Chapter 2). In the western end of Lake Melville (EpINETTE Basin), MARs are greatest (Table 3-2) because of the delivery of suspended sediment from the Churchill River runoff and the nearby Kenamu and NW River. In contrast, only a couple of smaller rivers drain into the eastern end of the LMS resulting in lower MARs.

To avoid overestimating the sediment sink in Lake Melville, we divided the Lake into two sections, west and east, and applied the average MAR for each region to the corresponding seafloor area (Table 3-2 and Figure 3-4).

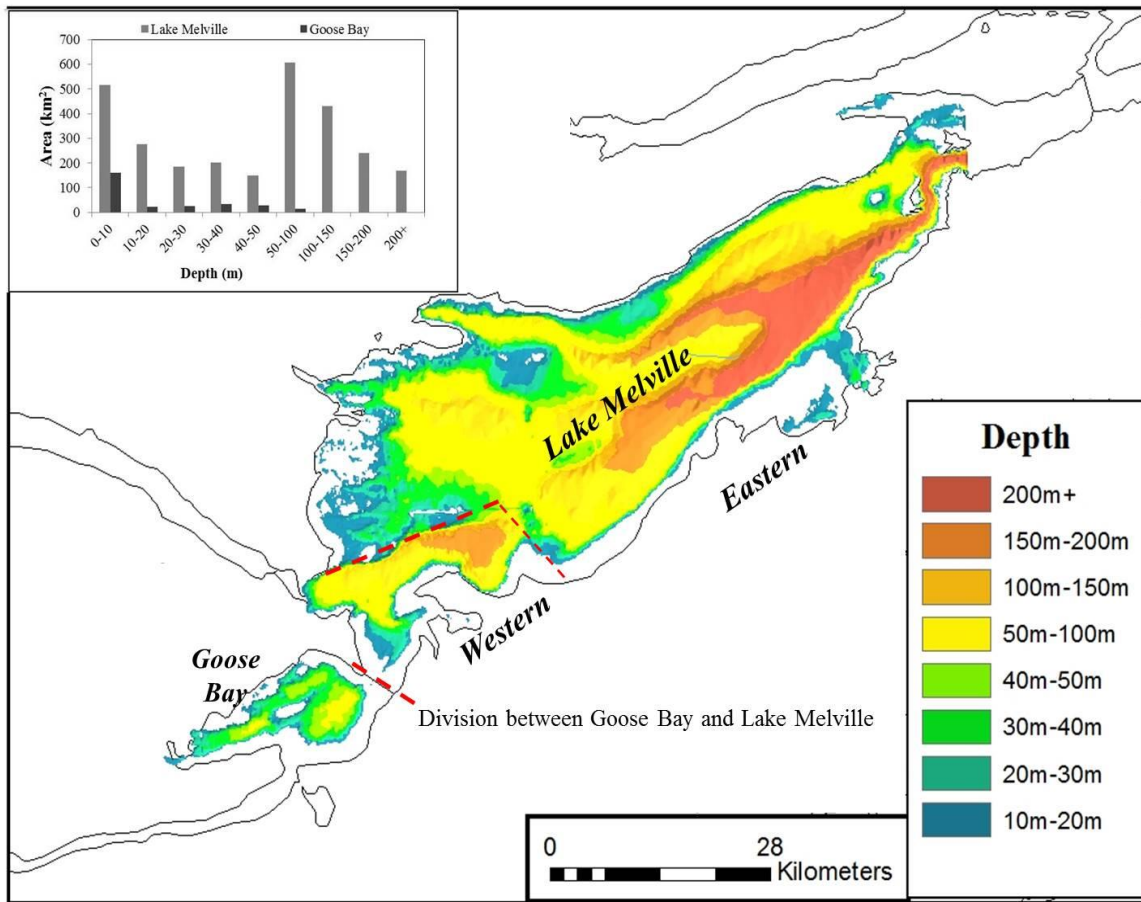
No net accumulation of sediment was assumed for water depths < 10 m (or 20% of the seafloor) due to processes such as ice scour and wave-driven resuspension. The seafloor area of the western section (201.7 km²) was measured from bathymetric data in ArcMap®. To establish the seafloor area of the eastern section (2059.3 km²), the area of the western section was subtracted from the total seafloor area of Lake Melville proper (minus water depths < 10 m) using hypsometry data provided by the Canadian Hydrographic Service. Applying the average MARs from each area to the corresponding seafloor yielded a sediment sink of 5.2 (± 2.6) x 10⁸ kg yr⁻¹ and 16.7 (± 6.2) x 10⁸ kg yr⁻¹ in the western and eastern end of Lake Melville, respectively (Table 3-2) for a total of 21.9 (± 6.7) x 10⁸ kg yr⁻¹.

Table 3-2. Summary of mass accumulation rates and area of sea floor used to calculated sediment sink.

Cores	Area (km ²)	Average MAR ¹ (±1SD g cm ⁻² yr ⁻¹)	Sink (±1SD x10 ⁸ kg yr ⁻¹)
<i>Goose Bay</i>			
I10, 26	282.8	0.22 ± 0.05	6.1 ± 2.3
<i>Western Lake Melville</i>			
I12, 35, 34	201.7	0.26 ± 0.13	7.5 ± 2.1
<i>Eastern Lake Melville</i>			
DB3, MT1	2059.3	0.08 ± 0.03	20.2± 2.5
I13, 30, DB6, BW1			
Sum Lake Melville			21.9 ± 6.7

¹Mass accumulation rates calculated from fitting profiles of ²¹⁰Pb_{ex} to a two layer advection diffusion model and validating with ¹³⁷Cs (Chapter 2).

Figure 3-4. Bathymetric map showing the division between Goose Bay and Lake Melville and between the western and eastern sections of Lake Melville (----). The inserted bar graph shows the seafloor area (km²) to water depths (m).



In Goose Bay, the average MAR, $0.22 \pm 0.08 \text{ g cm}^{-2} \text{ yr}^{-2}$ ($n=2$) was applied to the total area of the seafloor (282.8 km^2), yielding a sediment sink of $6.1 (\pm 2.3) \times 10^8 \text{ kg yr}^{-1}$. Unlike in Lake Melville, we chose to apply the average MAR to the whole seafloor area of Goose Bay (0-100 m water depth) because:

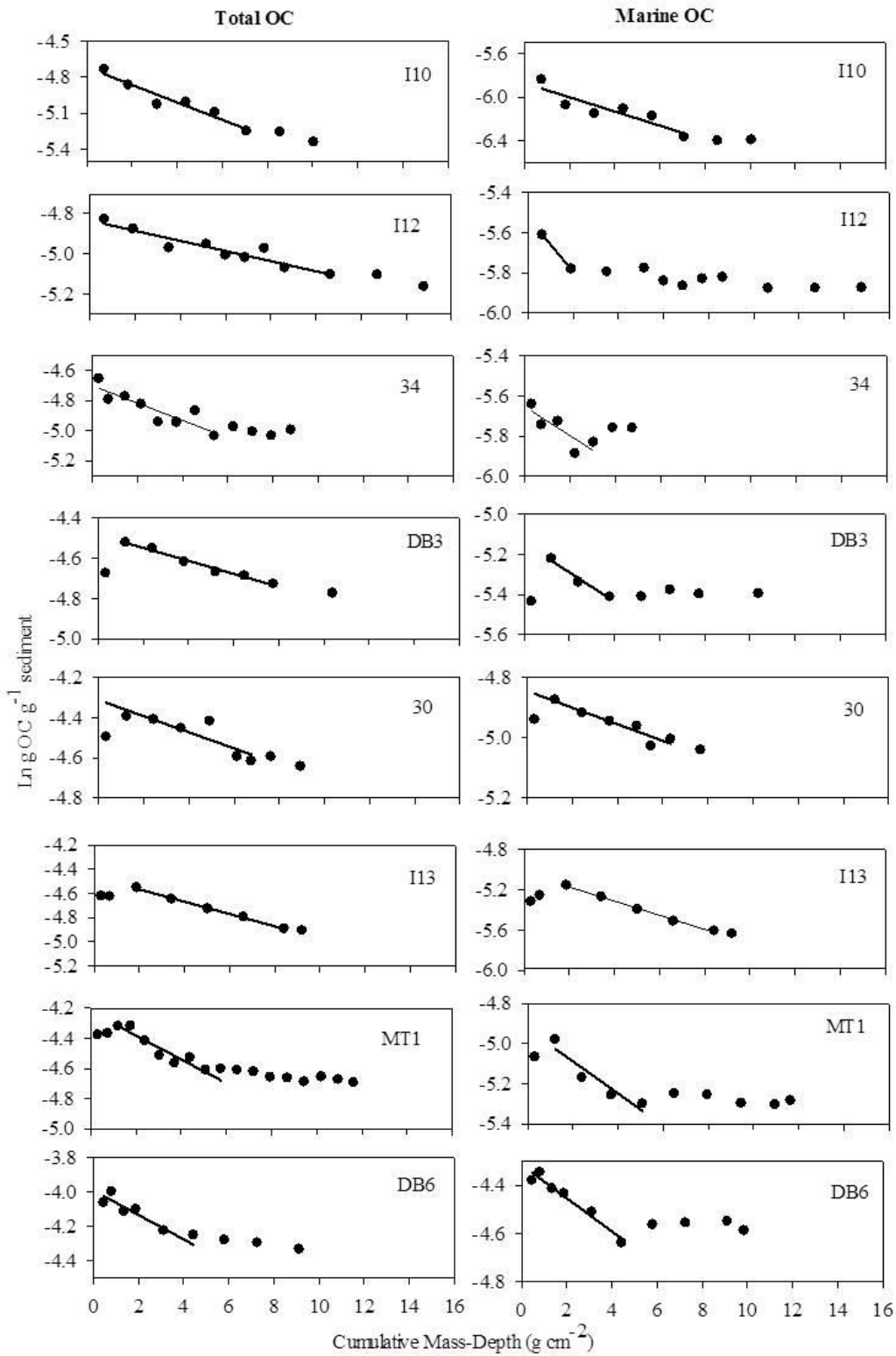
- 1) We have only two dated sediment cores for this area, thus no basis from which to assess the mean and variability of MARs in different water depth intervals.

- 2) Goose Bay is smaller with relatively shorter fetch than Lake Melville proper and ice melts in situ. Therefore, we expect less physical disturbance of the seafloor in the 0-20 m depth interval and hence greater sediment accumulation (Amec and BAE-Newplan., 2001).

3.5.2 Surface flux and rates of burial and oxidation of particulate organic carbon

In general, profiles of $\ln \text{OC}$ ($\text{g OC g sediment}^{-1}$) decreased exponentially with depth in the sediment cores until reaching low, relatively constant values at depths of 8-19 cm (Figure 3-5). The decreases in OC in the upper sediment layers suggest degradation of labile OC. The low and relatively constant %OC values below the depths of 8-19 cm probably reflect burial of refractory type OC undergoing negligible degradation (cf., Johannessen et al., 2003). In core 26, the burial depth of OC was not reached within the length of the core (10 cm). Therefore it was not possible to confidently determine the surface flux and rates of oxidation and burial. The OC profile in core 33 showed no clear trend with depth and could not be modelled. In four cores (DB3, I13, 30, and MT1), the OC content increased in the top 1-3 cm then showed exponential decrease with depth in the lower sections. Possible reasons for this low OC in the surface layers are loss of the fine organic surface during sampling and/or non-steady state conditions at these sites (Henrichs, 1992). For these cores, the top 1-3 cm sections were not included in modelling and instead the model was extrapolated to $m=0$ from the section of the core where OC showed exponential decay with depth. Because of this, the rates calculated for cores DB3, 33, 30, and MT1 are probably low (Table 3).

Figure 3-5. First-order decay model (black line) fitted to profiles of total and marine organic carbon (black dots) shown as $\ln \text{ g OC g sediment}^{-1}$ versus cumulative mass-depth (g cm^{-2}).



The calculated flux of total OC to surface sediment varies about four-fold across Lake Melville from $0.7 \times 10^{-3} \text{ g OC cm}^{-2} \text{ yr}^{-1}$ to $2.4 \times 10^{-3} \text{ g OC cm}^{-2} \text{ yr}^{-1}$ (mean = $1.3 \pm 0.2 \times 10^{-3} \text{ g OC cm}^{-2} \text{ yr}^{-1}$, n=7) (Table 3-3). The calculated OC flux in Goose Bay (core I10) lies within this range ($1.4 \times 10^{-3} \text{ g POC cm}^{-2} \text{ yr}^{-1}$, n=1). Of the total OC flux, an estimated 40 to 65% is comprised of terrestrial OC (OC_{terr}). An exception to this is site DB6 in the eastern end of Lake Melville, where only 27% of the OC is terrigenous. The terrestrial and marine proportion were applied to the calculated total flux of OC at the surface sediment and yielded OC_{terr} surface fluxes between $0.30\text{-}1.3 \text{ g OC cm}^{-2} \text{ yr}^{-1}$, with the lowest values at sites DB6 and MT1 in the eastern end of the LMS. Conversely, the highest flux of marine OC ($1.74 \times 10^{-3} \text{ g OC}_{\text{mar}} \text{ cm}^{-2} \text{ yr}^{-1}$) is found at site DB6 because of the greater influence of autochthonous (marine) primary production in the eastern end of the Lake. When compared to the Labrador shelf, east of Groswater Bay, the fluxes of total OC to surface sediments across Lake Melville and Goose Bay are three orders of magnitude higher than reported by Muzuka and Hillaire-Marcel (1999) (cf., site 1, $2.57 \times 10^{-6} \text{ g OC cm}^{-2} \text{ yr}^{-1}$).

Table 3-3. Organic carbon surface fluxes and rates of burial and oxidation.

Station	Surface ¹ Flux	Burial Rate ¹	Oxidation Rate ¹
(10 ⁻³ g C cm ⁻² yr ⁻¹)			
<i>TOC</i>			
Goose Bay			
I10	1.43	0.80	0.62
Lake Melville			
I12	1.35	1.00	0.35
34	1.82	1.35	0.46
DB3	1.36	1.02	0.34
30	1.21	0.87	0.34
I13	0.69	0.44	0.25
MT1	0.59	0.39	0.20
DB6	2.41	1.75	0.62
<i>OC_{mar}</i>²			
Goose Bay			
I10	0.5	0.27	0.23
Lake Melville			
I12	0.61	0.50	0.11
34	0.71	0.63	0.07
DB3	0.69	0.53	0.15
30	0.69	0.57	0.12
I13	0.39	0.21	0.18
MT1	0.30	0.20	0.10
DB6	1.69	1.32	0.37
<i>OC_{terr}</i>³			
Goose Bay			
I10	0.94	0.53	0.39
Lake Melville			
I12	0.74	0.50	0.24
34	1.11	0.72	0.39
DB3	0.67	0.49	0.19
30	0.52	0.30	0.22
I13	0.30	0.23	0.07
MT1	0.29	0.19	0.10
DB6	0.72	0.43	0.25

¹Surface flux and rates of burial and oxidation were calculated by applying a first-order degradation model to down-core profiles of OC, described in detail in methods section. ²Fraction of marine OC calculated using a two-endmember mixing model and marine endmember established from $\delta^{13}\text{C}_{\text{org}}$ signature from Muzuka and Hillaire-Marcel (1999). ³Calculated as the difference between TOC and OC_{mar} .

Overall, the mean burial rate of total OC in Lake Melville proper is $1.0 (\pm 0.5) \times 10^{-3} \text{ g C cm}^{-2} \text{ yr}^{-1}$ ($n = 7$), which is similar to the mean OC burial rate in Hudson Bay (Kuzyk et al., 2009). Consistent with surface flux, the burial of total OC on the Labrador shelf is three orders of a magnitude lower than in Lake Melville (cf., site 1, $1.53 \times 10^{-6} \text{ g C cm}^{-2} \text{ yr}^{-1}$, Muzuka and Hillaire-Marcel, 1999). These differences of OC flux and burial rates between Lake Melville and the Labrador Shelf reflect a greater sedimentation rate and proximity to river runoff in Lake Melville.

Across Goose Bay and Lake Melville, burial rates of total OC are spatially variable, ranging from $0.8 \times 10^{-3} \text{ g C cm}^{-2} \text{ yr}^{-1}$ in Goose Bay to $1.8 \times 10^{-3} \text{ g C cm}^{-2} \text{ yr}^{-1}$ in the eastern end of Lake Melville. This variation probably reflects both variable sedimentation rates and variation in the supply of marine and terrestrial OC. When the average burial rate for Goose Bay and Lake Melville are applied to the corresponding seafloor areas, the total OC burial fluxes are $2.3 \times 10^6 \text{ kg total OC yr}^{-1}$ and $20.8 \times 10^6 \text{ kg total OC yr}^{-1}$, respectively. In Goose Bay, which represents 11% of the total seafloor area of the system, burial flux of OC makes up 9.5% of the collective total OC buried in the system. This implies Goose Bay, for its size, is a fair trap for capturing and burying OC. Of the total OC buried in Goose Bay and Lake Melville, respectively, 35 and 61% is comprised of OC_{mar} , which yields total OC_{mar} burial fluxes of $0.8 \times 10^6 \text{ kg yr}^{-1}$ and $12.8 \times 10^6 \text{ kg yr}^{-1}$ and by difference $1.5 \times 10^6 \text{ kg OC}_{\text{terr}} \text{ yr}^{-1}$ and $8.0 \times 10^6 \text{ kg OC}_{\text{terr}} \text{ yr}^{-1}$.

Based on the down-core profiles of OC approximately 43% and 28% of the total POC deposited to the sea floor in Goose Bay and Lake Melville undergoes oxidation in surface sediment layers, respectively (see Table 3-3). The loss of POC through remineralization occurs in the top 8-19 cm of sediment cores collected across Lake Melville and Goose Bay. Overall, the mean loss of total POC in Goose Bay is $0.6 \times 10^{-3} \text{ g cm}^{-2} \text{ yr}^{-1}$, yielding a total OC loss of $1.8 \times$

10^6 kg yr^{-1} . In Lake Melville, the mean loss of POC is $0.4 \times 10^{-3} \text{ g cm}^{-2} \text{ yr}^{-1}$ ($n=7$) which yields a total POC loss of $8.3 \times 10^6 \text{ kg yr}^{-1}$. These oxidation rates are presented with a caveat because in most sediment cores this “burn-down” coincides with a decrease (lightening) in $\delta^{13}\text{C}_{\text{org}}$ in the surface sediment (see Chapter 2). These lighter $\delta^{13}\text{C}_{\text{org}}$ imply an increased supply of POC_{terr} within the 43 years before the sediment cores were collected. As such, the oxidation and burial rates, which are calculated from the decrease of OC down-core, are undoubtedly affected by an increased supply of POC_{terr} in recent years (i.e., to the upper most sections of the cores). Because of this increase in POC_{terr} , the oxidation rate of total POC and POC_{terr} are presumably overestimated here.

Of the POC_{terr} deposited to the seafloor in Goose Bay, $0.4 \times 10^{-3} \text{ g C cm}^{-2} \text{ yr}^{-1}$ is oxidized, while in Lake Melville the rate of POC_{terr} oxidation varies from $0.07 \times 10^{-3} \text{ g C cm}^{-2} \text{ yr}^{-1}$ to $0.4 \times 10^{-3} \text{ g C cm}^{-2} \text{ yr}^{-1}$ (mean = $0.2 \times 10^{-3} \text{ g C cm}^{-2} \text{ yr}^{-1}$, $n = 6$) with no obvious spatial trend. Applied to the seafloor area in Goose Bay and Lake Melville, the oxidation rates yield losses of $1.1 \times 10^6 \text{ kg POC}_{\text{terr}} \text{ yr}^{-1}$ and $4.1 \times 10^6 \text{ kg POC}_{\text{terr}} \text{ yr}^{-1}$, respectively. Although POC_{mar} is often considered to be more easily degraded (labile) than POC_{terr} , the loss of POC_{terr} at the sediment surface of Goose Bay is about two times greater than the loss of POC_{mar} ($0.2 \times 10^{-3} \text{ g C cm}^{-2} \text{ yr}^{-1}$, $n = 1$). This difference in oxidation rates probably reflects a greater flux of POC_{terr} (i.e., 65% OC_{terr} versus 35% OC_{mar}) in Goose Bay. In Lake Melville, POC_{mar} at the sediment surface is remineralized at a similar rate as POC_{terr} (mean = $0.2 (\pm 0.1) \times 10^{-3} \text{ g C cm}^{-2} \text{ yr}^{-1}$ $n= 6$), reflecting comparable influx of terrigenous and marine OC to the surface sediment of Lake Melville proper. Applied to the seafloor of Goose Bay and Lake Melville, the POC_{mar} oxidation rates yield a total loss $0.7 \times 10^6 \text{ kg yr}^{-1}$ and $4.0 \times 10^6 \text{ kg POC}_{\text{terr}} \text{ yr}^{-1}$, respectively.

3.5.3 Sediment input from rivers

The majority of fresh surface water in Lake Melville (ca. 30-40 km³) is sourced from four rivers: Churchill, Northwest (NW), Kenamu, and Goose (Bobbitt and Akenhead, 1982). The Churchill River is by far the largest supplier of freshwater, contributing on average $1,769 \pm 509$ m³ s⁻¹ (Environment Canada Hydrometric Database: station 03OE001) or 60% of the total freshwater input to the system. To estimate the suspended sediment load from the Churchill River into the Lake Melville system, we used monthly TSS measurements reported by Nalcor (2007). Measurements of TSS data were made on grab samples collected near the mouth of the Churchill River (station 51 in Nalcor, 2007) over the period of April 2006 to March 2007 (Table 3-4). Concentrations of TSS below the reported detection limit (5 mg L⁻¹) were assigned 1 mg L⁻¹. Seasonal variability was accounted for by applying monthly mean TSS concentrations to corresponding monthly mean discharge rates, measured continuously at a hydrometric gauging station, 03OE001. This station is located above Muskrat Falls, ca. 40 km from the river mouth. Because the river widens and transitions into a braided channel below Muskrat Falls, applying the discharge rate from this station could be a source of inaccuracy in our calculations (cf., Gebhardt et al., 2005). Nevertheless, using the discharged-weighted TSS concentrations as the best available data, we obtained a mean annual suspended sediment input of $25.2 (\pm 9.2) \times 10^8$ kg yr⁻¹ from the Churchill River. Here, we consider only suspended sediment load because the bedload fraction is presumed to settle out (forming sand bars) before reach the mouth of the river (Amec, 2008b).

Table 3-4. Churchill River monthly TSS and discharge data used to estimate the suspended sediment input into the Lake Melville system.

DATE	TSS (mg/L) ¹	Discharge (m ³ /s) ²
4/6/2006	1	1670
5/2/2006	1	3270
5/11/2006	127	3270
5/18/2006	87	3270
5/25/2006	33	3270
6/8/2006	1	1510
7/5/2006	8	1360
7/5/2006	14	1360
8/4/2006	13	1600
9/25/2006	17	1360
10/17/2006	30	1540
11/22/2006	14	1970
12/20/2006	8	1930
1/16/2007	36	1690
2/21/2007	32	1740
3/13/2007	106	1590

¹Total suspended sediment data from Nalcor (2007).

²Mean monthly discharge rates obtained from Environment Canada station 03OE001

Based on sparse data from the 1950s (cf., Coachman, 1953), the NW, Goose, and Kenamu Rivers have a mean discharge rate of 944, 204 and 266 m³ sec⁻¹, respectively. The peak discharge of the Goose and Kenamu Rivers occurs during spring freshet (May-June) followed by low flow during the rest of the year. Rainfall events in summer and fall can trigger episodic high flow (Bobbitt and Akenhead, 1982). These elevated flow events could accelerate bank erosion along the Goose and Kenamu Rivers, resulting in greater loads of suspended sediment and OC_{terr} than can be predicted from the scarce measurements available (cf., Milliman and Syvitski, 1992). In contrast, NW River drains the large and deep Grand Lake, which acts to stabilize seasonal shifts in flow and probably traps particulates (Coachman, 1953). In the 1970s, the primary source of freshwater to Grand Lake, the Naskapi River, was re-routed northward into the Smallwood Reservoir. This re-routing decreased the drainage basin of the Naskapi River from 23,310 to

12,691 km² (Anderson, 1985) and reduced the inflow of the Naskapi River into Grand Lake to one-half the original flow

To calculate the sediment input to the Lake Melville system from the NW and Goose Rivers, recently collected TSS data (Table 3-5) averaged from June 2013 and October 2014, were applied to the only available discharge rates for the Goose (204 m³ sec⁻¹) and NW (944 m³ sec⁻¹) Rivers (Coachman, 1953). This approach yielded values of 0.8 x10⁸ and 0.7 x10⁸ kg yr⁻¹ for the NW and Goose Rivers, respectively. Since the river discharge rates used in our calculations were measured more than 60 years ago, they are potentially a source of error in our calculations (i.e., Roberts et al., 2012) but likely minor because these rivers provide only 4% or less of the estimated suspended sediment of input the Churchill River. Suspended sediment input from the Kenamu River was estimated using the suspended sediment load of 100, 000 m³ yr⁻¹ predicted by Syvitski (1990) and assuming a suspended solid density of 1.5 g cm⁻³ (Sunderland et al., 2010). Using these values, the Kenamu River input is nearly two times that of the NW and Goose Rivers, at 1.5 x 10⁸ kg yr⁻¹.

Table 3-5. River TSS measurements.

Rivers	TSS (mg L ⁻¹)	
	June 2013	October 2014
Northwest	7.6	4.4
		4.6
Goose	7.6	8.0
		12.8

In addition to the four primary rivers, Lake Melville also receives inputs from numerous smaller rivers including the Mulligan and Sebaskachu Rivers that drain into the north shore and the English River that drains the Mealy Mountains (see Table 1 for river properties). To our

knowledge, flow rates and TSS data do not exist for these rivers. Thus, we estimated sediment inputs by scaling the inputs of the Goose River to the combined watershed size of the Mulligan, Sebaskachu, and English Rivers (2 282 km², approximately 66% the size of the Goose River watershed), obtaining a combined suspended sediment input of 0.5 x 10⁸ kg yr⁻¹.

3.5.4 Estimated inputs of terrestrial organic carbon from rivers

Inputs of POC_{terr} from the Churchill, Goose and NW Rivers are based on newly acquired POC measurements of filtered river water collected in June 2013 and October 2014 (Table 3-6 and 3-7).

Table 3-6. Concentrations of particulate organic carbon in river water.

River	Terrestrial POC in Particulate Matter (mg L ⁻¹)	
	June 2013	October 2014
Churchill	0.556	0.348
Goose	0.489	0.433
Northwest	0.227	0.191

Table 3-7. Monthly rates of POC_{terr} averaged to estimate the yearly inputs of POC_{terr} from the Churchill, Goose, and Northwest River.

Month	Estimated Monthly River POC _{terr} Load (x 10 ⁶ kg month ⁻¹)		
	Churchill ¹	Goose ²	Northwest ²
April	29.9	3.14	6.76
May	57.4	3.14	6.76
June	26.5	3.14	6.76
July	23.9	3.14	6.76
August	28.1	3.14	6.76
September	14.9	2.78	5.69
October	14.9	2.78	5.69
November	21.6	2.78	5.69
December	1.38	0.04	0.08
January	1.21	0.04	0.08
February	1.24	0.04	0.08
March	1.13	0.04	0.08
Monthly Average	18.5	2.0	4.3

¹For December to March, POC_{terr} inputs were estimated at 20% the mean POC_{terr} measured in June 2013 and October 2014 and equally distributed among the four months. This percentage was based on the percentage of TSS input for the months of December to February (i.e. 20% of yearly input). March was excluded because of an exceptionally high TSS concentration (106 mg L⁻¹). ²POC_{terr} inputs during ice-covered months (December to March) were estimated at 5% of the mean POC_{terr} concentration measured in June 2013 and October 2014.

This approach yielded values of 18.4 x 10⁶ kg POC yr⁻¹, 1.8 x 10⁶ kg POC yr⁻¹, and 4.3 x 10⁶ kg POC yr⁻¹ for the Churchill, Goose and NW Rivers, respectively. Although inputs of suspended sediment from the Goose and NW Rivers are comparable, the much higher POC_{terr} input from the NW River could be explained by a greater contribution of lacustrine organic matter (OM) produced in Grand Lake. This hypothesis is supported by a lighter δ¹³C_{org} signature in particulate matter of NW River (-31.1 ‰) compared to that in Goose River (-27.1 ‰) (Table 3-8).

Table 3-8. Measure $\delta^{13}\text{C}_{\text{org}}$ of riverine particulate organic matter.

Rivers	June 2013 $\delta^{13}\text{C}_{\text{org}}$ (‰)	October $\delta^{13}\text{C}_{\text{org}}$ (‰)	Mean $\delta^{13}\text{C}_{\text{org}}$ (‰ \pm 1SD)
Churchill	-31.4	-31.7	-31.6 \pm 0.2
Goose	-27.0	-27.2	-27.1 \pm 0.1
Kenamu	-28.8	-33.3	-31.1 \pm 3.1

Since there are no direct measurements of POC_{terr} from the Kenamu River, we presume the POC_{terr} influx parallels TSS inputs, which are 2.1 times greater than the Goose River. Using this relation, we estimate the POC_{terr} input from Kenamu River to be $4.2 \times 10^6 \text{ kg C yr}^{-1}$. Based on a combined drainage basin area of $2,282 \text{ km}^2$, the total POC_{terr} contribution from the Sebaskachu, Mulligan, and English Rivers was estimated as one-half the input from Goose River ($0.8 \times 10^6 \text{ kg POC yr}^{-1}$).

3.5.5 Estimated inputs from autochthonous primary production

The organic and inorganic components of the carbon cycle are linked through the fixation of carbon dioxide by photosynthesising primary producers (i.e., phytoplankton, ice algae). Coastal environments tend to have enhanced primary production relative to offshore environments because of nutrient influx from rivers, in addition to marine sources. In river dominated coastal systems, phytoplankton production and spatial extent are complexly linked to river runoff. Freshwater inflow promotes primary production by delivering nutrients, organic carbon, and warmer water (Cloern et al., 2014; Peierls et al., 2012). Additionally, river runoff drives estuarine circulation, causing the entrainment of nutrient rich marine water to the surface (R. Macdonald, personal communication). In some estuaries, such as the Fraser River Estuary, the supply of nutrients to surface water is dominated by the entrainment of marine water (Yin et al., 1995). On the contrary, systems strongly influenced by river runoff may limit phytoplankton production through shortened hydraulic residence times (cf., Lucas et al., 2009; Peierls et al.,

2012), increased light attenuation from elevated CDOM inputs (cf., Granskog et al., 2007) and a shallow euphotic zone from greater suspended solids (Sorokin and Sorokin, 1996).

To our knowledge, primary production has not been quantified in the LMS. Most authors assume that Lake Melville is oligotrophic (cf., Schartup et al., 2015). However, chlorophyll *a* biomass measurements are extremely scarce. The median chlorophyll *a* biomass measured in surface waters (nominally 1 m depth) in June 2013 was $1.2 \mu\text{g L}^{-1}$ (n=6), while the median in the 6-10 m depth range was only $0.20 \mu\text{g L}^{-1}$ (n=4) (A. Schartup, personal communication).

To estimate inputs of marine organic carbon (POC_{mar}) from new primary production for the budget, we applied the surface fluxes of POC_{mar} determined from the sediment core data to a rearrangement of the simple empirical relationship:

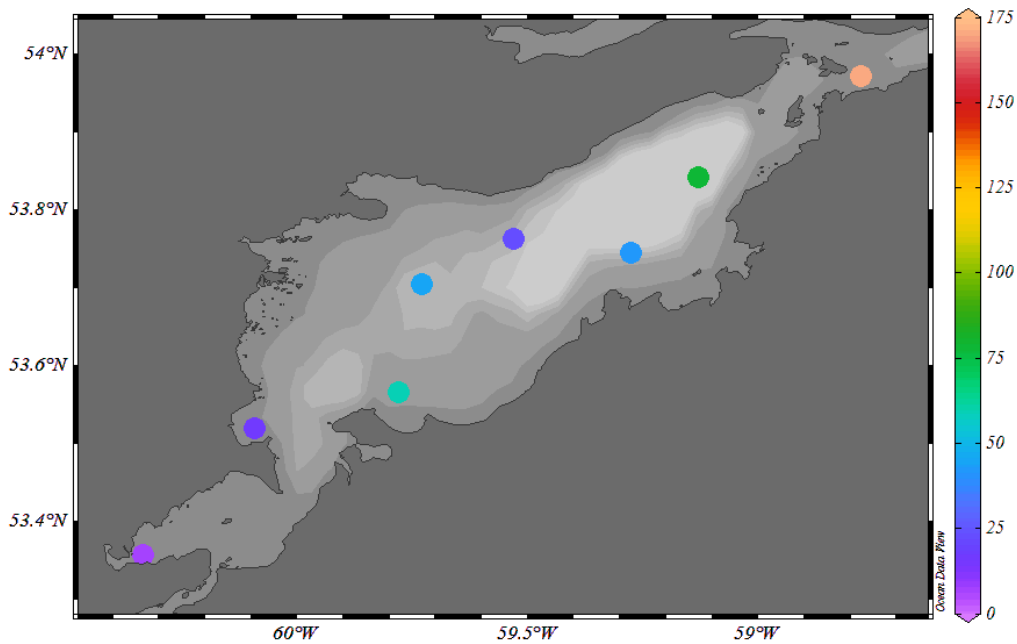
$$J=20PP/z \qquad \text{Eq. 5}$$

where *J* is the POC_{mar} flux, *PP* is the primary production ($\text{g POC m}^{-2} \text{yr}^{-1}$), and *z* is the corresponding water depth at the sampling site (Berger et al., 1988).

Overall, primary production of OC_{mar} estimated in this manner is significantly associated with distance to the Churchill River ($R^2 = 0.67$, $p < 0.05$, $n = 8$), increasing, step-wise eastward across Goose Bay and Lake Melville (Figure 3-6 and Appendix C). In Goose Bay, estimated new production of OC is lowest at $6.8 \text{ g POC}_{\text{mar}} \text{ m}^{-2} \text{ yr}^{-1}$ (site I10). From Goose Bay to a site immediately east of Goose Bay Narrows (site 34) in Lake Melville, new production increases nearly five times to $58.8 \text{ g POC}_{\text{mar}} \text{ m}^{-2} \text{ yr}^{-1}$. Overall, the general eastward increase is likely associated with entrainment of bottom saline water carrying salinity and nutrients to the surface and/or greater light penetration with increasing distance from the major river inputs (i.e., surface salinity = <1-15; mean secchi depth = $1.8 \pm 0.3 \text{ m}$, (n = 3) in Lake Melville versus surface salinity ca. 23; secchi depth = 4.4 m , (n = 1) in Groswater Bay). As fresh surface water transports

particulates from the Churchill River plume eastward across Goose Bay and hence Lake Melville, the water velocity decelerates after passing through Goose Bay Narrows, losing a large portion of its suspended sediment load. This sediment deposition is evidenced by the large MAR east of Goose Bay Narrows, $0.41 \text{ g cm}^{-2} \text{ yr}^{-1}$, as discussed in Chapter 2. Satellite images also support a dramatic change in optical properties of the surface layer in the area east of Goose Bay Narrows (not shown). At the two most easterly sites in Lake Melville (30 and DB6), new production was calculated as 75.9 and $165.6 \text{ g OC}_{\text{mar}} \text{ m}^{-2} \text{ yr}^{-1}$, respectively (Appendix C). We suspect the elevated primary production at side DB6 is a “hot spot” and potentially reflects a limited area at the east end of Lake Melville where lower turbidity and, hence a deeper euphotic zone coincides with elevated nutrient fluxes linked to upwelling on the eastern side of the Narrows (Aure et al., 2007; Lu et al., 2013).

Figure 3-6. Calculated new primary production ($\text{g m}^{-2} \text{ yr}^{-1}$) in Goose Bay and Lake Melville as estimated from a general empirical model and the surface fluxes of OC_{mar} in the sediment cores.



Both the mean ($60.1 (\pm 50.8) \text{ g C m}^{-2} \text{ yr}^{-1}$, $n=7$) and median ($42.5 \text{ g C m}^{-2} \text{ yr}^{-1}$, $n= 7$) new production are consistent with an oligotrophic status and are within the range of primary production over the Arctic Shelf ($45\pm 20 \text{ g C m}^{-2} \text{ a}^{-1}$ (Anderson et al., 1990)), the Atlantic Barents Sea ($40\text{-}70 \text{ g C m}^{-2} \text{ yr}^{-1}$), and Hudson Bay ($50\text{-}70 \text{ g C m}^{-2} \text{ yr}^{-1}$, (Sakshaug, 2004)). Due to the wide range of new production rates across Lake Melville, we selected to apply the median new production ($42.5 \text{ g C m}^{-2} \text{ yr}^{-1}$, $n= 7$) to the approximate surface area of Lake Melville (2261 km^2). Using this approach we obtained an input of $98.3 \text{ kg POC}_{\text{mar}} \text{ yr}^{-1}$. For Goose Bay, the estimated primary production rate $6.3 \text{ g POC}_{\text{mar}} \text{ m}^{-2} \text{ yr}^{-1}$ yields a total POC_{mar} input of $1.8 \times 10^6 \text{ kg POC}_{\text{mar}} \text{ yr}^{-1}$.

3.5.6 Inputs from coastal erosion and resuspension

The coastlines of Arctic and subarctic seas are under increasing pressure from larger storm surges due to reduced sea ice, rising relative-sea level (RSL), and melting permafrost (FitzGerald et al., 2008; Jorgenson et al., 2006; Macdonald et al., 2015; Overeem et al., 2011). In many regions, such as the Siberian Shelves, sediment input from coastal erosion exceeds inputs from rivers (cf., Rachold et al., 2000), while simultaneously contributing significant amounts of fresh and paleo type terrestrial organic matter (Goni et al., 2005; Karlsson et al., 2011; Vonk et al., 2012). In contrast, Lake Melville is experiencing falling RSL because of long term crustal rebound of the Labrador-Ungava Peninsula ($120\text{-}150 \text{ m}$ since last deglaciation) (Vilks et al., 1987). Currently the rebound rate is estimated at $1\text{-}4 \text{ mm yr}^{-1}$ (Batterson and Liverman, 2010; Henton et al., 2006; Sella et al., 2007). This crustal rebound, together with a dampened tidal range, relatively low wave energy (smaller fetch), and a high proportion of rocky coastline along the east and south shores, collectively imply relatively low coastal erosion rates in Lake Melville compared to other Arctic and subarctic coastal regions (cf., Liverman et al., 2001; Shaw et al.,

1998). Thus, we assume here that sediment and OC inputs to Goose Bay and Lake Melville from coastal erosion are less than river inputs.

In contrast to subaerial coastal erosion, subaqueous resuspension (i.e., via ice rafting, or wave and tide energy) and lateral transport of particulates from shallow areas (i.e., < 10 m) could be an important source of material, especially along the low lying north shore where shoals are common. In southern Hudson Bay, which also experiences falling RSL due to crustal rebound, Kuzyk et al. (2009) proposed that resuspension and lateral transport of particulates to deep water contributes ten times more sediment and about one and half times more terrigenous OC than river inputs. In Lake Melville, the transport of particulates from shallow to deep depths is likely not as significant as it is in Hudson Bay because water depth plays only a minor influence on MAR ($R^2=0.28$, $p=0.05$, $n=14$) in the LMS. Nevertheless, MODIS images occasionally reveal the presence of what appear to be turbid plumes associated with beaches along the north shore, northeast of the community of Northwest River. These images provide evidence of resuspension and lateral transport in Lake Melville. Furthermore, observations during sampling (i.e., rocky substrate, unsuccessful box cores) suggest some areas of the seafloor off Sebaskachu and Mulligan Bay are non-depositional environments. Quantifying irregular resuspension events is difficult especially in Lake Melville where data are sparse. Because of this, we estimate the sediment and OC input from coastal erosion/resuspension as the unbalanced term of the sediment budget ($5.3 \times 10^8 \text{ kg yr}^{-1}$) and assume 0.75% is OC ($5.1 \times 10^6 \text{ kg OC yr}^{-1}$).

3.4.7 Exchange with Groswater Bay

The exchange of particulate matter between Lake Melville and Groswater Bay is difficult to constrain because of uncertainties surrounding the exchange of water over the shallow (30 m)

sill in the Narrows. Lu et al. (2013), provides an overview of the estuarine circulation recorded by two moorings anchored from September 2012 to July 2013 west (inside) and east (outside) of the Narrows. The mooring data revealed that throughout the year there is an overall net export, during both ebb and flood tide, of surface water from Lake Melville to Groswater Bay, with the greatest velocity (0.7 m sec^{-1}) at 10 m. These results imply that there is a net export of sediment and POC from Lake Melville to Groswater Bay as well. Consistent with this hypothesis, the $\delta^{13}\text{C}_{\text{org}}$ signature of surface POC east of the Narrows ($-25.0 \pm 0.01 \text{ ‰}$) and of surface sediment in Groswater Bay ($-22.5 \pm 0.01\text{‰}$) are lighter than the expected marine endmember (ca. -21.3 ‰) and consistent with about 12 to 30% POC derived from vascular C_3 terrestrial plants ($\delta^{13}\text{C}_{\text{org}}$ ca. -34 to -24 ‰).

To estimate net export of particulates from Lake Melville to Groswater Bay, we used the only available freshwater flushing rate, $4.1 \times 10^{10} \text{ m}^3$ in 5.8 months, established by Bobbitt and Akenhead (1982). This flushing rate is based on 1981 data and thus, it is in line with the regulated flow of the Churchill River. Adjusting this flushing rate to one year ($8.6 \times 10^{10} \text{ m}^3 \text{ yr}^{-1}$) and applying it to a TSS of 7 mg L^{-1} in Groswater Bay yields a sediment export value of $6.0 \times 10^8 \text{ kg yr}^{-1}$ or 21% of river input. Applying the export percentage of 21% to POC_{mar} and POC_{terr} inputs yields estimated exports of $20.7 \times 10^6 \text{ kg yr}^{-1}$ and $6.2 \times 10^6 \text{ kg yr}^{-1}$, respectively.

3.6 Mass-balance and summary of budgets

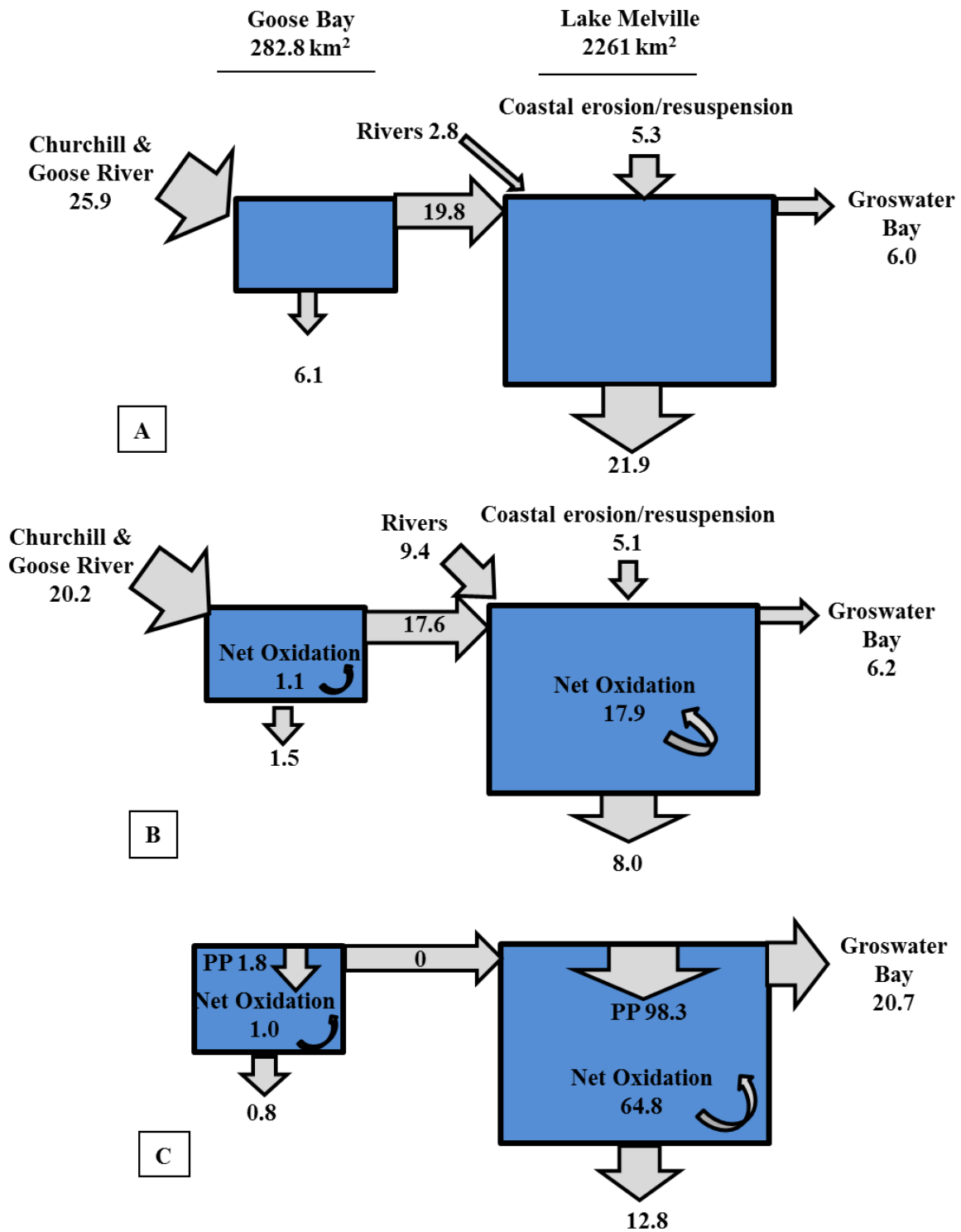
3.6.1 Sediment budget

Figure 3-7a shows the constrained boundary conditions of the sediment budget with Goose Bay and Lake Melville proper represented as two simplified and separate compartments. By simplifying the system into two separate boxes, the exchange of material from Goose Bay to Lake Melville and export out of the system was quantified. The total sediment input to the LMS

is $34 \times 10^8 \text{ kg yr}^{-1}$, with the majority, $28.7 \times 10^8 \text{ kg yr}^{-1}$, carried into the system by rivers. The Churchill River is the largest contributor (74%) of sediment, delivering $25.2 \times 10^8 \text{ kg yr}^{-1}$ to the system. Of the Churchill River's suspended sediment load, 21% is deposited in Goose Bay ($5.4 \times 10^8 \text{ kg yr}^{-1}$). Additionally, $0.7 \times 10^8 \text{ kg yr}^{-1}$ of sediment is delivered from Goose River to Goose Bay (total = $6.1 \times 10^8 \text{ kg yr}^{-1}$). The remaining sediment brought in by the Churchill River, $19.8 \times 10^8 \text{ kg yr}^{-1}$, is carried to Lake Melville. In addition to this sediment input from Goose Bay, Lake Melville receives an additional sediment load from the Kenamu, NW, Sebaskachu, Mulligan, and English Rivers ($2.8 \times 10^8 \text{ kg yr}^{-1}$). Thus, for Lake Melville proper, the total sediment input from rivers and Goose Bay is $22.6 \times 10^8 \text{ kg yr}^{-1}$ while 21% ($6.0 \times 10^8 \text{ kg yr}^{-1}$) of river inputs is assumed to be exported to Groswater Bay and the Labrador Sea.

Applying corresponding ^{210}Pb -based MAR's to the western and eastern area of Lake Melville (excluding water depths $< 10 \text{ m}$, see Figure 3-4) and summing the two regions gives a sediment sink of $21.9 \times 10^8 \text{ kg yr}^{-1}$. Thus, including the deposition in Goose Bay ($6.1 \times 10^8 \text{ kg yr}^{-1}$), the total sediment sink for the system ($28.0 \times 10^8 \text{ kg yr}^{-1}$) exceeds river inputs and exports by $5.3 \times 10^8 \text{ kg yr}^{-1}$. This unbalanced term is presumed to be sourced from lateral resuspension and/or coastal erosion.

Figure 3-7. Mass balance budgets of sediment ($\times 10^8 \text{ kg yr}^{-1}$) (a), POC_{terr} ($\times 10^6 \text{ kg yr}^{-1}$) (b), and POC_{mar} ($\times 10^6 \text{ kg yr}^{-1}$) (c). Arrows pointing towards a box represent inputs, arrows pointing downwards represent sinks, curved arrows represent net oxidation and PP is primary production.



3.6.2 Particulate organic carbon budgets

Particulate organic carbon in Goose Bay and Lake Melville contain both terrestrial and marine OC, reflecting contributions from river runoff and autochthonous primary production, respectively (Tan and Vilks, 1987). Since each type of POC is sourced, cycled and degraded differently, we follow the recommendation of Macdonald et al. (1998) and developed two separate POC budgets: terrestrial and marine (Figure 3-7b and 3-7c). Similar to the sediment budget, the budgets of POC are divided into two simplified compartments, Goose Bay and Lake Melville.

Terrestrial POC Budget

In total, the input of POC_{terr} to Goose Bay and Lake Melville from all rivers is 29.6×10^6 kg yr⁻¹ (Figure 3-7b). Of the total river input of POC_{terr} , 62% (18.4×10^6 kg POC yr⁻¹) is delivered to Goose Bay by the Churchill River. Applying ²¹⁰Pb_{ex} based MAR and burial flux of terrigenous OC to the seafloor area of Goose Bay yields a burial flux of 1.5×10^6 kg POC yr⁻¹. This burial flux is comparable to the amount of POC_{terr} (1.1×10^6 kg POC yr⁻¹) lost through oxidation in the surface sediment. We note that these rates of Goose Bay have large uncertainties because they were derived from a single core. Based on findings in other systems (i.e., Fraser River delta, Johannessen et al., 2003), we would expect greater POC_{terr} burial in river deltas in Goose Bay. Still, using the best available data, the difference between the inputs to Goose Bay and the amount buried and oxidized there is 17.6×10^6 kg POC_{terr} yr⁻¹ or 87% of river input; to balance Goose Bay, the remainder is presumed to be transported with surface waters through Goose Bay Narrows to Lake Melville. This suggests that the majority of POC_{terr} brought in by the Churchill River is transported farther eastward than Goose Bay.

In addition to the $17.6 \times 10^6 \text{ kg POC}_{\text{terr}} \text{ yr}^{-1}$ from Goose Bay, Lake Melville receives a total of $9.4 \times 10^6 \text{ kg yr}^{-1}$ of POC_{terr} from the NW, Kenamu, Sebaskachu, Mulligan, and English Rivers and $8.3 \times 10^6 \text{ kg yr}^{-1}$ from coastal erosion/lateral resuspension. In Lake Melville, the burial flux of POC_{terr} , $8.2 \times 10^6 \text{ kg yr}^{-1}$, and oxidation in surface sediment, $4.1 \times 10^6 \text{ kg POC}_{\text{terr}} \text{ yr}^{-1}$, represents 28% and 14% of total inputs, respectively. Compared to Goose Bay, Lake Melville properly buries six times more terrigenous OC in an area eight times larger than Goose Bay.

We presume the export of POC parallels suspended sediment exports to Groswater Bay (i.e., 21% of river inputs). Based on this assumption, we calculated a loss of POC_{terr} to Groswater Bay and Labrador Sea of $6.2 \times 10^6 \text{ kg yr}^{-1}$. In total, this leaves an unbalanced term of $13.8 \times 10^6 \text{ kg POC}_{\text{terr}} \text{ yr}^{-1}$ (47% of total river inputs). Ittekkot (1988) found on average about 35% of riverine POC is comprised of labile OM. Following this author's findings (within suitable uncertainties), we suggest the unbalanced term of $13.8 \times 10^6 \text{ kg POC}_{\text{terr}} \text{ yr}^{-1}$ in Lake Melville is lost by oxidation in the water column. Since Goose Bay is much smaller and surface water residence time much shorter (cf., Amec and BAE-Newplan., 2001), the oxidation of POC_{terr} is presumed to take place entirely in Lake Melville where particle residence time is longer.

Marine POC budget

Rates of autochthonous OC production in Goose Bay and Lake Melville were difficult to constrain because direct measurements, to our knowledge, do not exist. Accordingly, we utilized the marine fraction of OC in the sedimentary record, which in itself provides an archive of productivity in the system. Here, calculated POC_{mar} fluxes at the surface sediment were applied to an empirical relationship (Eq. 5) that takes into account degradation within the water column

(i.e., deeper water = longer residence time = greater degradation). Through this method, the rates of primary production (POC_{mar}) in Goose Bay and Lake Melville were calculated as $1.8 \times 10^6 \text{ kg yr}^{-1}$ and $98.3 \times 10^6 \text{ kg yr}^{-1}$, respectively (Figure 3-7c). Eight core profiles of sedimentary POC_{mar} revealed rates of burial and oxidation of $0.8 \times 10^6 \text{ kg POC}_{\text{mar yr}^{-1}}$ and $0.7 \times 10^6 \text{ kg POC}_{\text{mar yr}^{-1}}$ in Goose Bay and $12.7 \times 10^6 \text{ kg POC}_{\text{mar yr}^{-1}}$ and $4.0 \times 10^6 \text{ kg POC}_{\text{mar yr}^{-1}}$ in Lake Melville, respectively. These rates suggest that the Lake Melville system buries about 13% of new OC production, which is relatively high. For example, Hudson Bay buries 6% of in situ primary production (Kuzyk et al., 2009) while the Beaufort Shelf buries only about 2% (Macdonald et al., 1998). Similar to the POC_{terr} , we assume 21% ($19.5 \times 10^6 \text{ kg}$) of POC_{mar} produced in Lake Melville is exported in the surface water to Groswater Bay. Using mass balance calculations, $0.3 \times 10^6 \text{ kg POC}_{\text{mar yr}^{-1}}$ and $60.8 \times 10^6 \text{ kg POC}_{\text{mar yr}^{-1}}$ is presumed oxidized within the water column of Goose Bay and Lake Melville, respectively; a rate up to fifteen times greater than POC_{terr} .

3.7 Potential impacts of the Lower Churchill development on the sediment and particulate organic carbon budgets

Construction of a hydroelectric dam on the Lower Churchill River at Muskrat Falls, about 40 km from the Rivers mouth, began in 2014 and is expected to start generating power by 2017-18. A reservoir (100.7 km^2) behind the dam will begin holding back water in 2016, flooding 41 km^2 of land (Amec, 2008a). The river bank where flooding will take place is comprised of highly erodible, unconsolidated sandy sediment, as is the downstream reach to Goose Bay (Amec, 2007). Modelling by Minaskuat (2008) predicted that bank erosion from Muskrat Falls Reservoir to the town of Happy Valley will increase substantially in the first two years as the shoreline

readjusts to the new water level. This predicted increase of bank erosion in the first two years is expected to drive a pulse of suspended sediment, and consequently terrestrial OM downstream (Minaskuat, 2008), consistent with observations from other systems (cf., Anselmetti et al., 2007; Bogen and Bønsnes, 2001; Finger et al., 2006).

To investigate the potential changes to the sediment load of the Churchill River to Goose Bay and Lake Melville following impoundment at Muskrat Falls, we calculated the sediment increase using the median reservoir shoreline erosion potential of 5.25 m yr^{-1} per m shoreline reported by Amec (2008a). Following the authors assumptions, we assumed a 10 m bank height. Applying these values to an approximate reservoir shoreline of 35.5 km and assumed bulk density of $2,600 \text{ kg m}^{-3}$, the annual sediment load from shoreline erosion of the reservoir is expected to be $48.5 \times 10^8 \text{ kg yr}^{-1}$. Assuming about half the eroded soil remains trapped in the reservoir and sand bar downstream, the input of suspended sediment to Goose Bay and Lake Melville from the Churchill River could double to $49.5 \times 10^8 \text{ kg yr}^{-1}$ in the two years following impoundment.

Despite efforts to clear large vegetation and brush from the predicted reservoir area prior to flooding, leaf litter will remain on the soil surface upon flooding and is expected to increase DOC concentrations in the Lower Churchill River (Schartup et al., 2015). At the same time, we suspect leaf litter, OM in the soil horizon, and vegetation along the river bank from Muskrat Falls to Goose Bay will also correlate to a pulse of POC_{terr} . Using the relative proportion of OC_{terr} to TSS (ca. 1%) from June 2013 and October 2013, we could expect a $24.3 \times 10^6 \text{ kg yr}^{-1}$ increase in OC_{terr} downstream during the first two years after flooding.

This potential doubling of both suspended sediment and terrigenous OC fluxes to Goose Bay and Lake Melville post impoundment of the Churchill River could have implications on

phytoplankton productivity by reducing light penetration and narrowing the euphotic zone. Furthermore, an increase in the delivery of freshwater during late summer months could decrease freshwater residence time driving primary producers out of the system (Peierls et al., 2012). Similar to the Southern Indian Lake in Manitoba (cf., Newbury and McCullough, 1984), shoreline erosion and, thus, suspended sediment concentrations (and most-likely terrestrial OM), are expected to decline over a 20-50 years (Minaskuat, 2008) suggesting these changes could be long term.

Acknowledgments

Funding was provided by ArcticNet NCE program and NSERC CERC. Support was provided by the Centre for Earth Observation Science, University of Manitoba, and Arctic Scientific Partnership. Additional funding was provided by the Northern Scientific Training Program.

3.8 References

- Amec, 2008a, Bank stability study for the proposed Lower Churchill Hydroelectric Generation Project: Environmental baseline report.
- , 2008b, Lower Churchill Hydroelectric Generation Project: Sedimentation and Morphodynamics Study
- Amec, and BAE-Newplan., 2001, Aquatic Environment in the Goose Bay Estuary.
- Anderson, L. G., Dyrssen, D., and Jones, E. P., 1990, An assessment of the transport of atmospheric CO₂ into the Arctic Ocean: *Journal of Geophysical Research: Oceans* (1978–2012), v. 95, no. C2, p. 1703-1711.
- Anderson, T., 1985, *Rivers of Labrador: Canadian Special Publication of Fisheries and Aquatic Sciences* 81, Ottawa 1985. 389.
- Anselmetti, F., Bühler, R., Finger, D., Girardclos, S., Lancini, A., Rellstab, C., and Sturm, M., 2007, Effects of Alpine hydropower dams on particle transport and lacustrine sedimentation: *Aquatic Sciences*, v. 69, no. 2, p. 179-198.
- Aure, J., Strand, Ø., Erga, S. R., and Strohmeier, T., 2007, Primary production enhancement by artificial upwelling in a western Norwegian fjord.

- Barrie, L. A., Gregor, D., Hargrave, B., Lake, R., Muir, D., Shearer, R., Tracey, B., and Bidleman, T., 1992, Arctic contaminants: sources, occurrence and pathways: *Science of the total environment*, v. 122, no. 1, p. 1-74.
- Batterson, M., and Liverman, D., 2010, Past and future sea-level change in Newfoundland and Labrador: Guidelines for policy and planning: Current Research. Newfoundland and Labrador Department of Natural Resources Geological Survey, Report, p. 10-11.
- Berger, W., Fischer, K., Lai, C., and Wu, G., 1988, Ocean carbon flux: global maps of primary production and export production: Biogeochemical cycling and fluxes between the deep euphotic zone and other oceanic realms. *NOAA Natl Undersea Res Prog*, p. 88-81.
- Bobbitt, J., and Akenhead, S., 1982, Influence of controlled discharge from the Churchill River on the oceanography of Groswater Bay, Labrador: Research and Resource Services, Department of Fisheries and Oceans.
- Bogen, J., and Bønsnes, T. E., 2001, The impact of a hydroelectric power plant on the sediment load in downstream water bodies, Svartisen, northern Norway: *Science of The Total Environment*, v. 266, no. 1–3, p. 273-280.
- Brandt, S. A., 2000, Classification of geomorphological effects downstream of dams: *Catena*, v. 40, no. 4, p. 375-401.
- Brown, T., Reimer, K., Sheldon, T., Bell, T., Luque, B. S., Fisk, A., and Iverson, S., 2012, . A first look at Nunatsiavut Kangigialuk (‘fjord’) ecosystems: Nunavik and Nunatsiavut: From Science to Policy an Integrated Regional Impact Study (IRIS) of Climate Change and Modernization. ArcticNet Inc., Quebec City, Quebec, Canada.
- Burdige, D. J., 2006, *Geochemistry of marine sediments*, Princeton University Press Princeton.
- Carpenter, M., 2012, Benthic habitats of a sub-arctic fiord: the case study of Okak Bay, Labrador: Memorial University of Newfoundland (M.Sc. Thesis).
- Cloern, J. E., Foster, S., and Kleckner, A., 2014, Phytoplankton primary production in the world's estuarine-coastal ecosystems: *Biogeosciences*, v. 11, no. 9, p. 2477-2501.
- Coachman, L. K., 1953, River flow and winter hydrographic structure of the Hamilton Inlet-Lake Melville Estuary of Labrador, p. 21.
- Finger, D., Schmid, M., and Wüest, A., 2006, Effects of upstream hydropower operation on riverine particle transport and turbidity in downstream lakes: *Water Resources Research*, v. 42, no. 8, p. W08429.
- Finnis, J., and Bell, T., 2015, An analysis of recent observed climate trends and variability in Labrador: *The Canadian Geographer/Le Géographe canadien*.
- FitzGerald, D. M., Fenster, M. S., Argow, B. A., and Buynevich, I. V., 2008, Coastal impacts due to sea-level rise: *Annu. Rev. Earth Planet. Sci.*, v. 36, p. 601-647.
- Flynn, W., 1968, The determination of low levels of polonium-210 in environmental materials: *Analytica chimica acta*, v. 43, p. 221-227.
- Gebhardt, A. C., Gaye-Haake, B., Unger, D., Lahajnar, N., and Ittekkot, V., 2005, A contemporary sediment and organic carbon budget for the Kara Sea shelf (Siberia): *Marine Geology*, v. 220, no. 1–4, p. 83-100.
- Goni, M. A., Yunker, M. B., Macdonald, R. W., and Eglinton, T. I., 2005, The supply and preservation of ancient and modern components of organic carbon in the Canadian Beaufort Shelf of the Arctic Ocean: *Marine Chemistry*, v. 93, no. 1, p. 53-73.
- Granskog, M. A., Macdonald, R. W., Mundy, C.-J., and Barber, D. G., 2007, Distribution, characteristics and potential impacts of chromophoric dissolved organic matter (CDOM)

- in Hudson Strait and Hudson Bay, Canada: *Continental Shelf Research*, v. 27, no. 15, p. 2032-2050.
- Gray, J. T., 1969, Glacial history of the eastern Mealy Mountains, southern Labrador: *Arctic*, p. 106-111.
- Greene, B. A., 1974, *An Outline of the Geology of Labrador: 1974*.
- Hare, A., Stern, G. A., Macdonald, R. W., Kuzyk, Z. Z., and Wang, F., 2008, Contemporary and preindustrial mass budgets of mercury in the Hudson Bay Marine System: the role of sediment recycling: *Sci Total Environ*, v. 406, no. 1-2, p. 190-204.
- Henrichs, S. M., 1992, Early diagenesis of organic matter in marine sediments: progress and perplexity: *Marine Chemistry*, v. 39, no. 1, p. 119-149.
- Henton, J. A., Craymer, M. R., Dragert, H., Mazzotti, S., Ferland, R., and Forbes, D. L., 2006, Crustal motion and deformation monitoring of the Canadian landmass: *Geomatica*, v. 60, no. 2, p. 173-191.
- Ittekkot, V., 1988, Global trends in the nature of organic matter in river suspensions.
- Johannessen, S., Macdonald, R., and Paton, D., 2003, A sediment and organic carbon budget for the greater Strait of Georgia: *Estuarine, Coastal and Shelf Science*, v. 56, no. 3, p. 845-860.
- Johannessen, S. C., Macdonald, R. W., and Eek, K. M., 2005, Historical Trends in Mercury Sedimentation and Mixing in the Strait of Georgia, Canada: *Environmental Science & Technology*, v. 39, no. 12, p. 4361-4368.
- Jones, B. M., Arp, C., Jorgenson, M., Hinkel, K. M., Schmutz, J., and Flint, P., 2009, Increase in the rate and uniformity of coastline erosion in Arctic Alaska: *Geophysical Research Letters*, v. 36, no. 3.
- Jorgenson, M. T., Shur, Y. L., and Pullman, E. R., 2006, Abrupt increase in permafrost degradation in Arctic Alaska: *Geophysical Research Letters*, v. 33, no. 2.
- Karlsson, E., Charkin, A., Dudarev, O., Semiletov, I., Vonk, J., Sánchez-García, L., Andersson, A., and Gustafsson, Ö., 2011, Carbon isotopes and lipid biomarker investigation of sources, transport and degradation of terrestrial organic matter in the Buor-Khaya Bay, SE Laptev Sea: *Biogeosciences*, v. 8, no. 7, p. 1865-1879.
- Kuzyk, Z. Z. A., Gobeil, C., and Macdonald, R. W., 2013, 210Pb and 137Cs in margin sediments of the Arctic Ocean: Controls on boundary scavenging: *Global Biogeochemical Cycles*, v. 27, no. 2, p. 422-439.
- Kuzyk, Z. Z. A., Macdonald, R. W., Johannessen, S. C., Gobeil, C., and Stern, G. A., 2009, Towards a sediment and organic carbon budget for Hudson Bay: *Marine Geology*, v. 264, no. 3, p. 190-208.
- Lantuit, H., and Pollard, W., 2008, Fifty years of coastal erosion and retrogressive thaw slump activity on Herschel Island, southern Beaufort Sea, Yukon Territory, Canada: *Geomorphology*, v. 95, no. 1, p. 84-102.
- Lavelle, J. W., Massoth, G.J., Crecelius, E.A., 1985, Sedimentation rates in Puget Sound from 210Pb measurements: National Oceanic and Atmospheric Administration.
- Liverman, D., Batterson, M., Taylor, D., and Ryan, J., 2001, Geological hazards and disasters in Newfoundland and Labrador: *Canadian Geotechnical Journal*, v. 38, no. 5, p. 936-956.
- Lu, Z., DeYoung, B., and Foley, J., 2013, Analysis of physical oceanography data from Lake Melville, Labrador, July-September 2012: Department of Physics and Physical Oceanography, Memorial University of Newfoundland.

- Lucas, L. V., Thompson, J. K., and Brown, L. R., 2009, Why are diverse relationships observed between phytoplankton biomass and transport time?: *Limnology and oceanography*, v. 54, no. 1, p. 381-390.
- Macdonald, R., Solomon, S., Cranston, R., Welch, H., Yunker, M., and Gobeil, C., 1998, A sediment and organic carbon budget for the Canadian Beaufort Shelf: *Marine Geology*, v. 144, no. 4, p. 255-273.
- Macdonald, R. W., Kuzyk, Z. A., and Johannessen, S. C., 2015, It is not just about the ice: a geochemical perspective on the changing Arctic Ocean: *Journal of Environmental Studies and Sciences*, p. 1-14.
- Mason, R. P., Choi, A. L., Fitzgerald, W. F., Hammerschmidt, C. R., Lamborg, C. H., Soerensen, A. L., and Sunderland, E. M., 2012, Mercury biogeochemical cycling in the ocean and policy implications: *Environmental Research*, v. 119, p. 101-117.
- Milliman, J. D., and Syvitski, J. P., 1992, Geomorphic/tectonic control of sediment discharge to the ocean: the importance of small mountainous rivers: *The Journal of Geology*, p. 525-544.
- Minaskuat, 2008, Water and sediment modelling in the Lower Churchill River
- Muzuka, A. N., and Hillaire-Marcel, C., 1999, Burial rates of organic matter along the eastern Canadian margin and stable isotope constraints on its origin and diagenetic evolution: *Marine Geology*, v. 160, no. 3, p. 251-270.
- Nalcor, 2007, Water and sediment quality in the Churchill River: Environmental Baseline Report LHP 06-04: Minaskuat Limited Partnership for Newfoundland and Labrador Hydro, 2 of 5.
- Newbury, R., and McCullough, G., 1984, Shoreline erosion and restabilization in the Southern Indian Lake reservoir: *Canadian Journal of Fisheries and Aquatic Sciences*, v. 41, no. 4, p. 558-566.
- Overeem, I., Anderson, R. S., Wobus, C. W., Clow, G. D., Urban, F. E., and Matell, N., 2011, Sea ice loss enhances wave action at the Arctic coast: *Geophysical Research Letters*, v. 38, no. 17.
- Payette, S., Delwaide, A., Caccianiga, M., and Beauchemin, M., 2004, Accelerated thawing of subarctic peatland permafrost over the last 50 years: *Geophysical Research Letters*, v. 31, no. 18.
- Peierls, B. L., Hall, N. S., and Paerl, H. W., 2012, Non-monotonic responses of phytoplankton biomass accumulation to hydrologic variability: a comparison of two coastal plain North Carolina estuaries: *Estuaries and Coasts*, v. 35, no. 6, p. 1376-1392.
- Rachold, V., Grigoriev, M. N., Are, F. E., Solomon, S., Reimnitz, E., Kassens, H., and Antonow, M., 2000, Coastal erosion vs riverine sediment discharge in the Arctic Shelf seas: *International Journal of Earth Sciences*, v. 89, no. 3, p. 450-460.
- Roberts, J., Pryse-Phillips, A., and Snelgrove, K., 2012, Modeling the Potential Impacts of Climate Change on a Small Watershed in Labrador, Canada: *Canadian Water Resources Journal / Revue canadienne des ressources hydriques*, v. 37, no. 3, p. 231-251.
- Sakshaug, E., 2004, Primary and secondary production in the Arctic Seas, The organic carbon cycle in the Arctic Ocean, Springer, p. 57-81.
- Schartup, A. T., Balcom, P. H., Soerensen, A. L., Gosnell, K. J., Calder, R. S., Mason, R. P., and Sunderland, E. M., 2015, Freshwater discharges drive high levels of methylmercury in Arctic marine biota: *Proceedings of the National Academy of Sciences*, v. 112, no. 38, p. 11789-11794.

- Sella, G. F., Stein, S., Dixon, T. H., Craymer, M., James, T. S., Mazzotti, S., and Dokka, R. K., 2007, Observation of glacial isostatic adjustment in “stable” North America with GPS: *Geophysical Research Letters*, v. 34, no. 2.
- Shaw, J., Taylor, R. B., Forbes, D. L., Ruz, M., and Solomon, S., 1998, Sensitivity of the coasts of Canada to sea-level rise, *Geological Survey of Canada*.
- Smith, J. N., 2001, Why should we believe ^{210}Pb sediment geochronologies?: *Journal of Environmental Radioactivity*, v. 55, no. 2, p. 121-123.
- Sorokin, Y. I., and Sorokin, P. Y., 1996, Plankton and primary production in the Lena River estuary and in the south-eastern Laptev Sea: *Estuarine, Coastal and Shelf Science*, v. 43, no. 4, p. 399-418.
- Stein, R., and Macdonald, R., 2004, Organic carbon budget: Arctic Ocean vs. global ocean, *The organic carbon cycle in the Arctic Ocean*, Springer, p. 315-322.
- Sunderland, E. M., Dalziel, J., Heyes, A., Branfireun, B. A., Krabbenhoft, D. P., and Gobas, F. A., 2010, Response of a macrotidal estuary to changes in anthropogenic mercury loading between 1850 and 2000: *Environmental Science & Technology*, v. 44, no. 5, p. 1698-1704.
- Syvitski, J., Burrell, D., and Skei, J., 1987, *Fjords: Processes and Products*, New York, NY, Springer-Verlag, 379 p.:
- Syvitski, J., Schafer, C., 1990, ADFEX Environmental Impact Statement (EIS).
- Tan, F., and Vilks, G., 1987, Organic carbon isotope ratios and paleoenvironmental implications for Holocene sediments in Lake Melville, southeastern Labrador: *Canadian Journal of Earth Sciences*, v. 24, no. 10, p. 1994-2003.
- Uncles, R. J., and Cloern, J. E., 1987, Dynamics of Turbid Coastal Environments Turbidity as a control on phytoplankton biomass and productivity in estuaries: *Continental Shelf Research*, v. 7, no. 11, p. 1367-1381.
- Vilks, G., Deonarine, B., and Winters, G., 1987, *Lat Quaternary Marine Geology of Lake Melville, Labrador*: Geological Survey of Canada.
- Vonk, J., Sánchez-García, L., van Dongen, B., Alling, V., Kosmach, D., Charin, A., Semiletov, I., Dudarev, O., Shakhova, N., and Roos, P., 2012, Activation of old carbon by erosion of coastal and subsea permafrost in Arctic Siberia: *Nature*, v. 489, no. 7414, p. 137-140.
- Wardle, R. J., Gower, C. F., Ryan, B., Nunn, G. A. G., James, D.T., and Kerr, A., 1997, *Geological Map of Labrador; 1:1 million scale.*: Department of Mines and Energy, Geological Survey, Government of Newfoundland Map 97-07.
- Williams, G. P., and Wolman, M. G., 1984, Downstream effects of dams on alluvial rivers.
- Yin, K., Harrison, P. J., Pond, S., and Beamish, R. J., 1995, Entrainment of Nitrate in the Fraser River Estuary and its Biological Implications. II. Effects of Spring vs. Neap Tides and River Discharge: *Estuarine, Coastal and Shelf Science*, v. 40, no. 5, p. 529-544.
- Zaborska, A., Carroll, J., Papucci, C., and Pempkowiak, J., 2007, Intercomparison of alpha and gamma spectrometry techniques used in ^{210}Pb geochronology: *Journal of environmental radioactivity*, v. 93, no. 1, p. 38-50.
- Zhu, J., and Olsen, C. R., 2013, Sedimentation and Organic Carbon Burial in the Yangtze River and Hudson River Estuaries: Implications for the Global Carbon Budget: *Aquatic Geochemistry*, p. 1-1

Chapter 4 : Conclusion and suggestions for future work

4.1 Conclusions

This research was conducted as part of the “Lake Melville: Avativut, Kanuittailinnivut (Our Environment, Our Health)” project developed by the Nunatsiavut Government of Labrador and Memorial University of Newfoundland in collaboration with the University of Manitoba and funding from ArcticNet. The overall project objectives were: 1) to establish baseline conditions of Inuit health and well-being and ecosystem integrity in Lake Melville prior to hydroelectric development on the Lower Churchill River; and 2) to develop the science for monitoring any downstream effects of hydroelectric development in the context of ongoing climate change. Prior to this multidisciplinary research project, only a few studies had investigated Lake Melville, many of which focused on reconstructing the environmental history over a glacial timescale (i.e., Syvitski, 1993; Tan and Vilks, 1987; Vilks et al., 1987; Vilks., 1983) while a couple studies (i.e., Bobbitt and Akenhead, 1982b; Coachman, 1953) looked at the more recent hydrology and oceanography of the system. Because of this, basic fundamental processes within the collective Lake Melville system (i.e., Goose Bay and Lake Melville, hereafter referred to as LMS) and exchanges between the terrestrial environment, LMS, and the open ocean were poorly understood. Without an understanding of the most fundamental processes, the overall biogeochemical cycle and, consequently the cycling and fate of contaminants in the system could not be fully known.

To address the aforementioned knowledge gaps and contribute to the overall project objectives, this thesis applied new radioisotope and organic geochemical data (organic carbon, $\delta^{13}\text{C}$) for sediment cores distributed throughout the Lake Melville system to quantifying rates of

sedimentation and biomixing and enhancing our understanding of the major sources (i.e., terrestrial or marine), processes (i.e., deposition, lateral transport), and fate (i.e., oxidation, burial, export) of particulate organic carbon (POC) in the LMS. Through the examination of the sediment record, changes to the system in the most recently deposited sediment (i.e., last 100 years) was documented (Chapter 2). This documentation of change was used to conceptualize possible changes to the LMS following the hydroelectric development on the Lower Churchill River, while also considering the effects of a warming climate (cf., Finnis and Bell, 2015). In Chapter 3, sediment and POC (marine and terrestrial) budgets were constructed using new (Chapter 2 and 3) and previously published data in box-models, which separated Goose Bay and Lake Melville. Through the development of these budgets, the major processes in the organic carbon cycle taking place in Goose Bay and Lake Melville and exchanges between and out of the system were quantified. By establishing these baseline values, any changes to the system in the future can be assessed.

The study presented in Chapter 2 established the first contemporary (i.e., last 100 yr) mass accumulation rates (MARs) of the LMS. These MARs were established by modelling fifteen down-core profiles of $^{210}\text{Pb}_{\text{ex}}$ and validating the models with a separate transient tracer, ^{137}Cs . Overall, MARs are significantly inversely associated with distance to the Churchill River. Yet, the greatest MAR was found outside of Goose Bay near the mouth of the Kenamu River approximately 22 km from the Churchill River mouth. This variation in MARs was attributed to three main factors: 1) the large Churchill River plume that carries suspended sediment in the highly stratified, fast moving surface waters through Goose Bay Narrows and into the (larger) western end of Lake Melville, where water velocity slows and particles settle out; 2) additional inputs from smaller rivers, particularly the Kenamu River, whose channel morphology

(meandering), proneness to flooding, and tributaries that drain the Mealy Mountains, all favour disproportionate contributions to the sediment supply (c.f., Milliman and Syvitski, 1992); and 3) local topographic lows (troughs, basins, shoals, and shallow narrow channels) that influence the distribution of sediment by altering waves, tides and currents.

In Chapter 2, sources of sediment were investigated by comparing sedimentary inventories of $^{210}\text{Pb}_{\text{ex}}$ versus ^{137}Cs to the expected ratio in terrestrial soil (i.e., inventories expected from direct atmospheric fallout). This comparison concluded that sediment in the LMS is largely sourced from the terrestrial environment; high ^{137}Cs inventories near river mouths point to rivers as the greatest source of terrestrial material to the system. This conclusion was reinforced in Chapter 3, where budgets revealed that 78% and 81% of sediment and terrestrial POC inputs to the LMS is delivered by rivers, respectively.

A comparison of $^{210}\text{Pb}_{\text{ex}}$ to ^{137}Cs inventories in Chapter 2 revealed an opposing trend between the two radioisotopes, suggesting an additional source of $^{210}\text{Pb}_{\text{ex}}$ in the eastern end of Lake Melville. This additional $^{210}\text{Pb}_{\text{ex}}$ in the eastern end is consistent with inputs of dissolved $^{210}\text{Pb}_{\text{ex}}$ from landward flowing seawater and subsequent scavenging of $^{210}\text{Pb}_{\text{ex}}$ from the water column by particles (Kuzyk et al., 2013). The high sedimentary marine OC at this location suggests that elevated scavenging of $^{210}\text{Pb}_{\text{ex}}$ from the water column in the eastern most end of Lake Melville is also connected to a productive “hotspot”. This hypothesis was reinforced in Chapter 3, where the first estimates of primary production for the LMS were made using new surface sediment fluxes of marine OC (OC_{mar}) and a regression equation (from the literature) describing OC losses with depth in the water column. With this approach, primary production at the eastern most end of Lake Melville was 2-3 times greater ($165.6 \text{ g OC}_{\text{mar}} \text{ m}^{-2} \text{ yr}^{-1}$) than anywhere else in the LMS (median = $42.5 \text{ g C m}^{-2} \text{ yr}^{-1}$). We propose this productive “hotspot” is

linked to the renewal of nutrients from upwelling on the seaward side of the Narrows (c.f., Lu et al., 2013) and a deeper euphotic zone.

The distribution of deposited OC_{mar} and terrestrial OC (OC_{terr}) was investigated through the assessment of bulk OC and $\delta^{13}C_{\text{org}}$ in surface and down-core sediments in Chapter 2. River and marine $\delta^{13}C_{\text{org}}$ end-members, established from filtered river water and literature review, were applied to a simple two-endmember mixing model to determine the proportion of OC_{mar} and OC_{terr} . This approach revealed that OC_{terr} is greatest in sediment from the western end of the Lake, which is where the major rivers drain into the system. From west to east, the proportion of OC_{terr} decreased while OC_{mar} increased, with mostly OC_{mar} in the coastal sediment of Groswater Bay.

This mix of OC_{terr} and OC_{mar} in sediment across the LMS reflects the two-layer estuarine circulation of the system and supports findings by Tan and Vilks (1987). Since marine and terrigenous OC are sourced and cycled differently, budgets were developed for both marine and terrigenous OC, in addition to suspended sediment, in Chapter 3. Of the seven main rivers draining into the LMS, the Churchill River dominates, supply 65% of the total 38.5×10^8 kg sediment yr^{-1} and 53% of the total 34.5×10^6 kg POC_{terr} yr^{-1} of total river inputs. Although the Churchill River drains directly into Goose Bay, the majority of its inputs (79% sediment and 95% POC_{terr}) are transported into Lake Melville, demonstrating the large extent of influence of the Churchill River across the LMS. Rates of primary production were significantly inversely associated ($p < 0.05$) with distance to the Churchill River. This increase in primary production is associated with decreasing turbidity and DOM as the Churchill River plume moves eastward and gradually loses its load. Goose Bay captures only 18% of 33.8×10^8 kg yr^{-1} total sediment and 13% of 11.4×10^6 kg POC_{terr} yr^{-1} total POC_{terr} buried in the overall Lake Melville system.

Inspection of down-core profiles POC_{terr} , POC_{mar} , and $\delta^{13}\text{C}$ across the LMS in Chapter 2 revealed a small, but significant decrease of the $\delta^{13}\text{C}_{\text{org}}$ signature in sediment deposited predominantly (i.e., 90%) after 1970. A comparison of profiles of OC_{terr} and OC_{mar} (%) revealed that the portion of OC_{terr} has increased over time while OC_{mar} has remained relatively consistent down-core, suggesting an increase in the supply of OC_{terr} rather than a decline in OC_{mar} over the last ca. 43 years.

In seeking reasons for the increase in POC_{terr} , it is likely that the strongest source of POC_{terr} would be involved (i.e., the Churchill River). Specifically, changes in the seasonality of the Churchill River discharge because of hydroelectric development of Churchill Falls in the 1970s would have released POC_{terr} (c.f., Houel et al., 2006), thus likely increasing the delivery of such POC to Lake Melville, at least for some period until the system readjusted (Newbury and McCullough, 1984). Climate warming in the Labrador region (c.f., Finnis and Bell, 2015; Way and Viau, 2014) could also lead to increased freshwater runoff to the LMS (Roberts et al., 2012) while at the same time, a shorter season of sea ice cover and greater storm events could increase coastal erosion and the delivery of OC_{terr} (Goni et al., 2005; Lantuit et al., 2012).

Based on our new understanding of the LMS presented in chapters 2 and 3 and summarized here, we predict that the hydroelectric development on the Lower Churchill River will increase inputs of sediment and POC_{terr} to Lake Melville, at least in the first 2 year following impoundment. This increase in sediment and POC_{terr} is presumed to be greater than observed in the sedimentary record following the Churchill Falls development in the 1970s because of the nearness of Muskrat Falls to Goose Bay (ca. 40 km) and the highly erodible river bank at the reservoir site and along the lower reaches of the River (Amec, 2008b). Based on a similar system in Manitoba (c.f., Newbury and McCullough, 1984) and modelling of the lower Churchill River

suspended sediment load by Minaskuat (2008), bank erosion rates are expected to be greatest in the first 2 years following development and decline over a 20-50 year period. Applying erosion rates developed by Amec (2008a) to the expected shoreline length of the reservoir (35.5 km) suggests a doubling of the sediment ($49.5 \times 10^8 \text{ kg yr}^{-1}$) and POC_{terr} ($24.3 \times 10^8 \text{ kg yr}^{-1}$) delivered by the Churchill River in the first 2 years after impoundment.

4.2 Suggestions for future work

Because the Churchill River is by far the largest source of freshwater, sediment, and POC to the LMS, year-round monitoring of the Churchill River is needed to assess any changes during construction and the 2 years following impoundment when bank erosion will be greatest. Basic, seasonal assessments of the Goose, Northwest, and Kenamu Rivers, which have not been evaluated since the 1950s, are also needed to better constrain the role these rivers have on the LMS and how climate change could impact overall freshwater runoff to the system. Basic, yet essential measurements that should be implemented in future monitoring of rivers flowing into Lake Melville include: flow, total suspended sediment, organic carbon, and nutrients.

Within Lake Melville itself, our results show that the extent of the Churchill River plume is large, carrying suspended sediment and particulate organic matter through Goose Bay Narrows and into Lake Melville. Because of this wide distribution, it is presumed that the plume has a major impact on primary production (i.e., phytoplankton) by limiting the depth to which light penetrates the water column, delivering nutrients from land and driving estuarine circulation, which brings nutrient rich marine water to the surface. As the seasonal hydrology of the Churchill River shifts during and after impoundment at Muskrat falls, the plankton community could be affected. The rates of new production presented in Chapter 3 were constrained indirectly and need to be validated with direct measurements of chlorophyll *a* in the water

column and sediment surface, while an investigation into the ice algae community is, to our knowledge, still needed.

To conclude, the development of nutrient (PO_4^{3-} , NO_3^- , SiO_4^{4-}) budgets (inputs, losses, sinks) must be the next step to improve our understanding of the biogeochemical cycle in the LMS and potential impacts from hydroelectric and climatic change. By quantifying the cycling of nutrients in the LMS, insight into some uncertainties in the POC_{mar} budget presented here could be addressed. For example, how much nitrate is available for primary production? How much nitrate is brought to the surface waters by entrainment of marine bottom water versus river runoff and to what extent do these sources influence the distribution and rate of primary production? In addition to the budgets presented here, a nutrient budget would enable a more comprehensive understanding of the system, and provide a clearer connection between productivity and the fate of mercury in the LMS (Schartup et al., 2015).

4.3 References

- Amec, 2008a, Bank stability study for the proposed Lower Churchill Hydroelectric Generation Project: Environmental baseline report.
- , 2008b, Lower Churchill Hydroelectric Generation Project: Sedimentation and Morphodynamics Study
- Bobbitt, J., and Akenhead, S., 1982, Influence of controlled discharge from the Churchill River on the oceanography of Groswater Bay, Labrador: Research and Resource Services, Department of Fisheries and Oceans.
- Coachman, L. K., 1953, River flow and winter hydrographic structure of the Hamilton Inlet-Lake Melville Estuary of Labrador, p. 21.
- Finnis, J., and Bell, T., 2015, An analysis of recent observed climate trends and variability in Labrador: The Canadian Geographer/Le Géographe canadien.
- Goni, M. A., Yunker, M. B., Macdonald, R. W., and Eglinton, T. I., 2005, The supply and preservation of ancient and modern components of organic carbon in the Canadian Beaufort Shelf of the Arctic Ocean: Marine Chemistry, v. 93, no. 1, p. 53-73.
- Houel, S., Louchouart, P., Lucotte, M., Canuel, R., and Ghaleb, B., 2006, Translocation of soil organic matter following reservoir impoundment in boreal systems: Implications for in situ productivity: Limnology and oceanography, v. 51, no. 3, p. 1497-1513.

- Kuzyk, Z. Z. A., Gobeil, C., and Macdonald, R. W., 2013, 210Pb and 137Cs in margin sediments of the Arctic Ocean: Controls on boundary scavenging: *Global Biogeochemical Cycles*, v. 27, no. 2, p. 422-439.
- Lantuit, H., Overduin, P. P., Couture, N., Wetterich, S., Aré, F., Atkinson, D., Brown, J., Cherkashov, G., Drozdov, D., and Forbes, D. L., 2012, The Arctic coastal dynamics database: A new classification scheme and statistics on Arctic permafrost coastlines: *Estuaries and Coasts*, v. 35, no. 2, p. 383-400.
- Lu, Z., DeYoung, B., and Foley, J., 2013, Analysis of physical oceanography data from Lake Melville, Labrador, July-September 2012: Department of Physics and Physical Oceanography, Memorial University of Newfoundland.
- Milliman, J. D., and Syvitski, J. P., 1992, Geomorphic/tectonic control of sediment discharge to the ocean: the importance of small mountainous rivers: *The Journal of Geology*, p. 525-544.
- Minasquat, 2008, Water and sediment modelling in the Lower Churchill River
- Newbury, R., and McCullough, G., 1984, Shoreline erosion and restabilization in the Southern Indian Lake reservoir: *Canadian Journal of Fisheries and Aquatic Sciences*, v. 41, no. 4, p. 558-566.
- Roberts, J., Pryse-Phillips, A., and Snelgrove, K., 2012, Modeling the Potential Impacts of Climate Change on a Small Watershed in Labrador, Canada: *Canadian Water Resources Journal / Revue canadienne des ressources hydriques*, v. 37, no. 3, p. 231-251.
- Schartup, A. T., Balcom, P. H., Soerensen, A. L., Gosnell, K. J., Calder, R. S., Mason, R. P., and Sunderland, E. M., 2015, Freshwater discharges drive high levels of methylmercury in Arctic marine biota: *Proceedings of the National Academy of Sciences*, v. 112, no. 38, p. 11789-11794.
- Syvitski, J., Hinds, S.J., Burns, J.A., 1993, Marine geology of Lake Melville (Labrador), scale 1:100,000.
- Tan, F., and Vilks, G., 1987, Organic carbon isotope ratios and paleoenvironmental implications for Holocene sediments in Lake Melville, southeastern Labrador: *Canadian Journal of Earth Sciences*, v. 24, no. 10, p. 1994-2003.
- Vilks, G., Deonarine, B., and Winters, G., 1987, Late Quaternary Marine Geology of Lake Melville, Labrador: Geological Survey of Canada.
- Vilks, G. a. M., P.J., 1983, Evidence of postglacial paleoceanographic and paleoclimatic changes in Lake Melville, Labrador, Canada: *Arctic and Alpine Research*, v. 15, no. 3, p. 307-319.
- Way, R. G., and Viau, A. E., 2014, Natural and forced air temperature variability in the Labrador region of Canada during the past century: *Theoretical and Applied Climatology*, p. 1-12

Appendix A : Description of core locations used in this study.

Core	Region of Inlet	Latitude	Longitude	Water Depth (m)
I10	Goose Bay	53°21.42'N	60°19.98'W	25.6
26	Goose Bay	53°22.90'N	60°12.10'W	49
I11	Goose Bay	53°24.53'N	60°01.87'W	52
I12	Mouth of Northwest River	53°31.24'N	60°05.40'W	48
35	Mouth of Kenamu River	53°29.26'N	59°55.92'W	47
34	Eppinette Basin (Lake Melville)	53°33.97'N	59°46.80'W	161
28B	Sabaskatchu Bay	53°45.00'N	60°03.00'W	50
DB3	Sabaskatchu Trough (Lake Melville)	53°42.30'N	59°43.71'W	126
MT1	Mulligan Trough (Lake Melville)	53°45.78'N	59°31.84'W	149
DB5	Mulligan Trough (Lake Melville)	53°48.27'N	59°22.36'W	217
33	Grand Trough (Lake Melville)	53°40.06'N	59°28.65'W	175
I13	Grand Trough (Lake Melville)	53°49.39'N	59°48.21'W	213
30	Grand Trough (Lake Melville)	53°49.93'N	53°07.65'W	220
DB6	Grand Trough (Lake Melville)	53°58.33'N	58°46.61'W	196
BW1	Backway (Lake Melville)	54°04.86'N	58°16.58'W	98

Appendix B : Down-core data of radiochemistry, stable isotope, and organic carbon

Appendix B contains tables of the radiochemistry (^{210}Pb , ^{137}Cs , and ^{226}Ra), stable isotope ($\delta^{13}\text{C}_{\text{org}}$), and percentage of organic carbon (OC) data from fifteen sediment cores collected across Goose Bay and Lake Melville in 2013 and 2014. Total ^{210}Pb , ^{226}Ra , and ^{137}Cs were measured by gamma ray spectrometry at the Environmental Radiochemistry Laboratory (ERL) at U of M. Activities of ^{226}Ra were determined indirectly by counting ^{214}Pb , its granddaughter isotope, at 352 keV. Total ^{210}Pb and ^{137}Cs were counted at 47 and 661 keV, respectively. To assess the appropriateness of the gamma method in measuring ^{210}Pb in these cores, cores 26, DB3, MT1, and I13 were subjected to alpha ray spectrometry method and the results from this analysis are presented here. Unsupported or excess ^{210}Pb ($^{210}\text{Pb}_{\text{ex}}$) was calculated by subtracting ^{226}Ra from total ^{210}Pb . Stable isotope $\delta^{13}\text{C}_{\text{org}}$ and OC (%) were measured down select cores at the Stable Isotope for Innovative Research Laboratory (SIFIR) at U of M. The OC content was calculated from the difference between total carbon (TC) and inorganic carbon (IC), measured using an elemental analyser. Decarbonated sub-samples were analysed for $\delta^{13}\text{C}_{\text{org}}$ (‰ relative to VPDB) using an elemental analyser isotope-ratio mass spectrometer (EA-IRMS).

Core I10

Depth (cm)	Total ^{210}Pb (dpm g ⁻¹)	^{226}Ra (dpm g ⁻¹)	$^{210}\text{Pb}_{\text{ex}}$ (dpm g ⁻¹)	^{137}Cs (dpm g ⁻¹)	%OC	$\delta^{13}\text{C}_{\text{org}}$ (‰)
1	3.10	1.64	1.5	0.14	0.9	-27.9
2	3.48	1.63	1.8	0.42	0.8	-28.3
3	3.62	1.68	1.9	0.37		
4	3.45	1.19	2.3	0.53	0.7	-28.0
5	3.01	1.74	1.3	0.43		
6	4.29	1.25	3.0	0.38	0.7	-27.9
7	3.76	2.10	1.7	0.40		
8	3.52	1.58	1.9	0.26	0.6	-27.9
9	3.47	1.87	1.6	0.42		
10	2.59	1.87	0.7	0.30	0.5	-28.0
11	2.42	1.89	0.5	0.38		
12	3.34	1.88	1.5	0.43		
13	1.78	1.56	0.2	0.30	0.5	-28.1
14	1.74	1.69	0.1	0.45	0.5	-27.8
15	1.50	1.44	0.1	0.34	0.5	

Core 26

Depth (cm)	Total ^{210}Pb (dpm g ⁻¹) ¹	Total ^{210}Pb (dpm g ⁻¹) ²	^{226}Ra (dpm g ⁻¹)	$^{210}\text{Pb}_{\text{ex}}$ (dpm g ⁻¹)	^{137}Cs (dpm g ⁻¹)	%OC	$\delta^{13}\text{C}_{\text{org}}$ (‰)
1	3.80	2.32	1.94	1.49	0.38	0.4	-27.9
2	3.65	3.46	1.98	1.69	0.26	0.4	-28.1
3	4.06	2.95	1.55	3.06	0.31	0.4	-28.1
4	3.52	2.08	1.78	2.25	0.26	0.4	-28.3
5	3.52	2.92	1.35	2.84	0.28	0.4	-28.2
6	3.45	2.31	1.68	2.33	0.36	0.4	-28.1
7	3.33	2.97	1.84	1.92	0.16	0.4	-28.2
8	3.40	2.48	1.56	2.30	0.33	0.3	-28.4
9	3.03	2.55	1.63	1.83	0.34	0.3	-28.1
10	2.66	2.31	1.78	1.13	0.47	0.3	-28.3

Counted by ¹ gamma and ² alpha.

Core I11

Depth (cm)	Total ^{210}Pb (dpm g $^{-1}$)	^{226}Ra (dpm g $^{-1}$)	$^{210}\text{Pb}_{\text{ex}}$ (dpm g $^{-1}$)	^{137}Cs (dpm g $^{-1}$)	%OC	$\delta^{13}\text{C}_{\text{org}}$ (‰)
1	3.60	1.20	2.4	0.45	0.5	-27.8
2	4.20	1.80	2.4	0.34		
3	3.00	1.20	1.8	0.40		
4	3.00	1.20	1.8	0.44		
5	4.20	1.20	3.0	0.39		
6	3.00	1.20	1.8	0.42		
7	3.00	1.80	1.2			
8	3.00	1.80	1.2	0.47		
9	3.00	1.80	1.2			
10	3.60	1.80	1.8	0.61		
11	2.40	1.20	1.2	0.50		

Core I12

Depth (cm)	Total ^{210}Pb (dpm g $^{-1}$)	^{226}Ra (dpm g $^{-1}$)	$^{210}\text{Pb}_{\text{ex}}$ (dpm g $^{-1}$)	^{137}Cs (dpm g $^{-1}$)	%OC	$\delta^{13}\text{C}_{\text{org}}$ (‰)
1	7.01	2.05	4.96	0.49	0.8	-26.8
2	5.60	1.31	4.28	0.50		
3	4.61	1.77	2.84	0.53	0.8	-27.3
4	5.36	1.35	4.01	0.52		
5	4.11	1.54	2.57	0.63	0.7	-26.9
6	4.36	1.24	3.11	0.57		
7	3.59	1.91	1.68	0.82	0.7	-26.9
8	5.93	2.53	3.40	1.31	0.7	-27.0
9	3.33	2.10	1.23	1.23	0.7	-27.0
10	3.43	1.20	2.23	1.20	0.7	-27.1
11	2.06	2.29	1.20	0.74	0.6	-26.6
12	1.97	1.80	0.17	0.00		
13	1.80	1.73	0.07	0.79	0.6	-26.7
14	1.47	1.53	0.15	0.40		
15	1.85	1.20	0.48	0.00	0.6	-26.7
16	1.22	1.60	0.06	0.00		
17	1.20	0.60	0.06	0.00	0.6	-26.4

Core 35

Depth (cm)	Total ^{210}Pb (dpm g ⁻¹)	^{226}Ra (dpm g ⁻¹)	$^{210}\text{Pb}_{\text{ex}}$ (dpm g ⁻¹)	^{137}Cs (dpm g ⁻¹)	%OC	$\delta^{13}\text{C}_{\text{org}}$ (‰)
1	9.89	3.40	6.49	1.01	1.6	-27.6
2	4.53	1.76	2.77	0.69		
3	5.38	1.44	3.94	0.43		
4	5.27	1.66	3.61	0.52		
5	4.33	1.92	2.41	0.45		
6	5.42	1.82	3.60	0.48		
7	3.50	1.13	2.38	0.49		
8	4.48	1.50	2.98	0.51		
9	3.97	1.25	2.73	0.48		
10	4.84	1.47	3.37	0.55		
11	3.92	1.02	2.90	0.37		
12	3.81	1.36	2.45	0.50		
13	2.95	0.98	1.97	0.49		
14	3.23	1.30	1.94	0.41		
15	2.72	0.57	2.14	0.50		
16	3.68	1.63	2.05	0.46		
18	3.33	1.55	1.78	0.49		
22	2.71	1.48	1.23	0.40		
23	2.57	1.05	1.52	0.50		

Core 34

Depth (cm)	Total ^{210}Pb (dpm g $^{-1}$)	^{226}Ra (dpm g $^{-1}$)	$^{210}\text{Pb}_{\text{ex}}$ (dpm g $^{-1}$)	^{137}Cs (dpm g $^{-1}$)	%OC	$\delta^{13}\text{C}_{\text{org}}$ (‰)
1	9.18	1.76	7.42	0.45	0.9	-27.5
2	8.79	1.89	6.90	0.42		
3	6.87	1.80	5.07	0.53	0.8	-27.4
4	5.17	1.71	3.46	0.65		
5	7.30	2.69	4.61	0.71		
6	6.50	2.29	4.21	0.77		
7	3.81	1.76	2.04	0.27	0.8	-27.4
8	6.54	1.99	4.56	0.70		
9	3.92	1.88	2.04	0.29	0.8	
10	4.77	2.04	2.73	0.82		
11	4.20	1.84	2.36	0.99	0.7	-27.3
12	3.63	1.75	1.88	0.85		
13	3.42	1.81	1.61	0.78	0.7	-27.1
14	3.22	1.87	1.35	1.06	0.8	
15	2.11	1.86	0.25	0.75		
16	3.37	1.85	1.52	0.55		
17	2.35	2.09	0.25	0.00		
18	2.72	2.04	0.68	0.00	0.7	-26.4
19	3.09	1.99	1.10	0.00		
20	1.59	1.32	0.27	0.00	0.7	
21	1.53	1.46	0.07	0.00	0.7	
22	1.47	1.23	0.24	0.00	0.7	
23	1.32	1.16	0.16	0.00	0.7	-26.6

Core 28B

Depth (cm)	Total ^{210}Pb (dpm g ⁻¹)	^{226}Ra (dpm g ⁻¹)	$^{210}\text{Pb}_{\text{ex}}$ (dpm g ⁻¹)	^{137}Cs (dpm g ⁻¹)	%OC	$\delta^{13}\text{C}_{\text{org}}$ (‰)
1	10.16	1.98	8.18	0.54	1.1	-26.4
2	7.99	1.88	6.11	0.48		
3	5.89	1.78	4.11	0.42		
4	4.38	1.71	2.68	0.72		
5	4.17	1.63	2.54	0.62		
6	3.33	1.53	1.79	0.53		
7	2.59	1.54	1.06	0.00		
8	1.86	1.54	0.32	0.00		
9	1.62	1.48	0.15	0.00		
10	1.39	1.38	0.01	0.00		
11	1.51	1.39	0.11	0.00		
12	1.57	1.38	0.18	0.00		
13	1.54	1.38	0.16	0.00		
14	1.56	1.29	0.27	0.00		

Core DB3

Depth (cm)	Total ^{210}Pb (dpm g ⁻¹) ¹	Total ^{210}Pb (dpm g ⁻¹) ²	^{226}Ra (dpm g ⁻¹)	$^{210}\text{Pb}_{\text{ex}}$ (dpm g ⁻¹)	^{137}Cs (dpm g ⁻¹)	%OC	$\delta^{13}\text{C}_{\text{org}}$ (‰)
1	8.71	10.87	2.61	6.10	0.00	0.9	-26.7
2	9.89	10.44	3.23	6.66	0.88		
3	5.40	9.83	2.43	2.97	0.48	1.1	-26.4
4	7.13	10.03	1.92	5.20	0.76		
5	4.54	9.37	2.04	2.50	0.65	1.1	-26.8
6	6.03	8.61	2.16	3.87	0.85		
7	4.48	7.61	1.86	2.62	0.81	1.0	-26.8
8	5.29	6.48	2.34	2.95	1.12		
9	5.45	5.44	2.16	3.29	1.11	0.9	-26.6
10	3.72	4.35	1.99	1.72	0.58		
11	3.77	4.84	1.51	2.25	1.14	0.9	-26.3
12	3.08	3.79	2.05	1.03	0.46		
13	4.85	3.36	1.89	2.96	0.00	0.9	-26.2
14	3.21	3.02	2.24	0.97	0.00		
15	2.36	2.72	1.36	1.01	0.00		
16	2.35	2.72	1.72	0.64	0.00		
17	1.23	2.69	0.92	0.31	0.00	0.8	-26.0

Counted by ¹ gamma and ² alpha method.

Core MT1

Depth (cm)	Total ^{210}Pb (dpm g ⁻¹) ¹	Total ^{210}Pb (dpm g ⁻¹) ²	^{226}Ra (dpm g ⁻¹)	$^{210}\text{Pb}_{\text{ex}}$ (dpm g ⁻¹)	^{137}Cs (dpm g ⁻¹)	%OC	$\delta^{13}\text{C}_{\text{org}}$ (‰)
1	10.10	11.82	2.52	9.30	0.50	1.3	-26.3
2	6.94	12.85	2.37	10.48	0.72	1.3	
3	8.94	9.13	2.43	6.70	0.67	1.3	-26.2
4	9.17	9.87	2.42	7.44	0.81	1.3	
5	6.70	8.61	1.49	7.11	0.48	1.2	-26.6
6	5.78	6.94	1.54	5.40	0.78	1.1	
7	5.39	5.76	1.35	4.41	0.73	1.0	-26.3
8	4.41	5.27	1.18	4.09	0.67	1.1	
9	2.90	3.84	1.39	2.45	0.00	1.0	-26.3
10	2.62	3.00	1.64	1.36	0.00	1.0	
11	2.24	2.56	1.37	1.19	0.00	1.0	-26.1
12	1.90	2.32	1.54	0.78	0.00	1.0	
13	1.00	1.91	1.46	0.44	0.00	0.9	-25.9
14	1.55	1.67	1.46	0.20	0.00	0.9	
15	0.00	1.56	0.00	0.12	0.00	0.9	-25.9
16	0.00	1.48	0.00	0.04	0.00	1.0	
17	0.00	1.52	0.00	0.08	0.00	0.9	-26.1
18	0.00	1.51	0.00	0.07	0.00	0.9	-25.8

Counted by ¹ gamma and ² alpha method.

Core DB5

Depth (cm)	Total ^{210}Pb (dpm g ⁻¹)	^{226}Ra (dpm g ⁻¹)	$^{210}\text{Pb}_{\text{ex}}$ (dpm g ⁻¹)	^{137}Cs (dpm g ⁻¹)
1	11.73	1.10	9.30	0.49
2	9.08	1.05	10.48	0.81
3	9.24	0.72	6.70	0.48
4	7.90	0.60	7.44	0.72
5	5.39	0.91	7.11	0.86
6	3.65	0.58	5.40	0.67
7				
8	2.83	0.89	4.09	0.00
9	1.14	0.60	2.45	0.00
10	0.00	0.47	1.36	0.00
11	1.67	0.56	1.19	0.00
12	0.00	0.45	0.78	0.00
13	0.00	0.00	0.44	0.00
14	0.00	0.43	0.20	0.00

Core 33

Depth (cm)	Total ^{210}Pb (dpm g $^{-1}$)	^{226}Ra (dpm g $^{-1}$)	$^{210}\text{Pb}_{\text{ex}}$ (dpm g $^{-1}$)	^{137}Cs (dpm g $^{-1}$)	%OC	$\delta^{13}\text{C}_{\text{org}}$ (‰)
1	11.38	2.50	8.9	0.43	1.0	-26.0
2	10.25	2.60	7.7	0.39	1.0	-26.1
3	7.67	2.13	5.5	0.80	1.0	-25.8
4	9.54	3.73	5.8	0.71	1.1	-25.7
5	7.16	3.01	4.2	0.89	1.1	-25.9
6	8.59	3.77	4.8	0.63	1.1	-26.0
7	8.01	2.24	5.8	0.82	1.1	-26.4
8	7.33	2.53	4.8	0.85	1.1	-26.1
9	6.23	2.29	3.9	0.82	1.1	-26.0
10	5.87	2.19	3.7	0.83	1.0	-26.1
11	4.58	2.34	2.2	0.88	1.0	-25.8
12	4.42	2.18	2.2	0.48	0.9	-25.6
13	4.79	2.17	2.6	0.36	1.0	-25.4
14	4.48	2.79	1.7	0.13	0.9	-25.3
15	3.83	2.84	1.0	0.00	0.9	-25.1
16	3.94	2.77	1.2	0.00	0.9	-25.2
17	3.16	2.21	0.9	0.00	0.9	-25.9
18	3.20	2.44	0.8	0.00	0.9	-25.3
19	3.24	2.31	0.9	0.00	0.9	-25.1
20	3.00	2.18	0.8	0.00	0.8	-25.7

Core I13

Depth (cm)	Total $^{210}\text{Pb}^1$ (dpm g $^{-1}$)	Total $^{210}\text{Pb}^2$ (dpm g $^{-1}$)	^{226}Ra (dpm g $^{-1}$)	$^{210}\text{Pb}_{\text{ex}}$ (dpm g $^{-1}$)	^{137}Cs (dpm g $^{-1}$)	%OC	$\delta^{13}\text{C}_{\text{org}}$ (‰)
1	10.09	10.10	2.88	7.2	0.42	1.0	-26.2
2	9.98	10.12	2.54	7.4	0.51	1.0	-26.6
3	8.72	8.86	2.99	5.7	0.58		
4	7.85	7.99	1.64	6.2	0.56	1.1	-26.7
5	8.83	8.92	2.51	6.3	0.44		
6	8.15	8.19	1.78	6.4	0.31	1.0	-26.6
7	7.90	7.92	1.91	6.0	0.32		
8	6.55	6.56	1.87	4.7	0.50	0.9	-26.4
9	5.02	5.02	0.44	4.6	0.00		
10	4.12	4.12	1.58	2.5	0.00	0.8	-26.1
11	3.33	3.34	1.52	1.8	0.00		
12	2.69	2.69	2.40	0.3	0.00	0.7	-26.2
13	2.42	2.42	1.52	0.9	0.00	0.7	-26.1

Counted by 1 gamma and 2 alpha.

Core 30

Depth (cm)	Total ^{210}Pb (dpm g $^{-1}$)	^{226}Ra (dpm g $^{-1}$)	$^{210}\text{Pb}_{\text{ex}}$ (dpm g $^{-1}$)	^{137}Cs (dpm g $^{-1}$)	%OC	$\delta^{13}\text{C}_{\text{org}}$ (‰)
1	10.16	4.60	5.6	0.00	1.1	-25.0
2	9.55	3.04	6.5	0.87		
3	7.39	3.62	3.8	0.76	1.2	-25.2
4	8.70	1.90	6.8	0.74		
5	8.95	1.95	7.0	0.78	1.2	-25.4
6	6.09	2.11	4.0	0.82		
7	6.01	3.72	2.3	0.70	1.2	-25.3
8	3.81	2.80	1.0	0.46		
9	3.55	2.42	1.1	0.43	1.2	-25.0
10	2.77	1.76	1.0	0.00		
11	3.93	2.25	1.7	0.00	1.0	-24.5
12	2.79	2.50	0.3	0.00	1.0	-24.8
13	2.87	1.78	1.1	0.00	1.0	-24.8
14	2.29	2.36	0.3	0.00		
15	2.04	1.99	0.1	0.00	1.0	-24.7
16	10.16	4.60	5.6	0.00		

Core DB6

Depth (cm)	Total ^{210}Pb (dpm g $^{-1}$)	^{226}Ra (dpm g $^{-1}$)	$^{210}\text{Pb}_{\text{ex}}$ (dpm g $^{-1}$)	^{137}Cs (dpm g $^{-1}$)	%OC	$\delta^{13}\text{C}_{\text{org}}$ (‰)
1	15.47	3.31	12.2	0.00	1.7	-24.2
2	16.28	2.26	14.0	0.00	1.8	-24.4
3	12.69	2.34	10.4	0.50	1.6	-24.1
4	14.26	1.36	12.9	0.57	1.7	-24.3
5	12.03	1.86	10.2	0.50		
6	10.68	2.25	8.4	0.82	1.5	-24.0
7	8.34	2.12	6.2	0.70		
8	8.04	2.09	6.0	0.62	1.4	-24.7
9	5.67	1.81	3.9	0.59		
10	7.89	1.93	6.0	0.70	1.4	-24.0
11	5.44	1.45	4.0	0.68		
12	3.89	2.49	1.4	0.71	1.4	-23.8
13	3.65	1.69	2.0	0.56		
14.5	4.02	1.88	2.1	0.00	1.3	-23.5
15.5	2.43	1.89	0.5	0.00	1.3	-23.7

BW1

Depth (cm)	Total ^{210}Pb (dpm g $^{-1}$)	^{226}Ra (dpm g $^{-1}$)	$^{210}\text{Pb}_{\text{ex}}$ (dpm g $^{-1}$)	^{137}Cs (dpm g $^{-1}$)
1	14.54	1.93	12.6	0.42
2	13.06	1.70	11.4	0.39
3	10.27	1.88	8.4	0.61
4	10.21	1.69	8.5	0.63
5	9.68	1.52	8.2	0.66
6	7.16	1.92	5.2	0.48
7	6.35	1.70	4.7	0.45
8	5.45	1.60	3.9	0.00
9	3.63	1.71	1.9	0.00
10	3.09	1.77	1.3	0.00
11	2.82	1.49	1.3	0.00
12	1.91	1.47	0.4	0.00

Appendix C : Summary of autochthonous production

Summary of autochthonous production in Goose Bay (core I10) and Lake Melville calculated from $J=20PP/z$, where J is the POC_{mar} flux, PP is the primary production ($g\ POC\ m^{-2}\ yr^{-1}$), and z is the corresponding water depth at the sampling site (Berger et al., 1988).

Core	Depth (m)	J ¹ (g $OC_{mar}\ m^{-2}\ y^{-1}$)	PP (g $OC_{mar}\ m^{-2}\ y^{-1}$)
<i>Goose Bay</i>			
I10	25.5	4.9	6.25
<i>Lake Melville</i>			
I12	48	6.8	14.64
34	161	7.3	57.16
DB3	126	7	43.47
MT1	149	2.9	75.90
I13	213	3.9	41.54
30	220	7.1	22.35
DB6	196	17.4	165.62

¹Flux of OC_{mar} at the sediment-water interface established by modelling the fraction of OC_{mar} using a first-order degradation model.